Blitz-PRO

User's manual

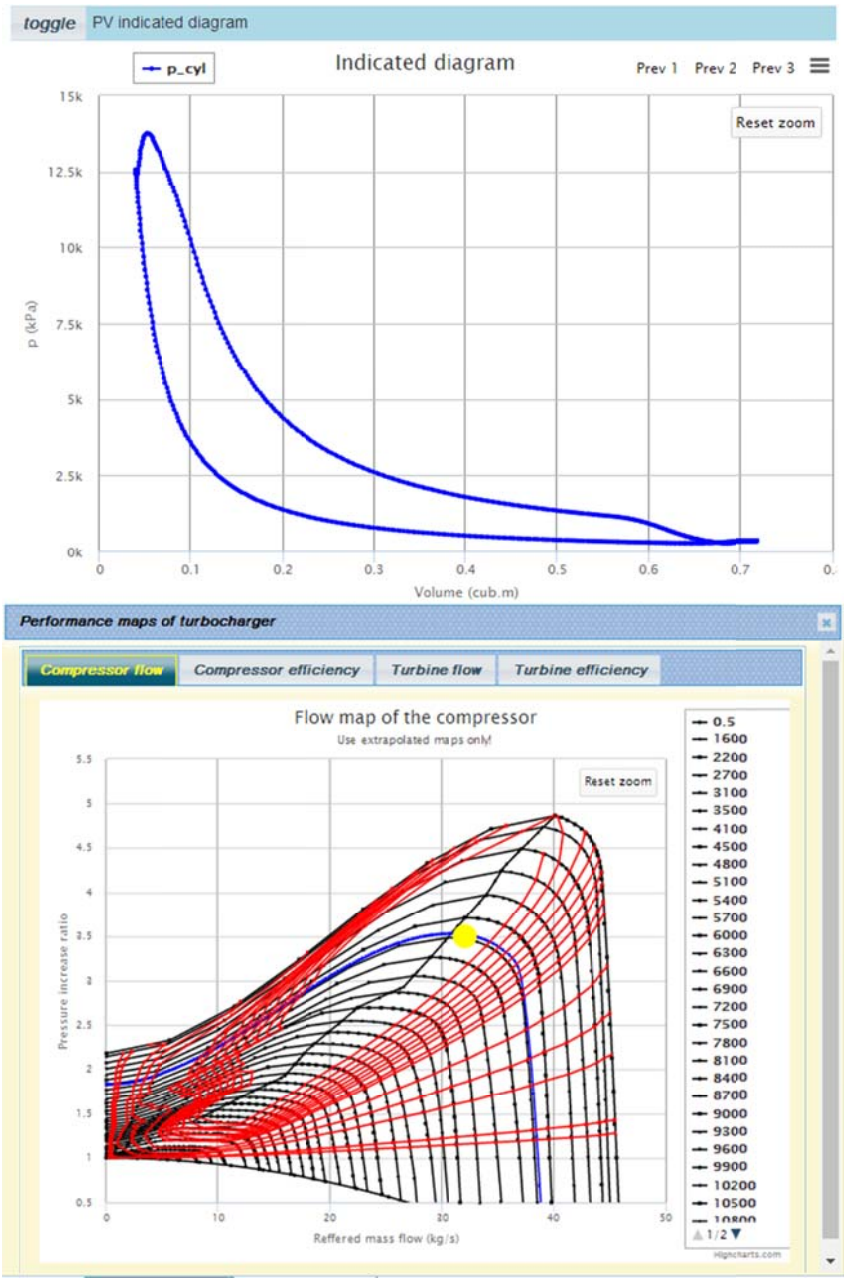

by D. S. Minchev

2018

Content:

List of terms

DF – dual-fuel engine, the gaseous main fuel is ignited by the pilot diesel fuel;
CI – compression-ignition (or diesel) engine;
ICE – internal combustion engine;
OTS – open thermodynamic system;
SI – spark-ignition engine;
Project – the separate file for input data and calculations results for the current engine;
Template – the pre-setup for calculations, example of the initial data setup for given type of engines;
User – the registered customer of software

1. Overview of the Blitz-PRO program.

1.1. Main definitions, features and application.

Blitz-PRO is the on-line simulation software for the Internal Combustion Engine operating cycle synthesis. It's available via the Internet Browser and doesn't have any installation distributive or local files.

The general idea is that the User creates its own profile (with unique login and password) and is able to create and manage projects for solving different tasks of ICE operating cycle simulation. The necessary input data for calculations execution as well as results of calculations are stored in Database, so the User can get immediate access to any project from any device under his profile credentials. To accelerate an initial setup of each Project the set of templates is suggested. Each template corresponds to some engine type and/or type of calculations, so the User approaches the stable calculations much faster.

Fig. 1.1.1. Blitz-PRO offers easy access to projects and calculations from any device with internet connection and web-browser support.

Blitz-PRO offers the following simulation options (the red font indicates options, which currently are under development):

1. Fuel ignition type:

Compression-ignition engines:

- direct multiple fuel injection;
- indirect fuel injection;
- HCCI combustion,

Spark-ignition engines:

- premixed;
- direct incylinder fuel injection,

Dual-fuel engines:

- premixed gas-air mixture;
- gas direct injection.

2. Stroke type:

Four-stroke

Two-stroke:

- loop-scavenging;
- uniflow-scavenging;
- opposed-piston scavenging,

Hybrid-stroke:

- eight-stroke (1 combustion for 4 crank revolutions);
- two-four-stroke switching.

3. Type of crank mechanism:

- conventional crank mechanism;
- ellipsograph-type crank mechanism;
- random piston motion law,

4. Supercharging:

Single-stage:

- turbocharger;
- driven supercharger,

Register :

- turbochargers;
- mechanical superchargers;
- turbocharger + mechanical supercharger,

Two-stage:

- turbochargers for 1st and 2nd stage;
- turbocharger for the 1st stage and mechanical charger for the 2nd stage;
- turbocharger for the 2nd stage and mechanical charger for the 1st stage.

5. Transient simulation:

Type-of-load apply:

- vehicle application:
  - *mechanical gearbox;*
  - *automatic gearbox;*
  - variator gearbox,
- ship application:
  - *direct & geared fixed pitch propeller;*
  - *direct & geared controllable pitch propeller;*
  - *electric gear;*
- test-bench application.

Turbocharger control:

waste-gate dynamics;
variable turbine's nozzle dynamics

The technological structure of the Blitz-PRO service contains the server's side and the User's side. The server's side includes Database, the Calculation Core and the Server's Side of Web Application. The User's side contains web browser and the stored files with results of calculations. The interactions between all these components are shown on the Fig. 1.1.2.

Simulation Core contains the routines of mathematical models for synthesis of the ICE operating processes. These routines are compiled into JAVA .war file. The initial data for calculations and the calculations results are stored in the Database. The Database also interacts with Web Application, performed under Zend Framework Environment (see Fig. 1.1.3 for the Web Application structure).

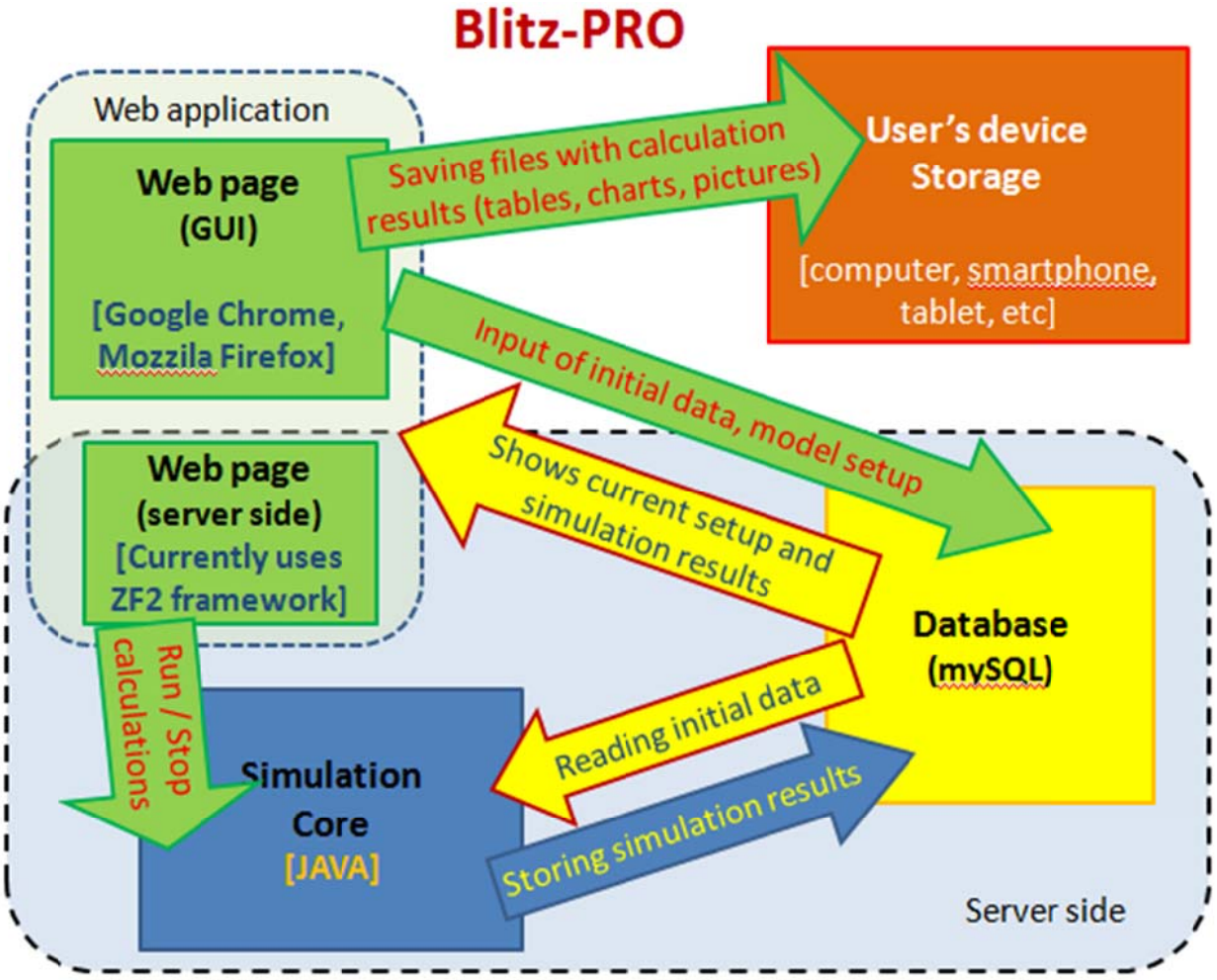

Fig. 1.1.2. The technological structure of the Blitz-PRO service.

Fig. 1.1.4 illustrates the projects managing by the User. The User can create, open and delete the Project, also he can save it by another name. The real Databese structure differs from the structure shown in Fig.1.1.4 and contains separated tables for projects, initial data (several tables) and calculation results (several tables).

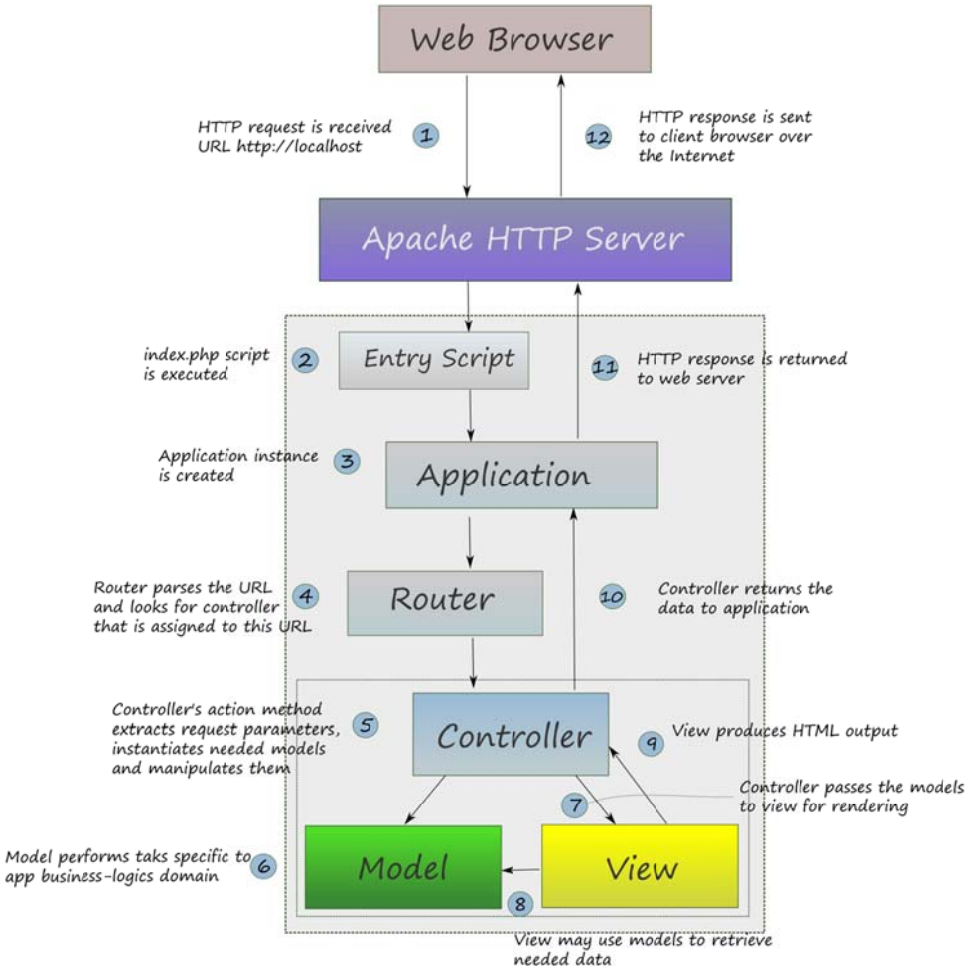

Fig. 1.1.3. Web Application structure.

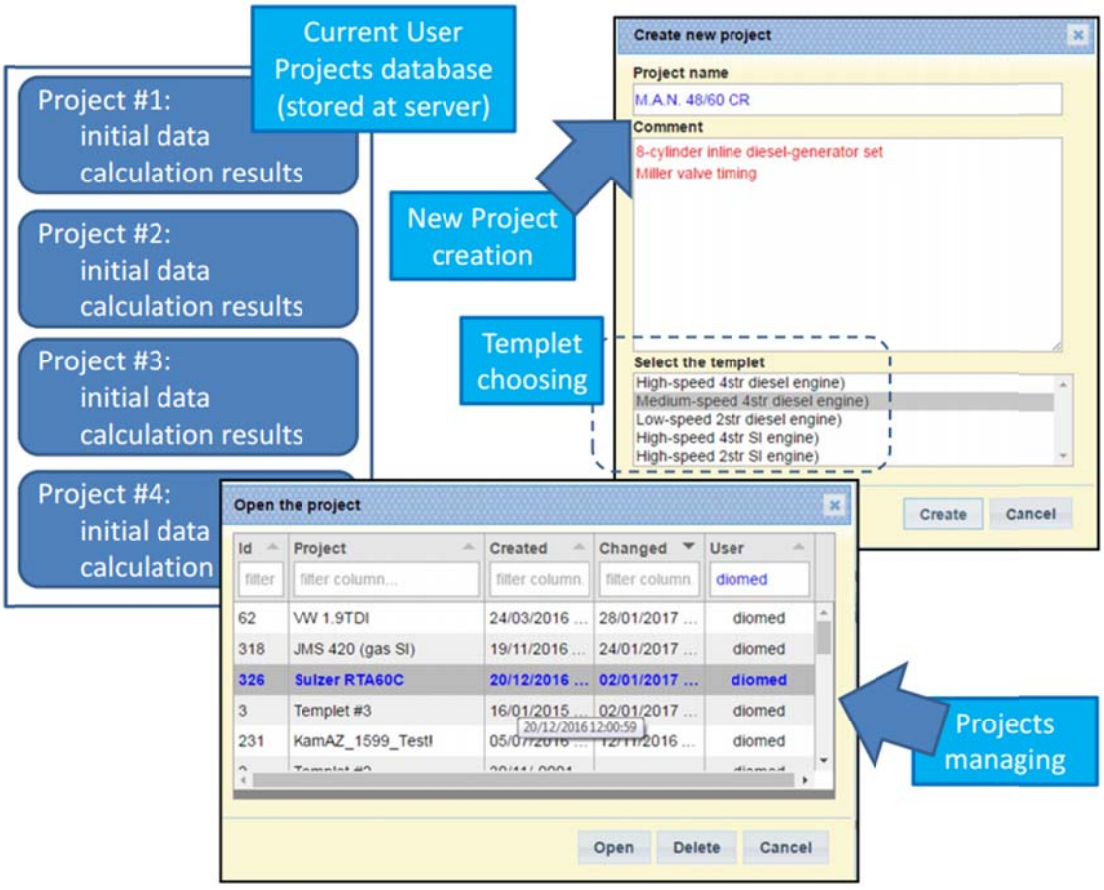

Fig. 1.1.4. Projects managing.

1.2. Equations and references

Blitz-PRO offers operating cycle synthesis for various configurations of ICE engines. Nevertheless for any engine configuration the basic approach remains the same: the engine is divided into couple of open thermodynamic systems (OTS), which interact each with other by energy and mass exchange processes.

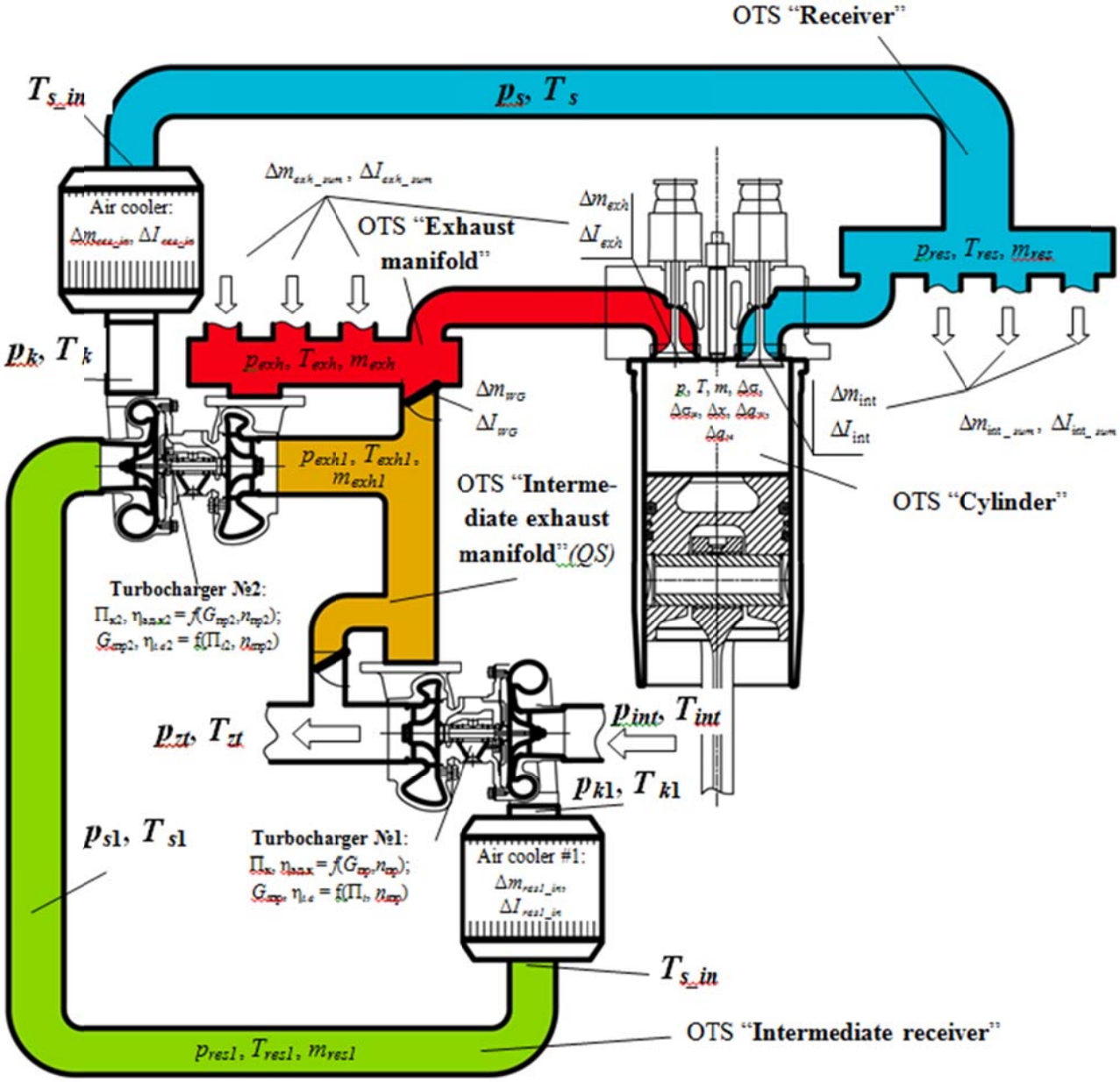

Fig. 1.2.1. Division of the engine layout into interacting open thermodynamic systems for the case of diesel engine with controllable two-stage turbocharging.

Figure 1.2.1 illustrates the approach of general thermodynamic system "Engine" division into number of interacting open thermodynamic systems for the case of diesel engine with controllable two-stage turbocharging. The actual layout depends on engine's operating cycle type (two-stroke, four-stroke), configuration of supercharging system, etc.

For open thermodynamic systems the universal set of equations is used. These equations are based on the concepts of the first-law of thermodynamics, equality of working gases properties for each point of the volume (0-D approach), gas-state law

and mass balance equations. The example of the open thermodynamic system is shown on Fig. 1.2.2 for the engine cylinder.

The first law of thermodynamics is expressed as:

$$\left(\frac{\mathrm{d}I_{fuel}}{\mathrm{d}\varphi}+\sum_{1}^{n_1}\frac{\mathrm{d}I_j}{\mathrm{d}\varphi}\right)+\frac{\delta Q_{comb}}{\mathrm{d}\varphi}+\sum_{1}^{n_2}\frac{\delta Q_{wall.i}}{\mathrm{d}\varphi}=c_{vm}T\left(\sum_{1}^{n_1}\frac{\mathrm{d}m_j}{\mathrm{d}\varphi}+\frac{\mathrm{d}m_{fuel}}{\mathrm{d}\varphi}\right)+c_v m\frac{\mathrm{d}T}{d\varphi}+mT\frac{d(c_v)_T}{d\varphi}+p\frac{\mathrm{d}V}{\mathrm{d}\varphi},$$

where $\mathrm{d}I_{fuel}/\mathrm{d}\varphi$, $\mathrm{d}I_j/\mathrm{d}\varphi$ – the rate of enthalpy change due to fuel evaporation and due to mass exchange processes, $\delta Q_{comb}/\mathrm{d}\varphi$ – heat release rate due to fuel combustion, $\delta Q_{wall.i}/\mathrm{d}\varphi$ – heat transfer rate to the walls of the system, $\mathrm{d}m_{fuel}/\mathrm{d}\varphi$, $\mathrm{d}m_j/\mathrm{d}\varphi$ – fuel mass flow and gases mass flow, n_1 – number of the interacting thermodynamic systems, involved into mass exchange process, n_2 – number of walls, involved into heat transfer process, p, T, V, m – pressure, temperature, volume, mass of the gases mixture in the OTS, c_v, c_{vm} – actual and average isochoric specific heat capacity.

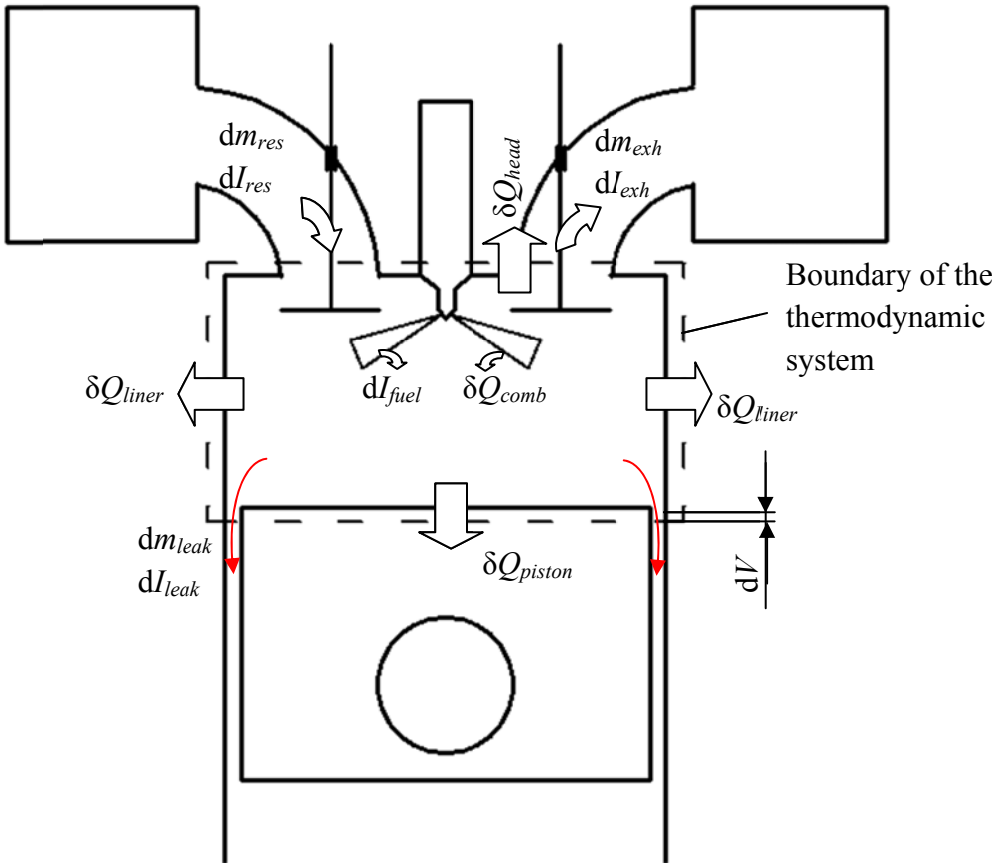

Fig. 1.2.2. Example of open thermodynamic system.

The thermodynamics first law equation is completed with the mass balance equation and with the gas-state equation:

$$\mathrm{d}m=\sum_{1}^{n_1}\mathrm{d}m_j+\mathrm{d}m_{fuel};$$

$$pV=Z\frac{m}{\mu}RT,$$

where Z is compression factor, calculated by the Berthelot equation:

$$Z=1+\frac{9}{128}\frac{\pi}{\theta}\left(1-\frac{6}{\theta^2}\right),$$

where $\pi = p/p_{crit}$ – relative to critical pressure, $\theta = T/T_{crit}$ – relative to critical temperature (see table 1.2.1).

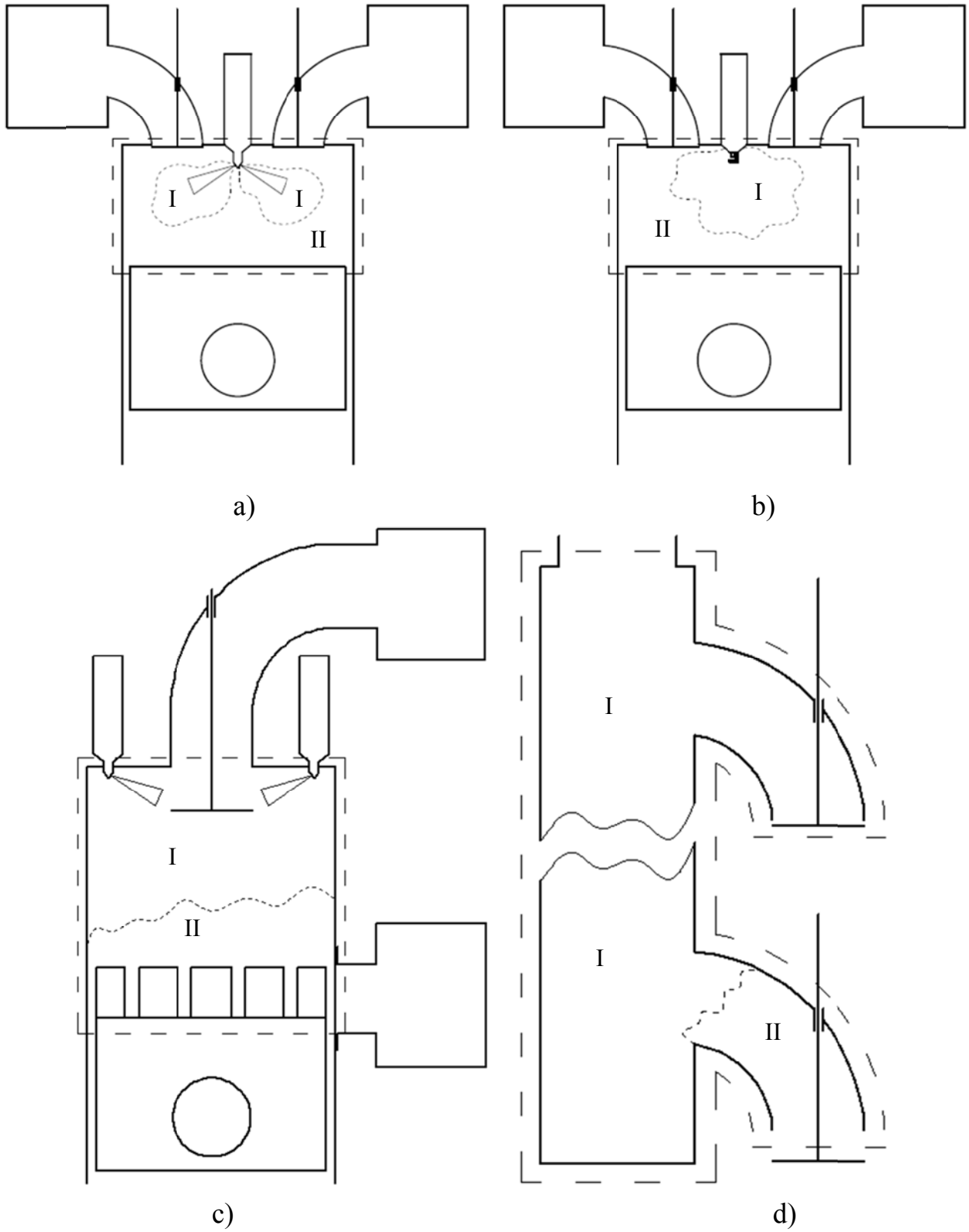

Fig. 1.2.3. Two-zone models for compression-ignition (a) and spark-ignition (b) combustion processes, two-stroke engines scavenging (c) and intake manifold burned gases reflux (d).
I – burned gases zone, II – fresh mixture zone

Table 1.2.1

Gas parameters in critical point, used in Berthelot equations

Gas	p_{crit}, MPa	T_{crit}, K
N_2	3.39	126.05
O_2	5.04	154.35
H_2	1.3	33.25
CO	3.5	134.15
CO_2	7.35	304.15
H_2O	22.13	647.35
CH_4	4.626	190.77
C_3H_8	4.32	370
CH_3OH	8.103	512.65
C_2H_5OH	6.3	514.15
Air	3.77	132.45
Petrol	1.633	570.3
Diesel oil	1.63	733

The specific heat of the gases mixture is calculated by Dalton's law, while the specific heat of each component is given by polynomial regressions, kJ/(kmole·K):

Air: $c_{v\mu} = 5{,}52411 \cdot 10^{-19} T^6 - 5{,}726799 \cdot 10^{-15} T^5 + 2{,}375597 \cdot 10^{-11} T^4 - - 4{,}951694 \cdot 10^{-8} T^3 + 5{,}1761 \cdot 10^{-5} T^2 - 1{,}9099 \cdot 10^{-2} T + 23{,}005$, $R^2 = 0{,}99999$;

CO_2: $c_{v\mu} = -3{,}5902 \cdot 10^{-19} T^6 + 4{,}11717 \cdot 10^{-15} T^5 - 1{,}9643 \cdot 10^{-11} T^4 + + 5{,}14242 \cdot 10^{-8} T^3 - 8{,}2174 \cdot 10^{-5} T^2 + 8.2126 \cdot 10^{-2} T + 10.333$, $R^2 = 1{,}0$;

CO: $c_{v\mu} = 6{,}66905 \cdot 10^{-19} T^6 - 6{,}87834 \cdot 10^{-15} T^5 + 2{,}838962 \cdot 10^{-11} T^4 - - 5{,}892362 \cdot 10^{-8} T^3 + 6{,}15177 \cdot 10^{-5} T^2 - 2{,}36488 \cdot 10^{-2} T + 23{,}739$, $R^2 = 0{,}99998$;

H_2: $c_{v\mu} = -9{,}269363 \cdot 10^{-19} T^6 + 8{,}875943 \cdot 10^{-15} T^5 - 3{,}321498 \cdot 10^{-11} T^4 + + 6.043425 \cdot 10^{-8} T^3 - 5.368376 \cdot 10^{-5} T^2 + 2.34933 \cdot 10^{-2} T + 16.878$, $R^2 = 0{,}99981$;

N_2: $c_{v\mu} = 4{,}062159 \cdot 10^{-19} T^6 - 4{,}487468 \cdot 10^{-15} T^5 + 1{,}993208 \cdot 10^{-11} T^4 - - 4{,}470124 \cdot 10^{-8} T^3 + 5{,}053716 \cdot 10^{-5} T^2 - 2{,}08783 \cdot 10^{-2} T + 23{,}56$, $R^2 = 0{,}99999$;

H_2O: $c_{v\mu} = - 4{,}897476 \cdot 10^{-20} T^6 + 3{,}447949 \cdot 10^{-17} T^5 + 2{,}656956 \cdot 10^{-12} T^4 - - 1{,}366663 \cdot 10^{-8} T^3 + 2{,}443866 \cdot 10^{-5} T^2 - 5{,}50647 \cdot 10^{-3} T + 25{,}104$, $R^2 = 0{,}99999$;

O_2: $c_{v\mu} = 1{,}211498 \cdot 10^{-18} T^6 - 1{,}142445 \cdot 10^{-14} T^5 + 4{,}197528 \cdot 10^{-11} T^4 - - 7{,}461907 \cdot 10^{-8} T^3 + 6{,}280219 \cdot 10^{-5} T^2 - 1{,}49757 \cdot 10^{-2} T + 21{,}623$, $R^2 = 0{,}99984$,

where R^2 – correlation factor.

Generally, for each open thermodynamic system the single-zone model is applied, that means the whole volume of the system is considered as homogeneous mixture of gases. But for several cases shown on Fig. 1.2.3 two-zone model is also implemented:

1. During combustion period to predict the burned gases and fresh charge temperatures for NO_x and CO formation calculation (*a*, *b* on Fig. 1.2.3).
2. During scavenging period for two-stroke engines to predict correctly gas exchange processes (*c* on Fig. 1.2.3).

3. To consider burned gases reflux from the cylinder into intake receiver (*d* on Fig. 1.2.3).

In the two-zone model the thermodynamic system is virtually divided into two interacting thermodynamic systems. The general concept for two-zone model is the equivalence of pressure for both zones and impenetrable flexible boundary surface between them. Basic equations are based on the first law of thermodynamics:

$$\begin{cases} \left(\frac{\mathrm{d}I_{fuel}}{\mathrm{d}\varphi} + \sum_1^{n_1} \frac{\mathrm{d}I_j^I}{\mathrm{d}\varphi} + \frac{\mathrm{d}I_{I-II}}{\mathrm{d}\varphi} \right) + \frac{\delta Q_{comb}}{\mathrm{d}\varphi} + \sum_1^{n_2} \frac{\delta Q_{wall.i}^I}{\mathrm{d}\varphi} + \frac{\delta Q_{I-II}}{\mathrm{d}\varphi} = \\ = c_{pm}^I T^I \left(\sum_1^{n_1} \frac{\mathrm{d}m_j^I}{\mathrm{d}\varphi} + \frac{\mathrm{d}m_{fuel}}{\mathrm{d}\varphi} \right) + c_p^I m^I \frac{\mathrm{d}T^I}{d\varphi} + m^I T^I \frac{d\left(c_v\right)_T^I}{d\varphi} + V^I \frac{\mathrm{d}p}{\mathrm{d}\varphi}; \\ \left(\sum_1^{n_3} \frac{\mathrm{d}I_j^{II}}{\mathrm{d}\varphi} - \frac{\mathrm{d}I_{I-II}}{\mathrm{d}\varphi} \right) + \sum_1^{n_4} \frac{\delta Q_{wall.i}^{II}}{\mathrm{d}\varphi} - \frac{\delta Q_{I-II}}{\mathrm{d}\varphi} = \\ = c_{pm}^{II} T^{II} \sum_1^{n_3} \frac{\mathrm{d}m_j^{II}}{\mathrm{d}\varphi} + c_p^{II} m^{II} \frac{\mathrm{d}T^{II}}{d\varphi} + m^{II} T^{II} \frac{d\left(c_v\right)_T^{II}}{d\varphi} + V^{II} \frac{\mathrm{d}p}{\mathrm{d}\varphi}, \end{cases}$$

where index "I" refers to the burned gases zone, and index "II" – to the fresh mixture zone, $\delta Q_{\text{I-II}}/\mathrm{d}\varphi$ – heat transfer rate between zones, $\mathrm{d}I_{\text{I-II}}/\mathrm{d}\varphi$ – enthalpy transfer rate between zones.

These equations are used together with general single-zone equation, which is used to find the pressure for the next time layer.

The mass flow between interacting thermodynamic systems is calculated on the traditional quasi-steady method coupled with prof. Orlin approach to consider unsteady effects.

The quasy-steady equations for gas flow velocity w_{static} from the volume with higher pressure "1" to the volume with lower pressure "2" are:

$$w_{static} = \begin{cases} \sqrt{\frac{2k_1}{k_1 - 1} R_\mu T_1^* \left[1 - \left(\frac{p_2}{p_1^*} \right)^{\frac{k_1 - 1}{k_1}} \right]}, \text{ if } \frac{p_1}{p_2} < \left(\frac{2}{k_1 + 1} \right)^{\left(\frac{k_1}{1 - k_1} \right)}; \\ \sqrt{\frac{2k_1}{k_1 + 1} R_\mu T_1^*}, \text{ if } \frac{p_1}{p_2} > \left(\frac{2}{k_1 + 1} \right)^{\left(\frac{k_1}{1 - k_1} \right)}, \end{cases}$$

where k_1 is the adiabatic exponent, "*" indicates total parameters.

To consider the unsteady phenomena the pulse conservation equation is used:

$$w \frac{\partial w}{\partial x} + \frac{\partial w}{\partial t} = -\frac{1}{\rho} \frac{\partial p}{\partial x}$$

It is converted according to prof. Orlin method [1] and expresses gas flow acceleration:

$$\frac{dw}{d\tau} = \frac{w_{static} \cdot |w_{static}| - w \cdot |w|}{2L},$$

where L is the "active" pipe length.

The active pipe length is to be set by the user for intake and exhaust valves/ports (see section 2.5), but for many other cases (turbine, compressor, inter-

cooler, etc) it is assumed automatically (usually divisible by channel's equivalent flow diameter).

The mass flow is calculated as:

$$\frac{dm}{dt} = \mu A w \frac{p_2}{R_\mu T_1^*} \left(\frac{p_2}{p_1^*} \right)^{\frac{1-k_1}{k_1}},$$

where μA – the effective flow area of the channel, μ – discharge coefficient.

Heat transfer calculations are based on Newton's law of cooling for quasi-steady heat transfer model. According to this model the wall temperatures for both hot and cold side are assumed constant and equal to their average values. Detailed information about models for heat transfer is presented in section 2.2.

Heat release rate from fuel combustion is given by Wiebe equation for spark-ignition engines and either Wiebe equation or by Razlejtzev mathematical model for compression-ignition engines (see section 2.4). Dual-fuel combustion is calculated with combined Wiebe-Razlejtzev model: the combustion of ignition fuel is calculated by Razleitzev model and the main fuel combustion is given by Wiebe equation.

Transient simulation of engine operation is based on consecutive (cycle-by-cycle) synthesis of engine's indicated process. The mechanical dynamics of engine and turbocharger is set with following equations:

$$\frac{\mathrm{d}n}{\mathrm{d}t} = \frac{60}{J_{rot}} \frac{P_e - P_{load}}{\left(\frac{\pi}{30} \right)^2 n},$$

$$\frac{\mathrm{d}n_{TC}}{\mathrm{d}t} = \frac{60}{J_{TC}} \frac{P_{turb} - P_{compr}}{\left(\frac{\pi}{30} \right)^2 n_{TC}},$$

where n, n_{TC} – crankshaft and turbocharger rotor speed, P_e, P_{load}, P_{turb}, P_{compr} – engine's brake power, power of the load resistance, power of turbine and compressor correspondently, J_{rot}, J_{TC} – reduced moment of inertia of engine, power consumer and transmission referred to the crankshaft speed and turbocharger's rotor moment of inertia.

Fuel injection and combustion for transient engine operation is to be set by the User with control maps *.csv files. For detailed information see section 2.7.

1.3. Getting started

To start the calculations the User needs to sign-in into application by clicking on the button “Sign-In” and passing the registration procedure.

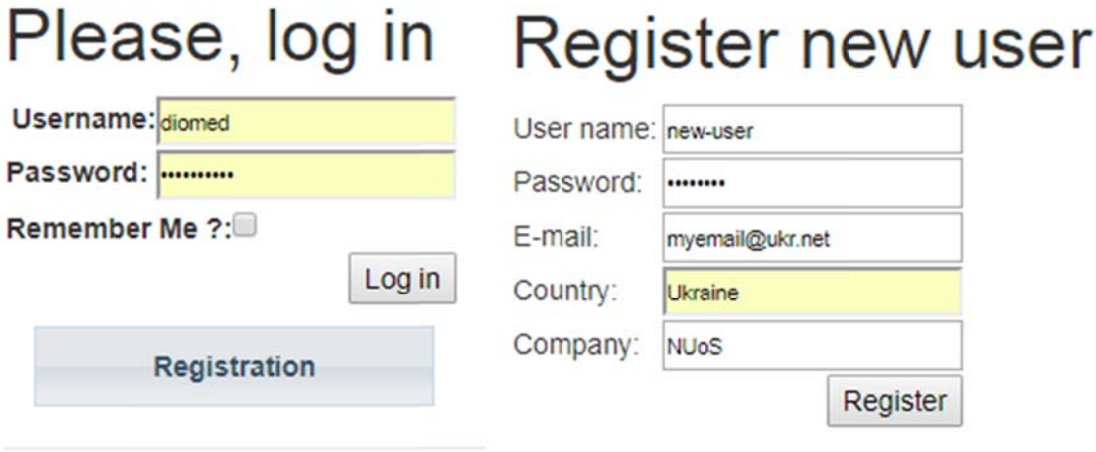

a) b)

Fig. 1.3.1. Registration of the new User.

The registration procedure starts by click on the button “Registration”. The User must fill all fields of the registration form. Please note that ***user name*** should contain from 8 to 12 symbols, while ***password*** – from 8 to 20 symbols. Then the User is to confirm the registration by pressing “Register” and to log-in into the Blitz-PRO application. If you want the Browser save your credentials, check the “Remember Me” option.

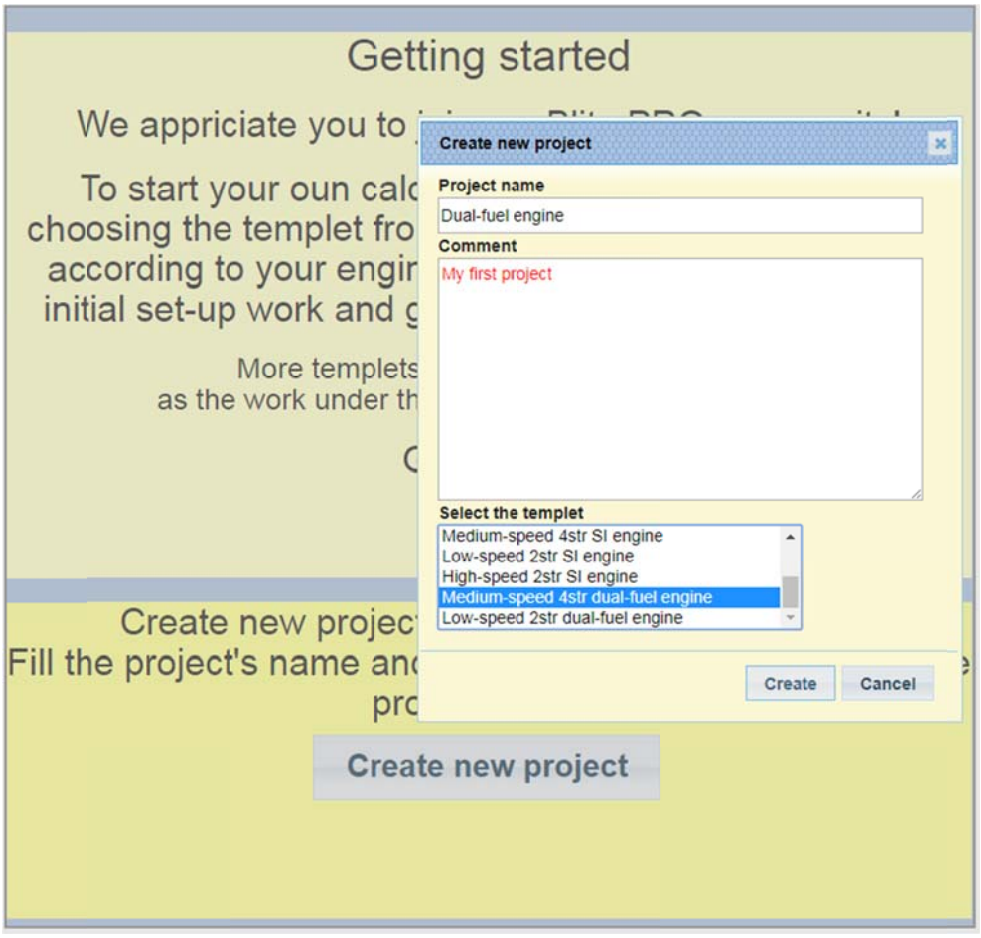

Fig. 1.3.2. Creating new Project.

Click on the “Start working!” button redirects the User to the start-working page, where he/she can create the first Project (by click on the button “Create new Project”).

To create the new Project the User states its name, short description and chooses the template for the Project from the selection list at the bottom. Templates are the set of calculations pre-setups for different types of ICE. Choosing the correct template helps to make the initial model setup much easier. Templates for two- and four-stroke, low-, medium and high-speed, compression ignition, spark-ignition and dual-fuel engines are currently available.

Note, that the limit for project name is 24 symbols. Each Project gets unique id number, so the User can create several Projects with the same project name. When the Project is created it gets reserved space in the Database, so the every change of any parameter is stored immediately in the Database, and there is no need for the User to save changes into the Project manually. At the same time, the undo/redo option is not available.

1.4. Projects managing.

The User can create, open, delete and copy the Project from the “New”, “Open”, “Seve as” buttons menu at the header of the main page.

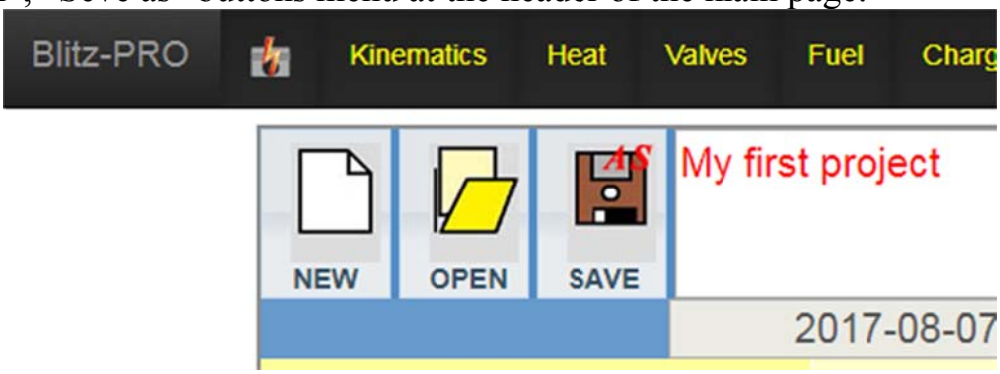

Fig. 1.4.1. Projects managing bar.

The “New” button opens the same dialog, described in section 1.4 (Fig. 1.3.2.).

The “Open” button opens the table of the User’s Projects as it is shown in Fig. 1.4.2, sorted by the date of last change of calculations results. The Project is assumed “changed” only when the User runs calculations, clicking “Calculate” button.

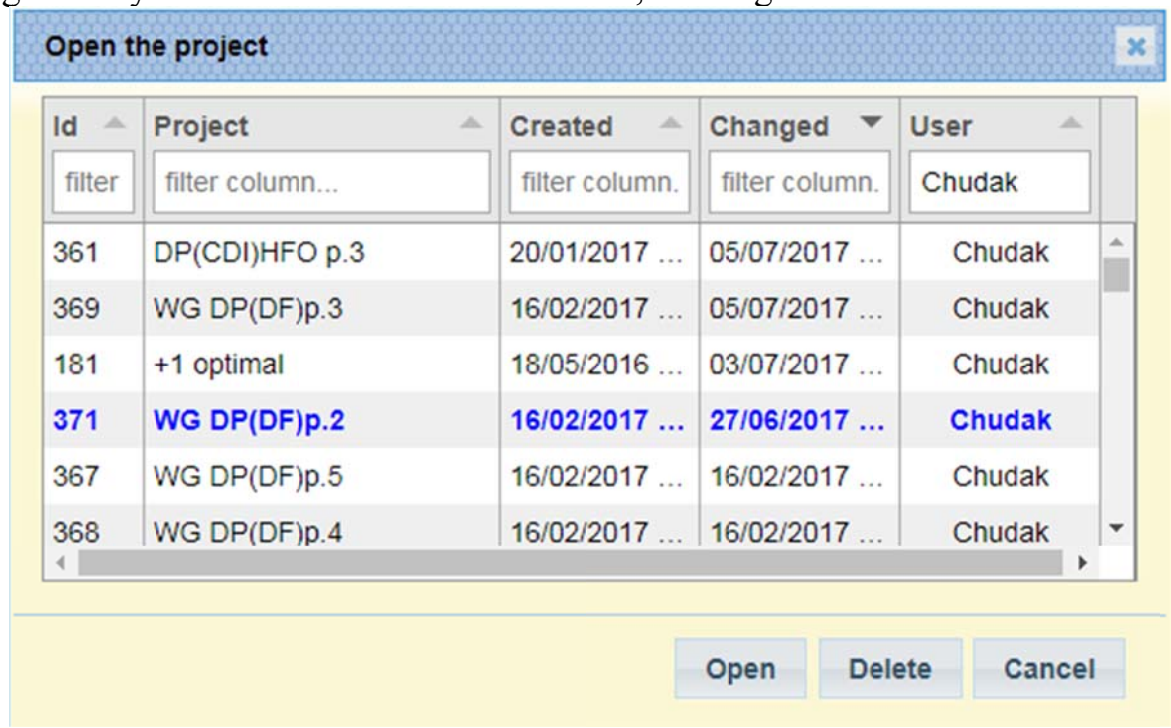

Fig. 1.4.2. Open Project dialog.

The User can sort Projects by any category (id, name, time of creation and last change), clicking on corresponding column header. He can also filter the Projects typing its id, name, etc.

To open the Project the User has to click on the Project from the list selecting it, and then press the “Open” button below. He can also delete the selected project. Note, that it is not permitted to delete active Project! The delete action cannot be un-done!

The User can copy the Project by pressing “Save as” button (see fig 1.4.3) and saving it with new name and description.

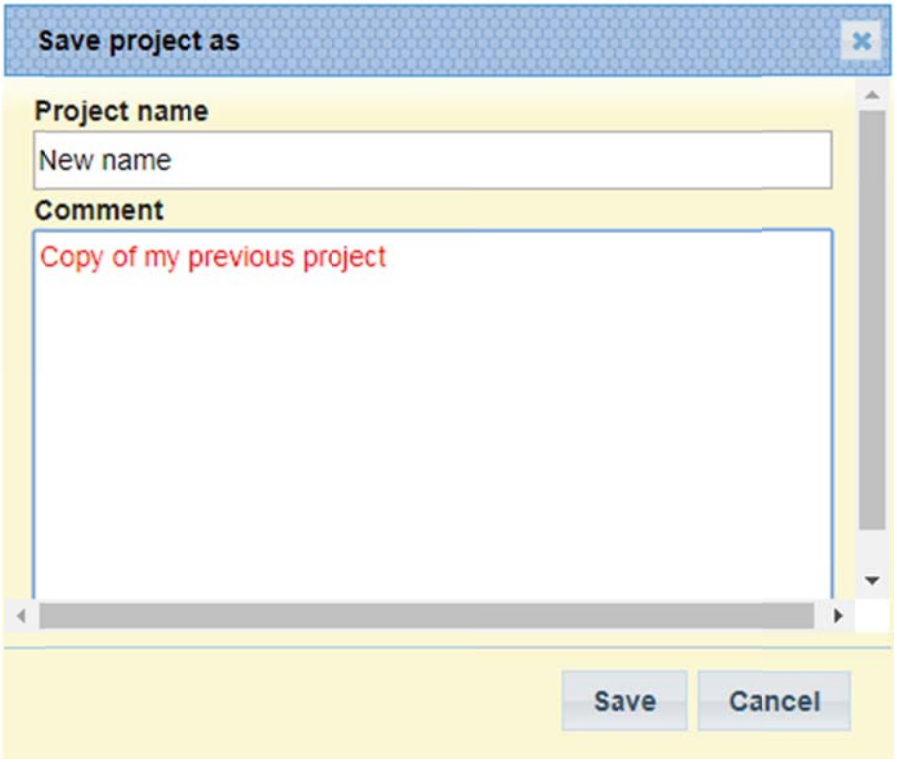

Fig. 1.4.3. Copy Project dialog.

1.5 Data import (.csv files structure)

For several cases Blitz-PRO offers to the User an option to import the data as the table form. These cases are:

1. Setup of the user-defined kinematics of the engine piston.
2. Setups of the user-defined intake/exhaust valves lift law or intake/exhaust ports area.
3. Setup of the user-defined fuel injection pattern.
4. Upload the performance maps for supercharging device.
5. Setup of the control maps for fuel injection or spark timing.
6. Setup of the user-defined ship resistance curve.
7. Import of the experimental data for engine transient operation.

Technologically the data import is made with .csv files (comma separated values files). For all cases the .csv file has the same structure: the rows of the data table are assembled in strings, with values for each column separated with comma "," (see Fig. 1.5.1 and 1.5.2):

$$x_{11}, x_{21}, x_{31}, \ldots x_{n1}$$
$$x_{12}, x_{22}, x_{32}, \ldots x_{n2}$$
$$x_{13}, x_{23}, x_{33}, \ldots x_{n3}$$
$$\ldots\ldots\ldots$$
$$x_{1m}, x_{2m}, x_{3m}, \ldots x_{nm}.$$

n_{crank}	q_{fuel}	φ_{inj}	$\varphi_{inj.start}$
rpm	g/cycle	c.a.d.	c.a.d.
650	0.0457	9.1	351.2
700	0.0547	10.3	352.8
780	0.057	10.4	353.8
860	0.058	10.76	354.2
940	0.0592	11.05	354.57
1020	0.0649	12.8	355.16
1100	0.0926	17.2	356.8
1180	0.1283	22.8	358.57
1260	0.1484	27.1	359.76
1340	0.145	27.76	359.57
1420	0.142	27.9	359.41
1500	0.1388	28	359.24
1580	0.1363	28.1	359.2
1660	0.1347	28.37	359.14
…	…	…	…

a)

```
650,0.0457,9.1,351.2
700,0.0547,10.3,352.8
780,0.057,10.4,353.8
860,0.058,10.76,354.2
940,0.0592,11.05,354.57
1020,0.0649,12.8,355.16
1100,0.0926,17.2,356.8
1180,0.1283,22.8,358.57
1260,0.1484,27.1,359.76
1340,0.145,27.76,359.57
1420,0.142,27.9,359.41
1500,0.1388,28,359.24
1580,0.1363,28.1,359.2
1660,0.1347,28.37,359.14
1740,0.1327,28.52,359.14
1820,0.1307,28.7,359.08
1900,0.1294,28.8,359.05
1969,0.1278,28.9,359.01
2060,0.1258,29,358.95
2140,0.1241,29.13,358.89
```

b)

Fig. 1.5.1 Example of .csv file structure for engine's control map.
a) table with data, b) screen shot of .csv file from text editor.

Table 1.5.1 contains information about the structure of .csv files for several cases, mentioned above.

Table 1.5.1

Structure of .csv files

Case:		x_1	x_2	x_3	x_4	x_5	x_6
Piston kinematics*	Param.	φ	V/V_s				
	Units	c.a.d.	-				
Valve relative lift*	Param.	φ	$\bar{h}_{\text{int}.v}$, $\bar{h}_{exh.v}$				
	Units	c.a.d.	-				
Port relative area*	Param.	φ	$\bar{A}_{\text{int}.p}$, $\bar{A}_{exh.p}$				
	Units	c.a.d.	-				
Fuel injection*	Param.	φ	σ				
	Units	c.a.d.	-				
Control maps for CI engine	Param.	n_{crank}	q_{fuel}	φ_{inj}	$\varphi_{inj.start}$		
	Units	rpm	g	c.a.d.	c.a.d.		
Control maps for SI engine	Param.	n_{crank}	χ_{thr}	$\varphi_{comb.start}$	φ_{comb}	m_{comb}	α
	Units	rpm	-	c.a.d.	c.a.d.	-	-
Transient data from experiment	Param.	τ	n_{crank}, n_{TC}, p_s, p_t, G_{int}, $p_{\max}$				
	Units	s	rpm, rpm, kPa, kPa, kg/s, kPa				

φ – crank angle revolution, V/V_s – relative displacement volume, σ – relative injected fuel mass, n_{crank} – crankshaft speed, q_{fuel} – amount of fuel, injected per cycle, $\varphi_{inj.start}$ – fuel injection start, χ_{thr} – throttle pressure drop, $\varphi_{comb.start}$ – start of combustion, φ_{comb} – duration of combustion, m_{comb} – Wiebe function exponent, α – air excess ratio, τ – time from transient start, n_{TC} – supercharger speed, p_s, p_t – intake receiver and exhaust manifold pressures, G_{int} - !intake mass flow, $p_{\max}$ – maximum pressure.
* - the range of φ is to be [0, 360/χ], including φ = 0 and φ = 360/χ (χ – stroke factor, equals 0.5 for four-stroke and 1.0 for two-stroke engines).

The .csv file for performance maps of the mechanical compressor or the turbocharger has its special structure and is to be formed with special software for generating, interpolating and extrapolating of the compressor and turbine characteristics.

The User can create .csv file with any text editor, or with special software (for example Microsoft Excel supports conversion of its electronic tables to .csv (MS-DOC) files. Please, make sure, the .csv file has the proper structure and extension!

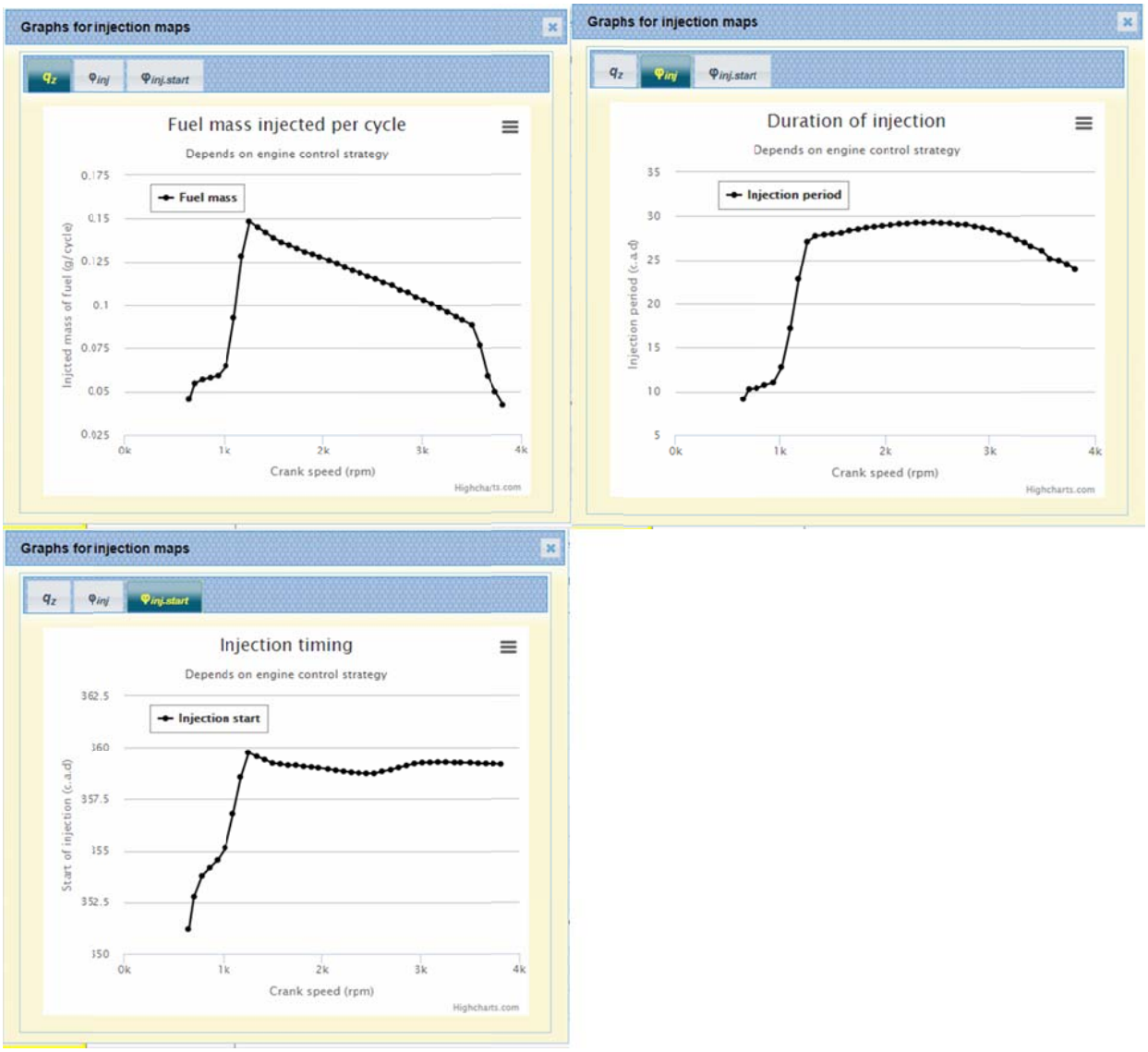

Fig. 1.5.2. Diesel engine control maps .csv file visualization.

2. Calculations setup

The User sets the basic engine configuration on the main page.

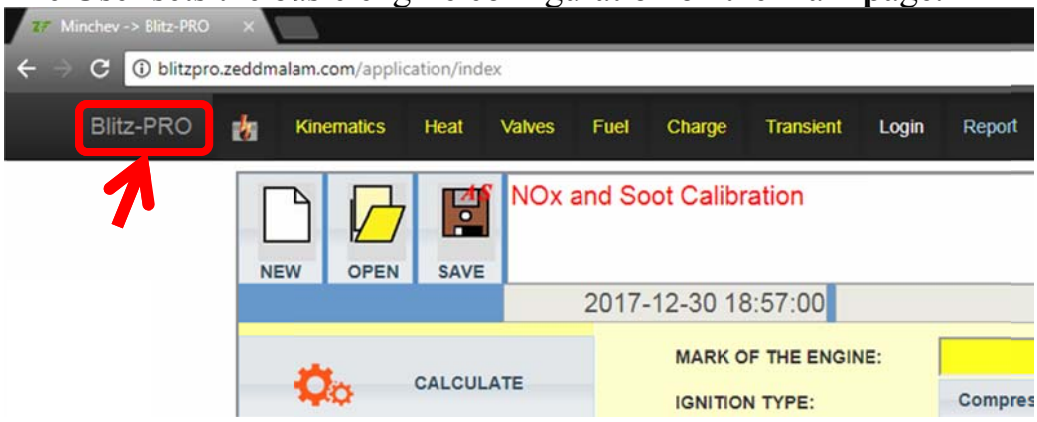

Fig. 2.1. Click the Blitz-PRO shortcut to navigate to the main page.

The type of ignition includes three options: compression-ignition, spark-ignition and dual-fuel ignition. The last is the case when gaseous fuel is ignited with diesel fuel pilot injection. The User should also choose between two-stroke and four-stroke operating cycle (eight-stroke cycle is currently not supported).

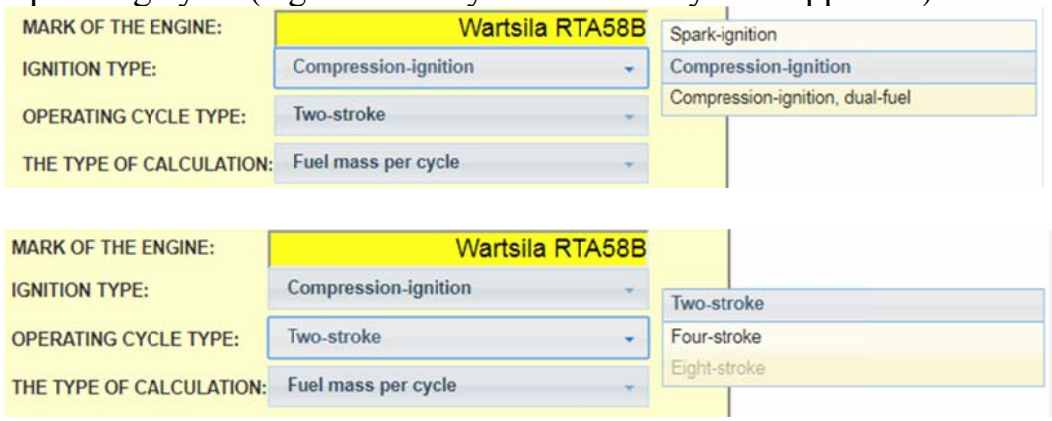

Fig. 2.2. Ignition type and operating cycle type options.

Synthesis of diesel engine operating cycle is available for three initial conditions: by setting of injected mass of fuel, by setting the value of the air excess ratio and by setting the desired brake power output. For spark-ignition engines and for dual-fuel engines there is the only option: to set the value of air excess ratio.

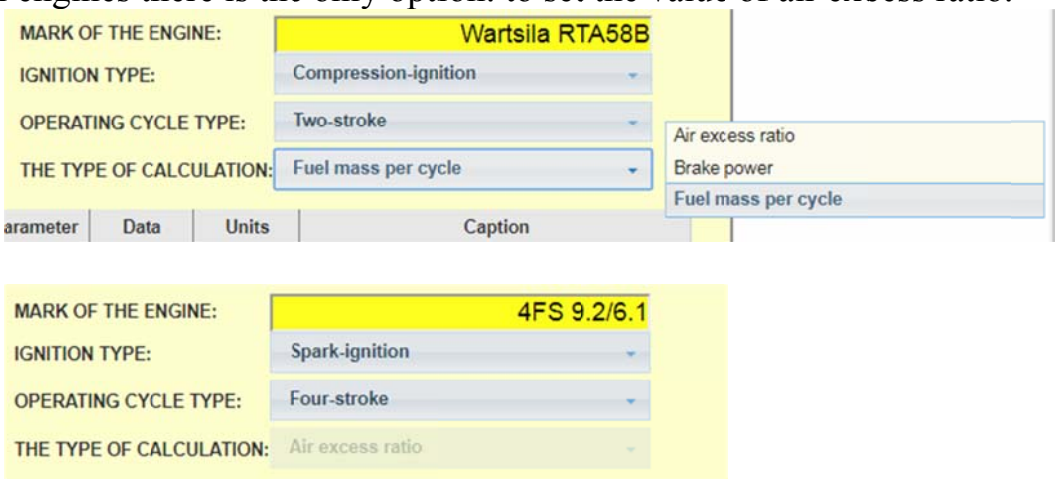

Fig. 2.3. Calculations modes for CI engines (above), SI and DF engines (below)

Most of parameters in the list of input data on the main page have duplication on the corresponding pages (“Kinematics”, “Heat transfer”, “Valves”, “Fuel and combustion”, “Supercharging”, “Transient”).

Exceptions are made for throttle plate pressure drop ratio χ_{thr}, currently avalible for spark-ignition engines only, and for relative volume of burned gases $\psi_{r.burned}$ (only for two-stroke engines), which can be set exclusively from the main page.

Throttle plate pressure drop ratio χ_{thr} is the ratio between absolute pressures before and after throttle plate. In the case of supercharged engines it is assumed, that throttle plate is placed before compressor.

The value of $\psi_{r.burned}$ is used to trigger between two-zone and single-zone gas-exchange model for two-stroke engines. If the fraction of the burned gases drops lower than $\psi_{r.burned}$, the calculations of scavenging switch to single-zone model (fast mixing model). For different scavenging systems the recommended values of $\psi_{r.burned}$ are: uniflow scavenging 3…15 %, ports scavenging 2…14 %, crankcase scavenging 10…30 %.

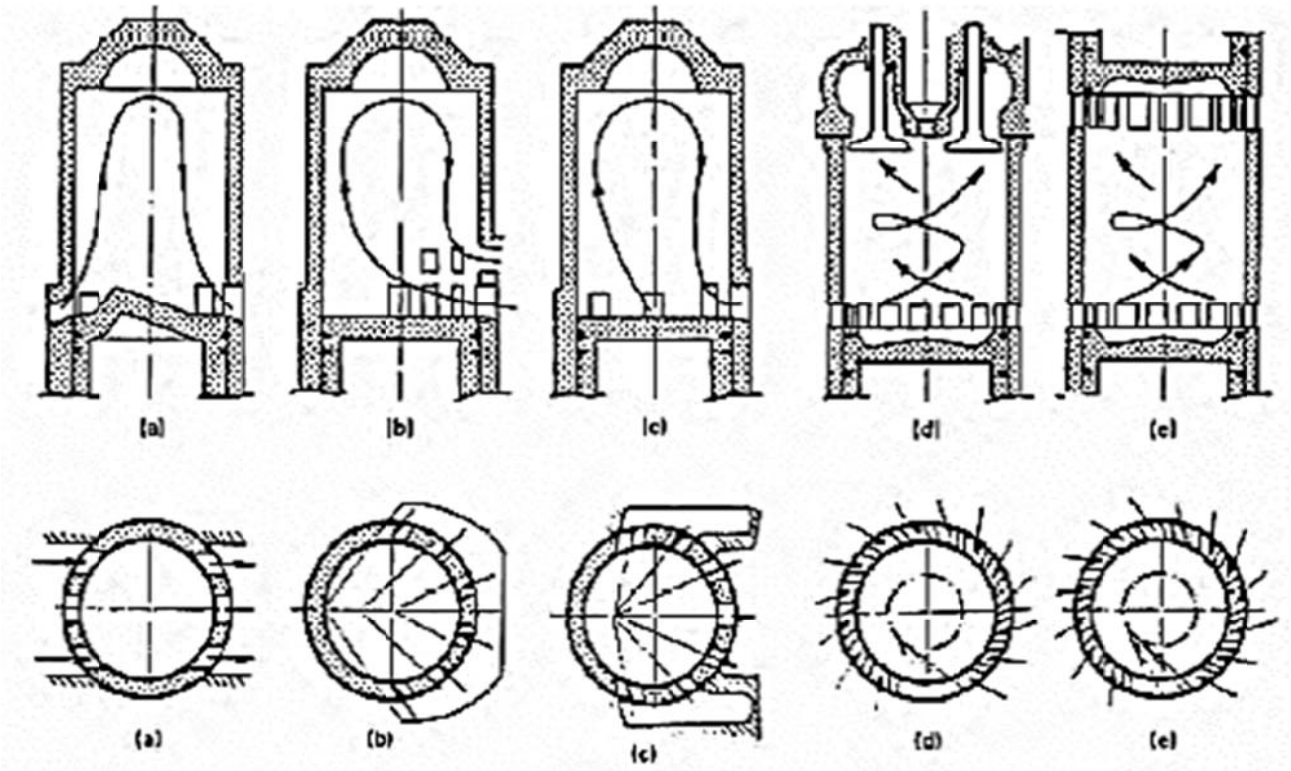

Fig. 2.4. Types of two-stroke engines scavenging:
Ports scavenging: a) cross-flow; b, c) loop;
Uniflow scavenging: d) with exhaust valves; e) opposed piston.

2.1. Kinematics and dynamics setup.

The page “Kinematics and Dynamics” serves to configure engine’s main geometrical properties: cylinder bore, piston stroke, number of cylinders, geometrical compression ratio.

Crank | Opposite pistons | Conrod free | Other — Mechanism of main motion

Parameter	Data	Units	Caption
D_{cyl}	108	mm	Cylinder bore
S_{pist}	127	mm	Piston stroke
i_{cyl}	4	-	Number of cylinders
ε	17	-	Geometrical compression ratio
μF_{leak}		mm^2	Piston&Rings equivalent leakage area
λ_{crank}	0.25	-	Crank ratio *ratio between crank radius and connection rod length*
k_{pist}		-	Relative eccentricity of the crank *ratio between piston pin eccentricity and crank radius*
m_{osc}	5	kg	Total oscilating mass *check the value of the oscilating mass, reffered to the piston surface [low-speed: 2500...6000, medium-speed: 1000...3000, high-speed: 200...700], kg/m²:* **428.7**
m_{rot}	6	kg	Total rotational mass *check the value of the rotatinal mass, reffered to the piston surface [low-speed: 700...12000, medium-speed: 1500...2500, high-speed: 300...1200], kg/m²:* **514.4**

Fig. 2.1.1. General view of kinematics page.

The following types of piston kinematics setup are supported: 1) central and deaxised crank mechanism, 2) opposed-piston central and deaxised crank mechanism, 3) ellipsographical conrod-free mechanism and 4) define the piston kinematics directly, skipping calculations of main motion mechanism kinematics. The radio button set at the top left corner of the page is used to choose the proper type of setup.

By pressing button “Mechanism of main motion”, the User can view the picture with description (see Fig. 2.1.2).

The fallowing equations are used:

$$\lambda_{crank} = \frac{R}{L} - \text{connecting rod (or crank) ratio;}$$

$$k_{pist} = \frac{e}{R} - \text{relative eccentricity of the crank.}$$

For central and deaxised crank mechanism:

$$s(\varphi) = R\left[\sqrt{\left(1-\frac{1}{\lambda_{\text{crank}}}\right)^2 - k_{pist}^2} - \frac{1}{\lambda_{\text{crank}}}\sqrt{1-\lambda_{\text{crank}}^2\left(\sin\varphi - k_{pist}\right)^2} - \cos\varphi\right];$$

$$V(\varphi) = \frac{\pi D_{cyl}^2}{4}\frac{S_{pist}}{\varepsilon - 1} + \frac{\pi D_{cyl}^2}{4}s(\varphi),$$

where s – piston travel; V – cylinder volume.

Please note! The User setups the piston stroke S_{pist}, so the crank radius R is calculated by the program to provide this value of the piston stroke. In the case of central crank mechanism $R = S_{pist}/2$, but it is different for deaxised mechanism. The calculated crank radius is displayed on the “Report” page.

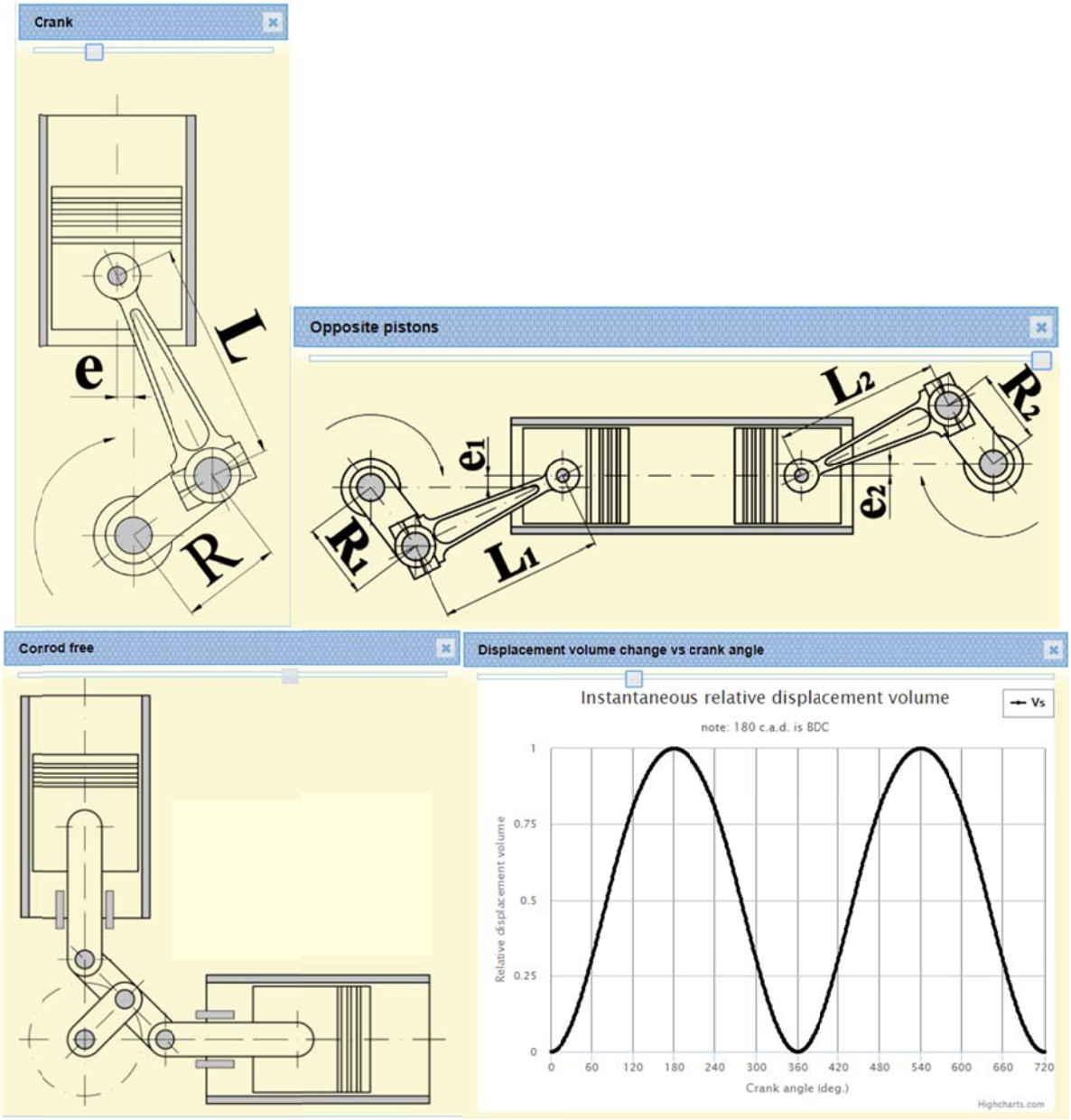

Fig. 2.1.2. Types of main motion mechanism kinematics setup.

For the conrod-free ellipsographical mechanism the sinus piston motion law is utilized:

$$s(\varphi) = R(1 - \cos\varphi).$$

The User can also upload custom piston motion law choosing the option “Other” and attaching the .csv file (see the instruction in section 1.5).

Dynamics calculation setup considers only two parameters: oscillating mass m_{osc} and rotating mass m_{rot}. These parameters are used for the inertial forces calculations. The oscillating masses include the mass of the piston, gudgeon pin, piston rings and connecting rod oscillating mass (generally 33 % of the conrod total mass):

$$m_{osc} = m_{pist} + m_{pin} + m_{rings} + m_{conrod.ocs}.$$

The rotational masses include the unbalanced rotational mass of the crank and rotational mass of the connecting rod (generally 67 % of the conrod total mass):

$$m_{rot} = m_{crank.rot} + m_{conrod.rot}$$

2.2. Heat transfer setup.

The “Heat-transfer” page serves to configure the engine friction losses, heat flow from the intake receiver, exhaust manifold and incylinder fluids to the corresponding boundary walls.

Engine’s friction losses include: friction between the piston rings, piston skirt and cylinder wall; friction in the wrist pin, big end, crankshaft, and camshaft bearings; friction in the valve mechanism; friction in the gears, or pulleys and belts, which drive the camshaft and engine accessories and losses to drive engine accessories (the fan, the water pump, the oil pump, the fuel pump, the generator, etc.).

All the friction losses dissipate as the heat and then are rejected to the cooling agents (air, water or oil).

The pumping work of the gas-exchange strokes of the four-stroke engines and the work of driving the mechanical supercharger are excluded from the friction losses setup and considered separately.

The following equation for friction mean effective pressure is utilized:

$$p_{fr} = a_{fr} + b_{fr} p_z + \frac{c_{fr} n}{1000},$$

where a_{fr}, b_{fr}, c_{fr} – empirical coefficients: a_{fr} – considers the static friction losses and solid friction components; b_{fr} – helps to estimate the impact of incylinder maximum gas pressure on the friction losses value; c_{fr} – is used for correlation of the friction losses with the engine speed.

Approximate values of the coefficients are given in the table 2.2.1.

Table 2.2.1

Friction equation coefficients

Engine type	a_{fr}	b_{fr}	c_{fr}
	kPa	kPa/MPa	kPa/rpm
Low-speed CI and dual-fuel	18…50	3…5	15…40
Medium-speed CI and dual-fuel	40…90	4…7	30…55
High-speed CI	45…95	4…8	30…60
High-speed SI	35…75	4…8	20…50

The ***incylinder*** heat transfer calculation is based on 1-D quasy-steady simplified approach. Newton's law of cooling is used for calculations of instantaneous heat flow dQ_{wall} to the wall:

$$dQ_{wall} = \alpha_{gas} F (T - T_{wall}) d\tau,$$

where α_{gas} – heat transfer coefficient from incylinder gases to the cylinder wall, F – wall surface area, T_{wall} – the wall surface temperature.

For heat transfer coefficient calculation the Woschni equation is used [2]:

$$\alpha_{\text{gas}} = A \frac{(10p)^{0,8}}{T^{0,53} D_{cyl}^{\ 0,2}} \left[C_1 c_m + C_2 \frac{(p - p_{mot}) V_s T}{1000 p V} \right]^{0,8},$$

where A, C_1, C_2 – coefficients, p_{mot} – incylinder pressure at motored running condition.

Coefficient A is in the range of 90…128, tending to decrease with the lower engine speed. Coefficients C_1 and C_2:

$C_1 = 6.18 + 0.417 c_\tau / c_m$ – for gas exchange processes;

$C_1 = 2.28 + 0.308 c_\tau / c_m$ – for compression and combustion processes;

$C_2 = 6{,}22\ \mathrm{K}^{-1}$ – for indirect combustion systems (swirl chamber, pre-chamber);

$C_2 = 3{,}24\ \mathrm{K}^{-1}$ – for quiescent combustion chamber,

where c_τ – the tangential velocity of the incylinder vortex (could be assumed $c_\tau \approx 0$ for four-stroke engines without vortex generators at the intake), c_m – mean piston speed.

Table 2.2.2

Values of coefficient A of Woschni equation

Engine type	A
Low-speed CI and dual-fuel	60…100
Medium-speed CI and dual-fuel	90…130
High-speed CI	100…140
High-speed SI	120…220

The average wall surface temperature $T_{wall.m}$ for cylinder head, piston head and manifolds is calculated on the assumption of quasy-steady heat-transfer process. The value of $T_{wall.m}$ is assumed constant for the entire operating cycle (the oscillations in the range of 5…40 ºC are neglected), while the heat transfer coefficient from gases to wall and the temperature of the gases are assumed as resulting values. The following equation is used:

$$T_{wall.m} = T_{gas.res} - \frac{k_m \left(T_{gas.res} - T_w \right)}{\alpha_{gas.m}}.$$

The resulting heat transfer coefficient for gases $\alpha_{gas.m}$ and resulting gas temperature $T_{gas.res}$ are calculated for the entire operating cycle as:

$$T_{gas.res} = \frac{1}{720\,\alpha_{gas.m}} \int_0^{720} \alpha_{gas} T \mathrm{d}\varphi,\ \alpha_{gas.m} = \frac{1}{720} \int_0^{720} \alpha_{gas} \mathrm{d}\varphi,$$

and the mean heat transfer coefficient from the gas and cooling fluid k_m is assumed on the basics of steady heat-transfer equations:

$$\begin{cases} q_m = k_m \left(T_{gas.res} - T_w \right); \\ q_m = \alpha_{gas.m} \left(T_{gas.res} - T_{wall.m} \right); \end{cases} k_m = \frac{1}{\dfrac{1}{\alpha_{gas.res}} + \dfrac{\delta_{wall}}{\lambda_{wall}} + R_{wall} + \dfrac{1}{\alpha_w}},$$

where q_m – specific heat flow; α_w – resulting heat transfer coefficients from cooling surface to cooling fluid respectively; T_w – resulting cooling fluid temperature; δ_{wall} – wall thickness; R_{wall} – wall thermal resistance.

For the cylinder liner the wall's temperature gradient is considered. The simplified approach includes cutting the liner to a number of slices ($N > 20$) and calculation of the mean hot wall temperature for each slice separately with the same quasy-steady method, described earlier:

$$\alpha_{gas.mi} = \frac{\int_{\varphi_o}^{360-\varphi_o} \alpha_{gas} d\varphi + \int_{\varphi_o+360}^{720-\varphi_o} \alpha_{gas} d\varphi}{720}; \quad T_{gas.res} = \frac{\int_{\varphi_o}^{360-\varphi_o} \alpha_{gas} T d\varphi + \int_{\varphi_o+360}^{720-\varphi_o} \alpha_{gas} T d\varphi}{720\alpha_{gas.mi}},$$

where α_{gas} – heat transfer coefficient from incylinder gases, φ_o – crank angle of the current cylinder slice opening.

The example of the calculated cylinder liner hot surface temperature is shown on the fig 2.2.1. This diagram is available from the "Report" page.

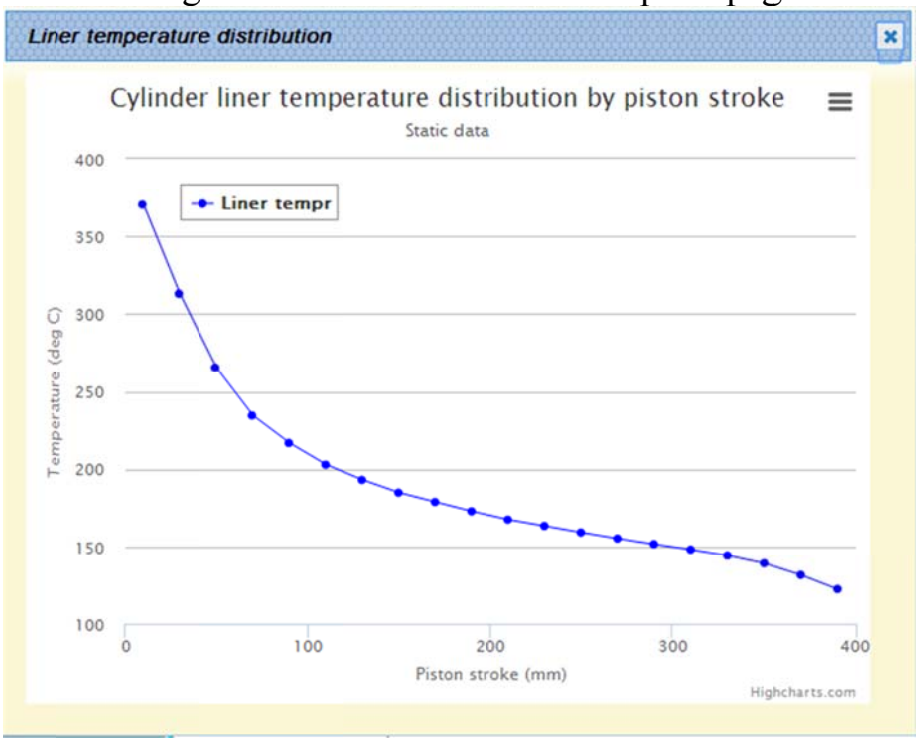

Fig 2.2.1. Temperature distribution on the cylinder liner hot surface.

To provide the calculations the average wall thickness for the piston, cylinder head and liner together with heat conductivity coefficients of their materials must be stated (see Fig. 2.2.2 – these pictures could be displayed by clicking the "Heat transfer to the cylinder walls" button).

To consider possible soot or deposits coating on the hot or cooling side of the corresponding wall, the User can choose the value for additional thermal resistance R (as an example: 0.25 mm soot layer provides $R \approx 4$ m^2·K/kW).

For air receiver the walls temperature is predicted with fallowing equations:

$T_{wall.\text{int}} = T_s + a_{\text{int}} T_s + b_{\text{int}}$ for conventional receiver, and

$T_{wall.\text{int}} = T_s + a_{\text{int}} T_t + b_{\text{int}}$ for receiver with heating from exhaust manifold,

where a_{int}, b_{int} – coefficients, T_s, T_t – average fresh charge and exhaust gases temperature correspondently.

The heat transfer coefficient from the fresh charge to the receiver walls is given by the equation:

$$\alpha_{\text{int}.res} = 47260 \cdot C_{\text{int}} \left(\frac{p_s}{100} \right)^{0.67} T_s^{-0.919},$$

where $C_{int} = 0.2 \ldots 1.2$ – correction coefficient.

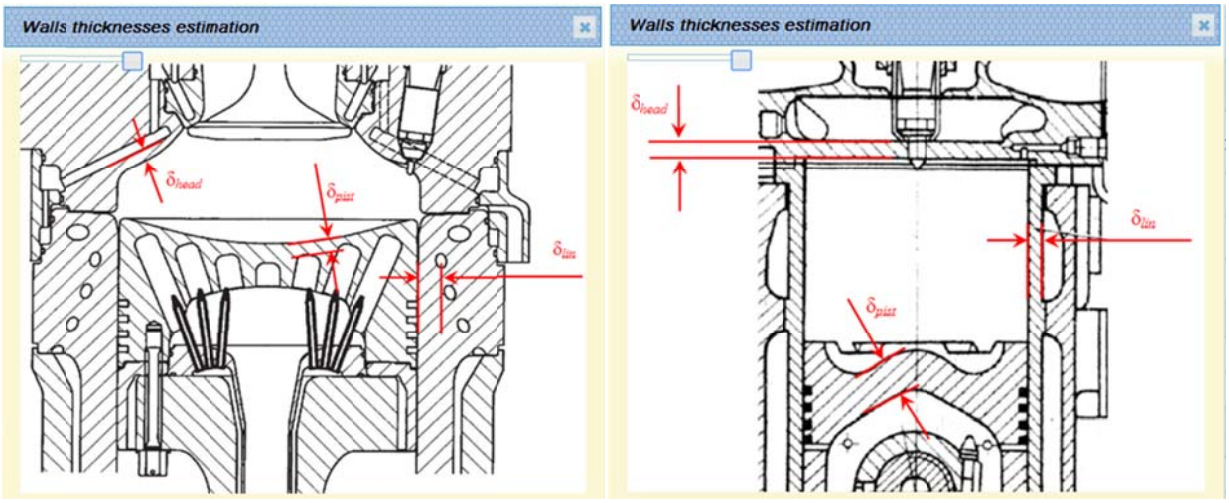

a) b)

Fig. 2.2.2. Examples of average walls thicknesses estimation for two-stroke (*a*) and four-stroke (*b*) engines.

For exhaust manifold heat transfer calculations two options of manifold design are supported: manifold without or with solid insulation and the manifold with water jacket insulation (see Fig. 2.2.3).

The heat transfer coefficient from the exhaust gases to the exhaust manifold walls is given by the equation:

$$\alpha_{exh} = 0.188 \cdot C_{exh} \frac{\lambda_{EG}}{d_{exh.eq}} \mathrm{Re}^{0.67},$$

where C_{exh} = 0.2…1.2 – correction coefficient, λ_{EG} – heat conductivity coefficient for exhaust gases, $d_{exh.eqv}$ – equivalent exhaust manifold diameter, $\mathrm{Re} = d_{exh.eqv} \cdot w_{exh} / \nu_{EG}$ – Reynolds number for exhaust gases flow.

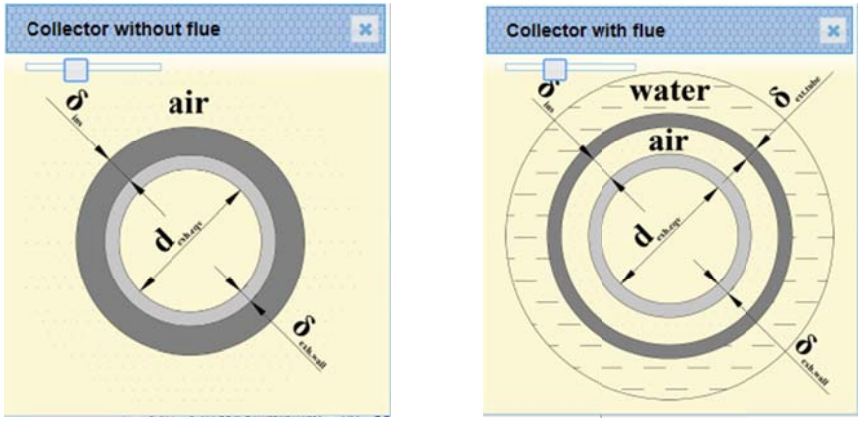

Fig. 2.2.3. Exhaust manifold cooling options:
with solid insulation (left) and with air insulation and water jacket (right)

Note that heat transfer coefficient is proportional to $\mathrm{Re}^{0.67}$, so with the rise of the exhaust gases speed the heat transfer to exhaust manifold wall intensifies. To keep it in the limits change manifold equivalent diameter.

In the case of the exhaust manifold with water jacket, the heat transfer coefficient from the air layer to the walls is taken proportional to the α_{exh}:

$$\alpha_{air} = C_{g/a} \alpha_{exh},$$

where $C_{g/a}$ = 0.2…1.2 – correction coefficient.

The exhaust manifold average wall temperature is calculated identically as the temperatures of the incylinder surfaces, so the wall thicknesses, heat conductivities and additional thermal resistance due to deposites must be given by the User.

For the cooling side of engine's parts the approximate values of heat transfer coefficients are given in table 2.2.3.

Table 2.2.3

Values of heat transfer coefficients for the cooling agents

Type of cooling agent	Cooling method	α_w, kW/(m^2·K)
Water	Free convection	0.4…2.0
	Forced convection	1.0…4.0
	Nucleate boiling	2.0…10.0
Antifreeze (water/ethylene glycol 50/50)	Free convection	0.3…1.5
	Forced convection	0.75…3.0
	Nucleate boiling	1.5…7.5
Oil	Spray cooling	0.2…2.0
	Circulation cooling	0.8…2.0
	Shake cooling	1.5…3.5
Air	Free convection	0.03…0.1
	Forced convection	0.05…0.5

2.3. Gas exchange devices (valves and ports setup).

The page “Valves and ports areas” serves to configure the gas exchange devices effective flow areas change with the crank angle progress.

Two types of gas exchange devices are supported for the two-stroke engines: ***valves*** and ***ports***. For four-stroke engines ***valves*** are the only option.

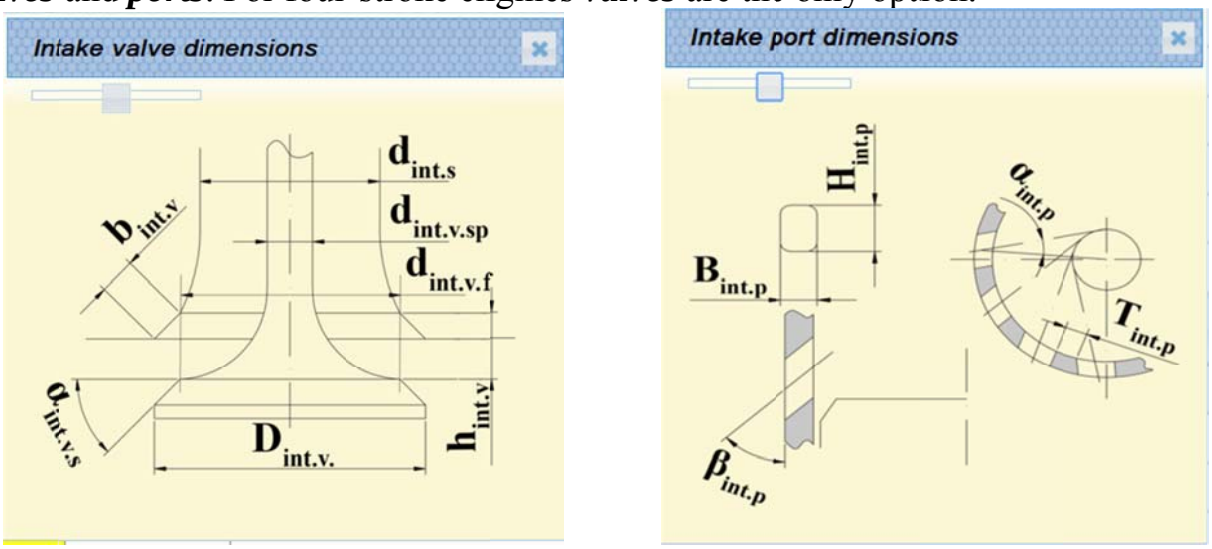

a) b)

Fig. 2.3.1. Gas-exchange devices options:
a) valve; b) ports.

Effective flow area A could is defined as a product of geometrical flow area A_{geom} and the discharge coefficient μ_v: $A = \mu_v A_{geom}$.

For valves the geometrical flow area could be calculated via two different equations, depending on the value of the instantaneous valve lift $h_v(\varphi)$:

if $h_v(\varphi) < b_v/\sin\alpha_{v.s}$:

$$A_{geom}(\varphi) = \pi h_v(\varphi)\cos\alpha_{v.s}\left(d_{v.f} + 0.5h_v(\varphi)\sin(2\alpha_{v.s})\right),$$

if $h_v(\varphi) > b_v/\sin\alpha_{v.s}$:

$$A_{geom}(\varphi) = 0.5\pi(d_s + D_v)\sqrt{\frac{(D_v - d_{v.f})^2}{4} + \left(h_v(\varphi) - 0.5(D_v - d_{v.f})\tan\alpha_{v.s}\right)^2}.$$

For discharge coefficient the regression is applied:

$$\mu_v(\varphi) = 0.96 - a_\mu \frac{h_v(\varphi) - b_v/\sin\alpha_v}{d_{v.f}},$$

where a_μ is the coefficient which is calculated from the equation:

$$a_\mu = \frac{(0.96 - \mu_{v.\min})d_{v.f}}{h_{v.\max} - b_v/\sin\alpha_v},$$

where $\mu_{v.\min}$ – minimal value of the discharge coefficient (at the valve maximum lift).

The recommended value for $\mu_{v.\min}$ is calculated for the User at the caption field (see Fig. 2.3.2). The calculations are based on experimental data (see Fig. 2.3.3).

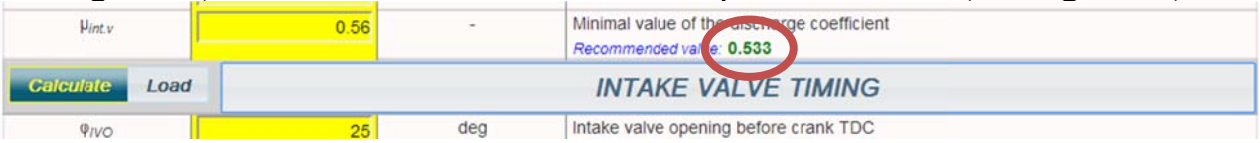

Fig. 2.3.2. Recommended value for minimal discharge coefficient.

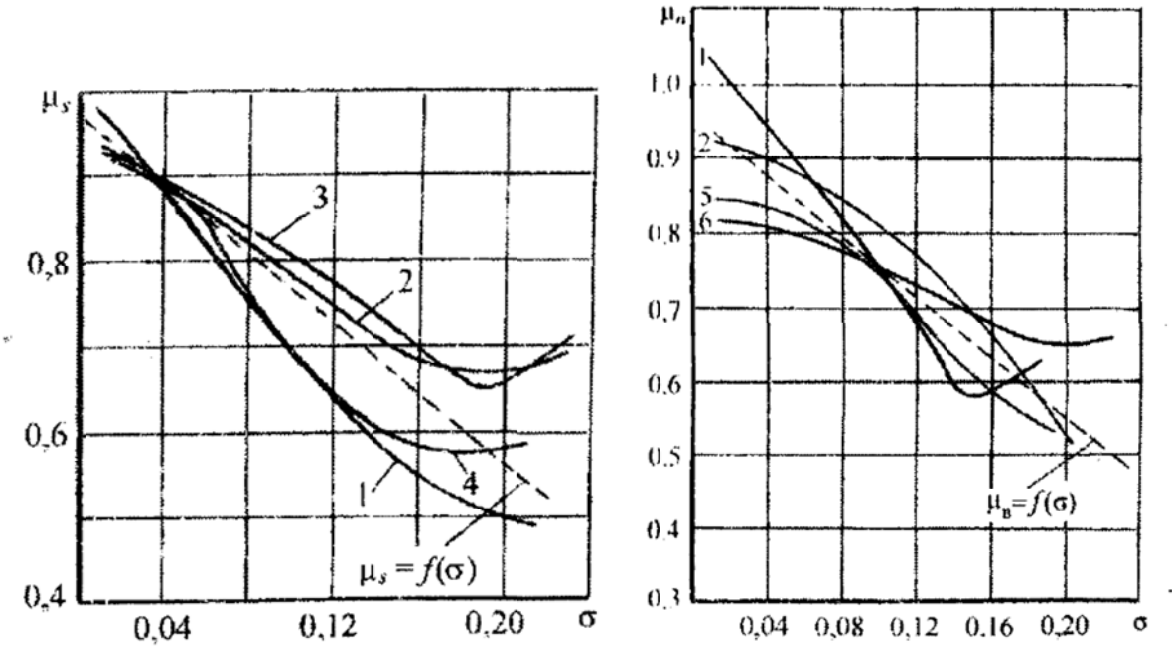

a b

Fig. 2.3.3. Discharge coefficients in relation with valve relative lift $\sigma = (h_v - b_v/\sin\alpha_{v.s})/d_s$ [3]: a) – intake valves, b) – exhaust valves.

If calculated value of effective flow area $A(\varphi)$ is smaller than the effective area of the valve pipe A_{pipe}, then it should be equaled to this area:

$$A_{pipe} = 0.95\pi\frac{\left(d_s^2 - d_{v.sp}^2\right)}{4},$$

$$\text{if } A(\varphi) = \mu_v(\varphi)A_{geom}(\varphi) > A_{pipe}, \text{ then } A(\varphi) = A_{pipe}.$$

Notice that predicted reasonable value of the valve lift (Fig. 2.3.4.) is calculated from equality $A(\varphi) = A_{pipe}$, but actual valve lift could be chosen 10% greater, than predicted.

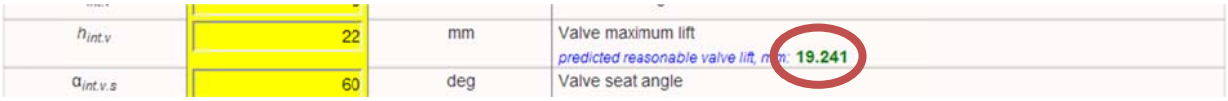

Fig. 2.3.4. Assistance for reasonable valve lift.

To synthesize the valve opening and closing law the following functions are used:

$$\text{valve opening: } h_v(\varphi) = 0.5h_v\left(1 - \cos\left(\frac{\pi(\varphi - \varphi_{VO})}{\varphi_{v.o.t}}\right)\right);$$

$$\text{valve closing: } h_v(\varphi) = 0.5h_v\left(1 + \cos\left(\frac{\pi(\varphi - (\varphi_{VC} - \varphi_{v.c.t}))}{\varphi_{v.c.t}}\right)\right),$$

where φ_{VO} and φ_{VC} – moments of valve opening and closing respectively, $\varphi_{v.o.t}$ and $\varphi_{v.o.t}$ – the period of valve opening and closing respectively.

User also can upload custom ***relative*** valve lift law choosing the option "Load" and attaching corresponding .csv file (see the instruction of preparing .csv files, section 1.5).

Valve timing is to be set with four parameters for both exhaust and intake valves as it is explained on Fig. 2.3.5.

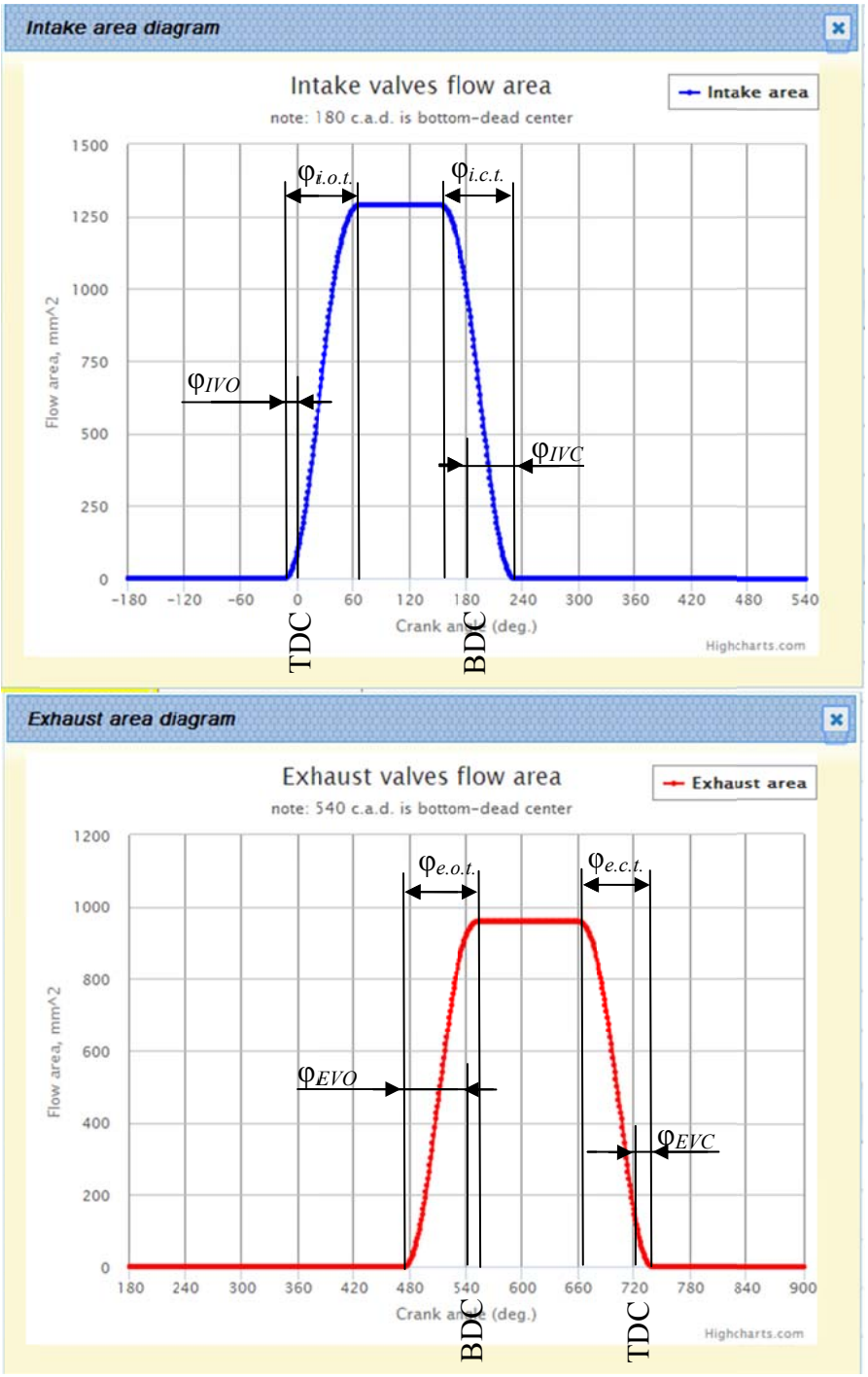

Fig. 2.3.5. Intake and exhaust valves timing explain
for the four-stroke engine example

The ports area $A(\varphi)$ calculation is supported for rectangular-shaped ports only. The change in ports flow area is caused by the piston motion and the ports position in liner.

The complete geometrical ports area A_{port} is calculated by equation:

$$A_{ports} = H_p \sin\beta_p B_p \cos\alpha_p N_p .$$

The effective instantaneous flow area is calculated by:

$$A(\varphi) = \mu_p A_{ports} H_{p.op}(\varphi)/H_p,$$

where $H_{p.op}(\varphi)$ – the opened port height at the moment φ, which is calculated from the piston cinematics, μ_p – ports discharge coefficient (supposed constant).

To choose correctly the number of the ports, please notice the predicted value of the distance between ports T_p (supposed even, see Fig. 2.3.1 and 2.3.6): its value must be positive.

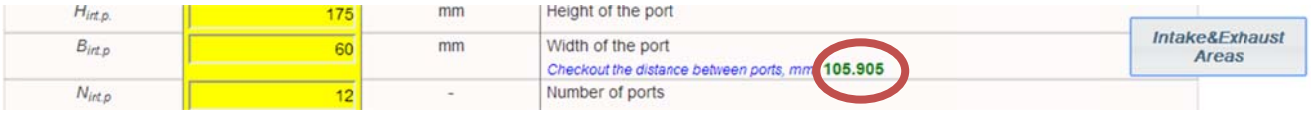

Fig. 2.3.6. Prediction of the distance between ports.

As it is known, ports timing is totally controlled by piston movement. The User should only point the piston position at the moment when the ports starts to open (φ_{IPO} for intake and φ_{EPO} for exhaust).

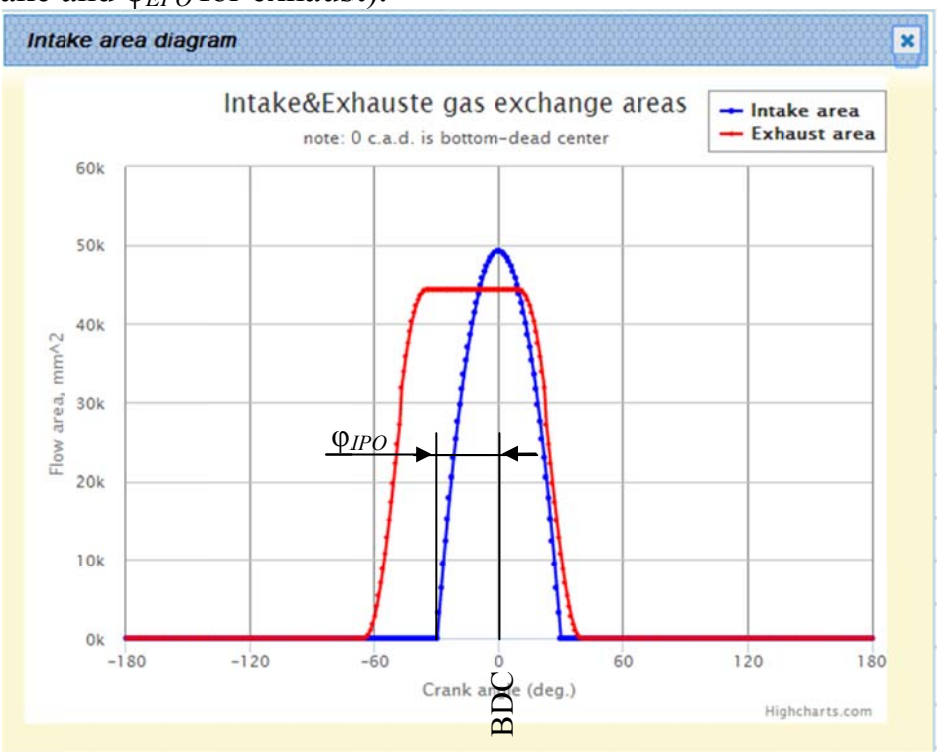

Fig. 2.3.7. Intake ports and exhaust valve timing setup for the two-stroke uniflow scavenged engine example.

The custom flow area law for ports could be uploaded choosing the option “Load” and attaching corresponding .csv file (see the instruction of preparing .csv files, section 1.5).

2.4. Fuel properties and combustion setup.

Blitz-PRO currently supports the combustion process simulation for spark-ignition, compression-ignition and dual-fuel engines. The last one means that ignition of the main gaseous fuel is provided by injection of some amount of ignition fuel in liquid state, ignited by compression.

For spark-ignition engines the Wiebe combustion model is applied, while for compression-ignition engines there is an option to choose between Wiebe combustion model and advanced Razlejtzev model. For dual-fuel engines the combination of these two models is used: Razlejtzev model for ignition fuel combustion and Wiebe model for main fuel combustion.

All three cases support the two-zone simulation routine – the calculation of thermodynamic parameters for fresh charge and burned gases zones separately. The main reason is to provide sophisticated prediction of toxic emissions, CO and NO_x particularly.

Fuel properties setup.

Fuels properties are divided by three groups: chemical properties (activation energy, octane and cetane number and calorific value), mass composition of the fuel and physical properties (density, temperature, viscosity, surface tension and molar mass).

It is important, that the sum of mass shares of chemical elements of the fuel must give 100%, i.e.:

$$g_C + g_H + g_S + g_O = 1.$$

Although the User can setup all fuel properties manually, it is necessary to choose the correct fuel type of fuel from the select list, as it is shown on Fig. 2.4.1. Selection of the fuel type triggers the correct correlations for fuel vapor specific heat and enthalpy of vaporization. Also, selection of the fuel type provides predefined fuel properties for this fuel type (the User can change these properties for the current Project).

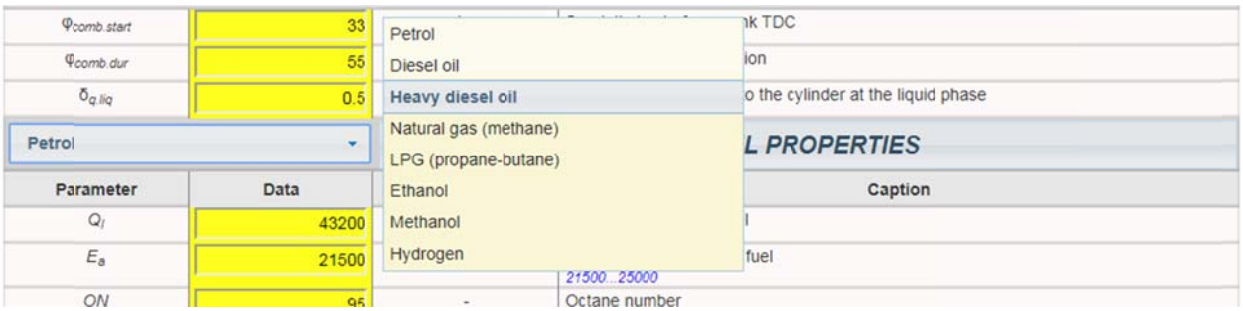

Fig. 2.4.1. Selection of the fuel type.

Spark-ignition engine combustion setup.

For spark-ignition engines the combustion of homogeneous fuel-to-air mixture is currently supported, that means that fuel is fully evaporated before combustion and premixed well with the air.

However, it is available to set-up the share of the fuel $\delta_{q.liq}$, trapped into cylinder in liquid state. The $\delta_{q.liq}$ is defined as the ratio between the mass flow of fuel, inducted into the cylinder in liquid state to the total mass flow of inducted fuel:

$$\delta_{q.liq} = \frac{dm_{liq.fuel}}{dm_{fuel}}.$$

The evaporation of the trapped liquid fuel starts after it comes into the cylinder during intake and compression. Such an approach helps to provide more accurate calculations for gas-exchange processes as well as to take into account heat absorption from working medium due to fuel evaporation at the compression period. But, as it is mentioned, all fuel is supposed to be evaporated before the spark will initiate the combustion. The calculations of the fuel evaporation are similar to the calculations of injected fuel evaporation for compression-ignition engine, expressed below.

The well-known Wiebe combustion model is very simple, and is described by following equation:

$$\frac{dx}{d\varphi} = -\ln(1-x_z)\frac{m+1}{\varphi_{comb.dur}}\left(\frac{\varphi-\varphi_{comb.start}}{\varphi_{comb.dur}}\right)^m \exp^{\ln(1-x_z)\left(\frac{\varphi-\varphi_{comb.start}}{\varphi_{comb.dur}}\right)^{m+1}},$$

where $dx/d\varphi$ indicates the relative rate of fuel combustion.

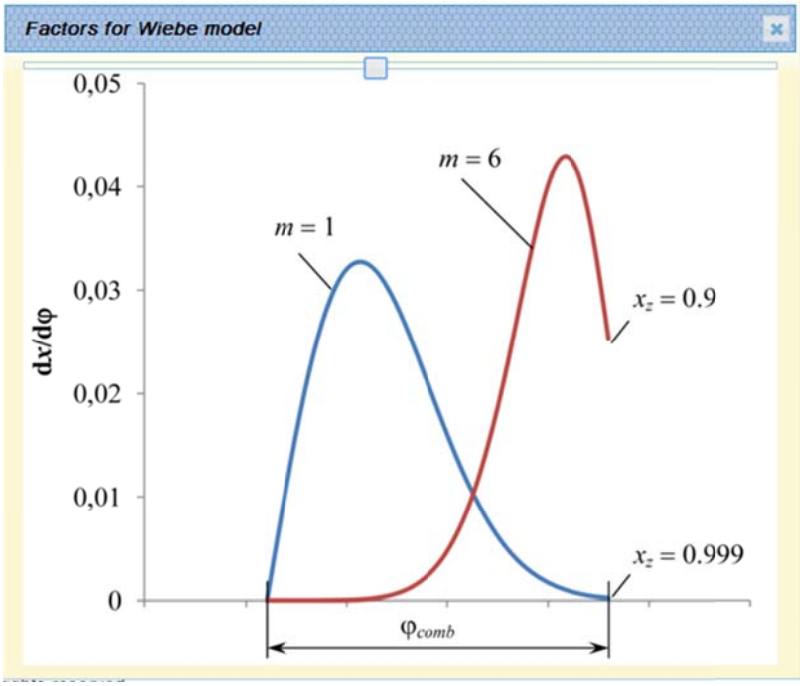

Fig. 2.4.2. Influence of x_z and m factors on the shape of fuel burning rate diagrams given by Wiebe equation.

It is obvious, that combustion law is totally defined if the User sets four values: combustion start moment $\varphi_{comb.start}$, duration of combustion $\varphi_{comb.dur}$, total burned fraction of fuel x_z, modifying factor m. The influence of the last two parameters is illustrated by Fig. 2.4.2. The typical value of m for spark-ignition engines lies in the range of 3…6, while x_z equals 0.95..0.999 and $\varphi_{comb.dur}$ = 30…90 c.a.d.

Drawbacks of the Wiebe combustion model are also well known: the User should know the duration and the shape of combustion curve. It is quite unacceptable for many cases when changing the engine setup the User should consider the effects

of these changes on the combustion process. For three main factors: air excess ratio α, crankshaft speed n and the density of fresh charge after the throttle plate ρ_s the following equations could be suggested:

$$\varphi_{comb.dur} = \varphi_{comb.dur}^{rated}\left(\frac{\alpha^{rated}}{\alpha}\right)^{0.6}\left(\frac{n}{n^{rated}}\right)^{0.5}; m = m^{rated}\left(\frac{\varphi_{comb.dur}^{rated}}{\varphi_{comb.dur}}\right)^{0.6}\left(\frac{n^{rated}}{n}\right)^{0.8}\left(\frac{\rho_s^{rated}}{\rho_s}\right),$$

where index "rated" indicates the conditions of engine operation at rated power and rated speed.

Compression-ignition engine combustion setup.

For compression-ignition engines, as it is known, the combustion process depends greatly on the peculiarities of the preliminary processes – the fuel injection and fuel evaporation. Blitz-PRO currently supports single, double and triple fuel injection (Fig. 2.4.3.). Duration of each fuel injection and its timing should be stated directly.

Single | Double | Triple — FUEL INJECTION TIMING

Parameter	Data	Units	Caption
Use control maps to set fuel injection dynamically (see "General settings" @ Transient datasheet)			
$\varphi_{start.inj}$	25	deg	First-stage injection timing (CAD before crank TDC)
$\varphi_{start.inj2}$	10	deg	Second-stage injection timing (CAD before crank TDC)
φ_{inj}	3.5	deg	Duration of the first-stage (single) injection
φ_{inj2}	23.5	deg	Duration of the second-stage injection
δq_{c1}	5	%	The relative amount of the first-stage injection

Fig. 2.4.3. Selection of the fuel injection type (single, double or triple injection) and setup the fuel injection timing.

Shares of each stage of injection are given by δq_{c1} and δq_{c2}:

$$\delta q_{c1} = \frac{q_{fuel1}}{q_{fuel}};\ \delta q_{c2} = \frac{q_{fuel2}}{q_{fuel}},$$

where q_{fuel1}, q_{fuel2} – the fuel mass, injected into the cylinder at the first and at the second stage correspondently, q_{fuel} – the total mass of fuel, injected into the cylinder at all injection stages together.

The shape of the fuel injection curve could be given in to ways: first – using the equations for approximate injection diagrams shaping, second – by loading the .csv file with the diagram for relative fuel injection rate.

The equations used for fuel injection curves generation are proposed by Razlejtsev [4]. The sum of two functions with ability of flexible setup gives the desired shape of injection rate curve:

$$\frac{d\sigma}{d\bar{\varphi}} = \left(\frac{d\sigma}{d\bar{\varphi}}\right)_1 + \left(\frac{d\sigma}{d\bar{\varphi}}\right)_2;$$

$$\frac{d\sigma}{d\bar{\varphi}} = \left[a\cdot\left(\bar{\varphi}^{m_1-1} - b\cdot\bar{\varphi}^{m_2-1}\right)\right]_0^{\bar{\varphi}=\Phi_{inj1}} + c\cdot\left(\bar{\varphi}^{m_3-1} - \bar{\varphi}^{m_4-1}\right),$$

where $\bar{\varphi} = \varphi/\varphi_{inj}$ – the relative injection angle, Φ_{inj1} – the relative angle for the first function, a, b, c, m_1, m_2, m_3, m_4 – adjustable factors.

Example of different fuel injection diagrams, generated with these equations are given on Fig. 2.4.4. The area under the line of fuel injection rate dσ/dφ gives the

relative fuel injection mass. For multiple injection all stages of injection are to be generated with the same set of adjustable factors (see Fig. 2.4.5.).

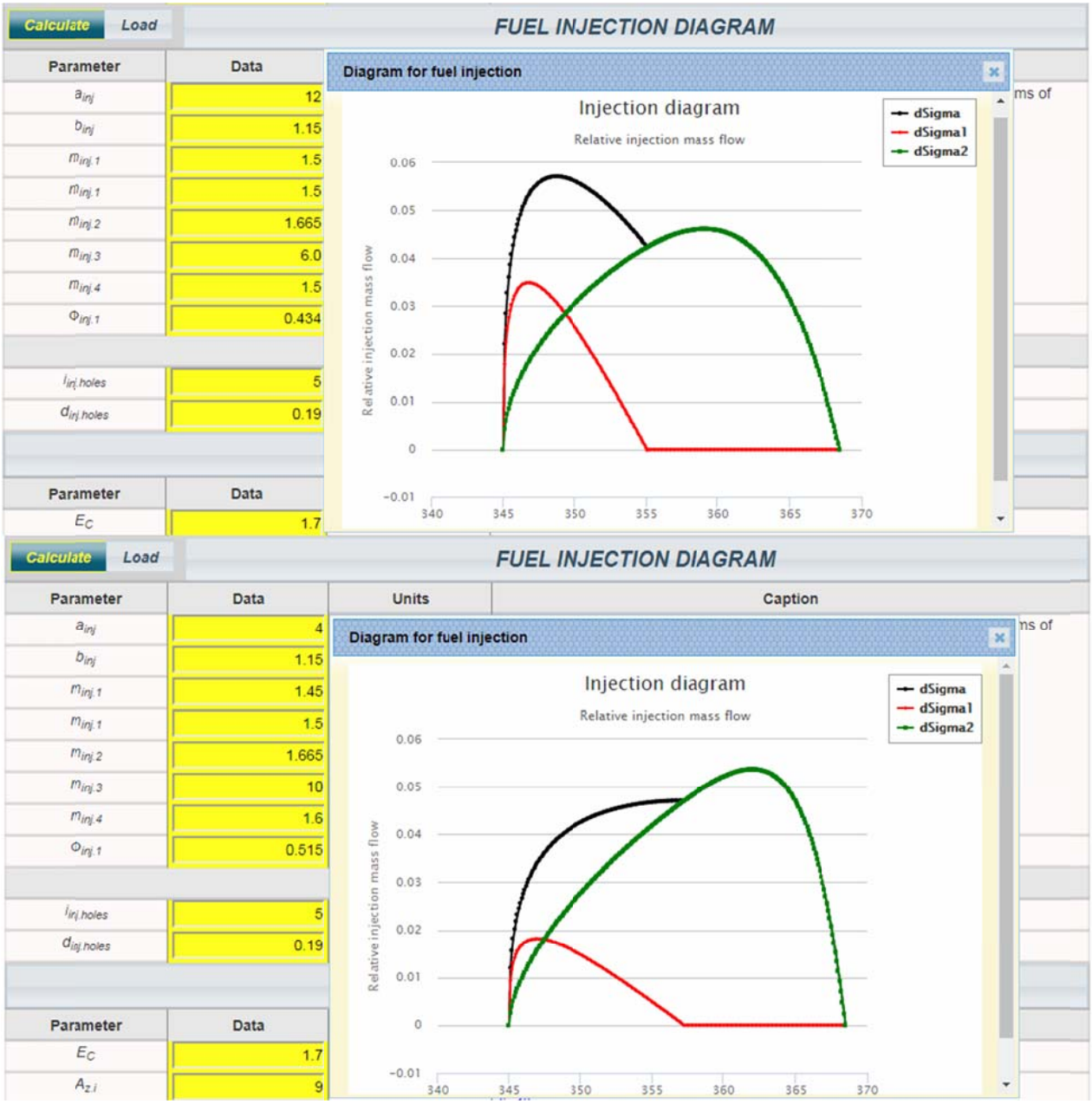

Fig. 2.4.4. Fuel injection diagrams for different sets of adjustable factors in the Razlejtzev approximating equations. Black line indicates the total fuel injection rate $d\sigma/d\varphi$, red and green – first $d\sigma/d\varphi_1$ and second $d\sigma/d\varphi_2$ functions respectively.

Fuel evaporation

Before to be involved into combustion process the liquid fuel must be vaporized. The fuel evaporation model is based on Sreznevskiy law according to equations, suggested by Razlejtzev for fuel evaporation rate [4]:

$$\frac{d\sigma_{ev}}{d\varphi} = \int_{\varphi_{inj.start}}^{\varphi} \frac{3}{2}\chi b_{ev}\left(1-\chi b_{ev}\frac{\varphi-\varphi_{inj.start}}{6n}\right)^{0.5}\frac{d\sigma}{d\varphi}d\varphi,$$

where σ – relative share of injected fuel; σ_{ev} – relative share of evaporated fuel; b_{ev} – evaporation constant; χ – the relative reduction of the fuel evaporation rate due to interaction of sprays with combustion chamber walls.

This integral shows the total evaporation of all fuel drops injected before the current moment during the time referred to current dφ.

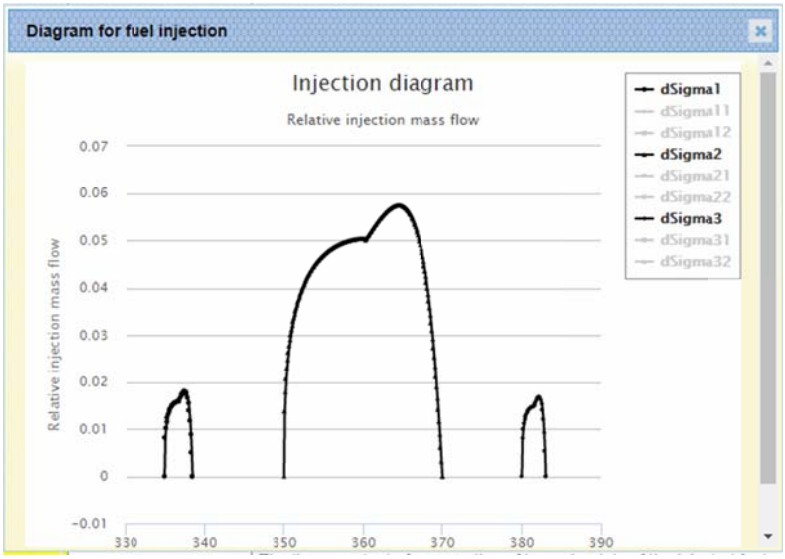

Fig. 2.4.5. Triple fuel injection diagrams example.

The evaporation constant is the adjustable parameter, which allows control of the fuel evaporation speed:

$$b_{ev} = \frac{10^{12}}{d_{32}^2}\frac{1}{p_c}\left(\frac{n}{1000}\right)^{m_Y},$$

where d_{32} – average droplet size by Sauter (the ratio of total volume of fuel drops to their total surface), p_c – incylinder pressure at the injection start, m_Y – the exponent number for the evaporation speed multiplier.

The user can alter the evaporation speed by changing m_Y. Normally m_Y is in the range of 0.65…1.0, but if the engine speed is lower than 1000 rpm the value of m_Y could be selected from the diapason of 0.45…0.8.

Another important factor – droplet size d_{32} is calculated from equation (according to Lyshevskiy [5]):

$$d_{32} = 10^6 E_c d_{inj.holes}\frac{M^{0.0733}}{\left(\bar{\rho}We\right)^{0.266}};$$

$$M = \frac{\mu_{fuel}^2}{d_{inj.holes}\rho_{fuel}\sigma_{fuel}};\ \bar{\rho} = \frac{\rho_c}{\rho_{fuel}};\ We = \frac{u_{inj}^2 d_{inj.holes}\rho_{fuel}}{\sigma_{fuel}},$$

where μ_{fuel}, ρ_{fuel}, σ_{fuel} – dynamic viscosity, density and surface tension of the fuel, E_c – coefficient (equals 1.7 for normal fuel injectors), $d_{inj.holes}$ – diameter of the fuel injector nozzle.

The relative reduction of the fuel evaporation rate due to interaction of sprays with combustion chamber walls is calculated by equation:

$$\chi = 1 - \left(\frac{1-\chi_0}{0.485}\right)\cdot 0.707\left(\frac{\varphi-\varphi_{wall}}{\varphi_{fr}}\right)\cdot\frac{2}{\sqrt{\pi}}e^{-0.5\left(\frac{\varphi-\varphi_{wall}}{\varphi_{fr}}\right)^2};$$

$$\varphi_{fr} = A_{st}\cdot 2\varphi_{wall}\frac{\bar{\rho}^{-0.5}We^{0.32}}{M^{0.07}},$$

where φ_{wall} – the moment of the time, when the fuel spray reaches the wall of combustion chamber, χ_0 – the minimal value of relative fuel evaporation rate reduction (is

set by the User), φ_{fr} – duration of interaction between the fuel spray and cylinder walls; A_{st} - coefficient in the cone angle of the fuel spray.

Note that it is very important to set properly the distance of the fuel spray free flight L_{wall} (roughly: the distance from the injector nozzle to the cylinder walls), which is involved into equations of φ_{wall} calculation.

Thus the User can change the fuel evaporation behavior by altering the fuel injection law, adjusting the constant of fuel evaporation speed (via m_Y), changing the injector's nozzle geometry and the setup for estimation of fuel evaporation rate drop due to interaction between fuel sprays and cylinder walls.

Choosing the injector's nozzle geometry

The injection nozzle geometry is to be set with only two parameters: number of injection holes $i_{inj.holes}$, and the diameter of the injection hole $d_{inj.holes}$. If the engine has more than one fuel injector per the cylinder, $i_{inj.holes}$ means the total number of injection holes of all injectors.

The values of $i_{inj.holes}$ and $d_{inj.holes}$ have a great influence on the injection process, particularly on the injection pressure, injection spray penetration and geometry, fuel atomization (expressed by the Sauter average diameter d_{32}).

If the information of the actual fuel injector nozzle is absent, the User can use the prediction of average fuel injection pressure and Sauter average diameter as it is shown on Fig. 2.4.6. In this case the adjustment of injector's nozzle geometry is to be made together with the fuel injection duration φ_{inj}.

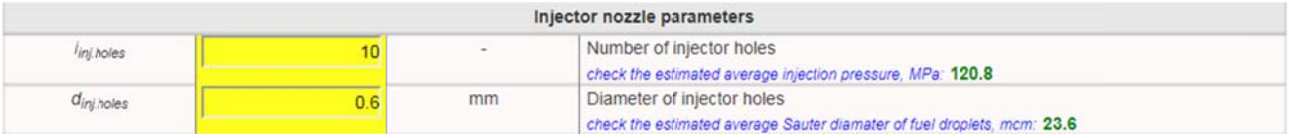

Fig. 2.4.6. The injector's nozzle geometry setup and injection paremeters estimation.

The accuracy of the p_{inj} and d_{32} prediction depends on the mode of the calculation: the best accuracy gives the direct setup of the injected fuel mass q_f (calculation mode "Fuel mass per cycle"), if the User chooses the calculation by setting the air excess ratio (calculation mode "Air excess ratio"), it is assumed for prediction, that engines volumetric efficiency is $\eta_v \approx 80$ %, and if calculation mode is "Brake power" the calculations are made for brake specific fuel consumption $b_e = 210$ g/(kW·h). At any calculation mode the predicted values of p_{inj} and d_{32} will differ from the values from the "Report" page.

The average injection pressure is calculated from the equations:

$$p_{inj} = \rho_{fuel} \frac{u_{inj}^2}{2} + p_{cyl}\ ;\ u_{inj} = \frac{q_f}{\rho_{fuel} \mu f_{nozzle}} \frac{\varphi_{inj}}{6n}\ ;\ \mu f_{nozzle} = 0.75 \frac{\pi d_{inj.holes}^2}{2} i_{inj.holes},$$

where μf_{nozzle} – the effective flow area of the injector's nozzle.

Table 2.4.1 shows the recommended ranges of p_{inj}, d_{32} and φ_{inj} for different injection systems.

Table 2.4.1

Ranges of ***rated*** average injection pressure p_{inj}, Sauter fuel droplets diameter d_{32} and injection duration φ_{inj}.

Injection system type	p_{inj}, MPa	d_{32}, μm	φ_{inj}, c.a.d
In-line fuel injection pumps	40…130	14…19	18…25
Distributor injection pumps	30…120	14…20	16…26
Single-plunger pumps	80…240	12…18	20…34
Unit-injectors	150…300	10…16	18…28
Common rail accumulator injection system	120…300	10…16	18…30

Ignition delay prediction

For ignition delay prediction the modified Tolstov equation is used [6]:

$$\tau_i = B_0(1-k_n n)\sqrt{\frac{p_{cyl}^{inj.start}}{T_{cyl}^{inj.start}}}e^{\frac{E_a}{RT_{cyl}^{inj.start}}}\frac{70}{25+CN},$$

where B_0, k_n – coefficients, $p_{cyl}^{inj.start}$, $T_{cyl}^{inj.start}$ - pressure and temperature in the engine cylinder at the start of fuel injection, E_a – activation energy, CN – cetane number of the fuel.

The recommended values of B_0, k_n are given in table 2.4.2.

Table 2.4.2

Coefficients for Tolstov equation

Rated crank speed, rpm	k_n	B_0
< 2500	0.00016	0.0000038
> 2500	0.00018	0.000002

Razlejtzev combustion model

The predefined combustion model for compression-ignition engines is based on Razlejtzev equations of combustion kinetics, though the User can still choose the Wiebe combustion model, which has simpler setup.

Basic set of equations for Razlejtzev combustion model is as following [4]:

$$\frac{dx}{d\varphi}=\begin{cases}\dfrac{1}{6n}\left(\left(P_0+6n\dfrac{d\sigma_{ev}}{d\varphi}\right)\Big/\left(1+A_1\left(P_0+6n\dfrac{d\sigma_{ev}}{d\varphi}\right)\right)\right)\Bigg|_{x=0}^{x=\sigma_i}\\ \dfrac{1}{6n}\left(P_2+6n\dfrac{d\sigma_{ev}}{d\varphi}\right)\Big/\left(1+A_1 6n\dfrac{d\sigma_{ev}}{d\varphi}\right)\Bigg|_{\sigma=\sigma_i}^{\varphi=\varphi_{\text{inj.end.}}+\Delta\varphi_{k.ext}}\\ \dfrac{1}{6n}A_3\dfrac{\xi_{a.c}\alpha}{x}(1-\Delta_{U.F}-x)x\Big|_{\varphi=\varphi_{\text{inj.end}}+\Delta\varphi_{k.ext}}^{\varphi=\varphi_{\text{comb.end}}}\end{cases},$$

where σ_i represents the amount of fuel, injected during ignition delay, $\varphi_{inj.end}$ – the moment of injection end, $\Delta\varphi_{k.ext}$ – extension of the time for second equation usage, $\Delta\varphi_{comb.end}$ – end of the combustion process, $\xi_{a.c}$ – function of air usage, $\Delta_{U.F}$ – unburned fuel fraction.

The functions P_0, P_2, A_0, A_2 are calculated with the equations:

$$P_0 = \frac{A_0\, q_{fuel}(\sigma_{ev} - x_0)}{V(\varphi_{comb.start})}(b_0\sigma_{ev} + x_0); \qquad A_0 = a_0(n \cdot H)^{m_{comb}};$$

$$A_1 = a_1(n \cdot H)^{m_{comb}};$$

$$P_2 = \frac{A_2\, q_{fuel}(\alpha - x)}{V_c}(\sigma_{ev} - x); \qquad A_2 = a_2(n \cdot H)^{m_{comb}},$$

where H is the swirl number (ratio between the rotational speed of the fresh charge swirl in the cylinder at the end of compression and the crankshaft rotational speed), a_0, a_1, a_2, b_0, m_{comb} – coefficients (see table 2.4.3).

Table 2.4.3

Approximate values for Razlejtzev combustion model setup

Engine type	$a_0 \cdot 10^{-3}$	$a_1 \cdot 10^{2}$	a_2	b_0	m_{comb}	H	m_Y
n = 50…250 rpm, two-stroke	5…12	5…10	10…15	0.1…0.2	0.6…0.8	1.5…3	0.3…0.65
n = 400…750 rpm, four-stroke	8…15	4…9	8…13	0.05…0.15	0.5…0.7	1…1.1	0.45…0.7
n = 750…1500 rpm, four-stroke	10…40	3…7	4…8	0.05…0.1	0.5…0.7	1…1.2	0.5…0.75
n > 1500 rpm, four-stroke	15…30	3…6	3…7	0.04…0.08	0.6…0.8	1.2…2	0.5…0.9

The Razlejtzev combustion model considers combustion as the tree-stage process, with the corresponding equation for each stage. These stages are:

1) combustion of the fuel vapor formed during ignition delay,

2) combustion during injection period,

3) combustion after injection (afterburning).

The equations switch for each stage activates at the defined moments of time: when $x = \sigma_i$ from the first stage equation to the second stage equation and when $\varphi = \varphi_{inj.end} + \Delta\varphi_{k.ext}$ from the second stage equation to the third stage.

The extended period for second stage equation (combustion during injection) $\Delta\varphi_{k.ext}$ can be set up with the $\Delta\varphi_k$ and $\Delta\tau_k$ parameters. Generally at the full load $\Delta\varphi_k$ = 0, reaching up to 5…12 at idling, while $\Delta\tau_k$ is recommended to choose from 0.3 ... 0.8 for direct fuel injection and from 0.5...0.9 for indirect fuel injection.

The afterburning process is mainly guided by the air usage function $\zeta_{a.c}$ which can be calculated from the following equation:

$$\xi_{a.c} = 1 - 1.46(1 - \xi_{a.c0})\frac{\Phi_z}{\Phi_{z0}}\frac{2}{\sqrt{\pi}}e^{-0.5\left(\frac{\Phi_z}{\Phi_{z0}}\right)^2},$$

where Φ_z – relative combustion duration, $\zeta_{a.c0}$, Φ_{z0} – coordinates of the minimum point for the function $\zeta_{a.c} = \zeta_{a.c}(\Phi_{z0})$.

The approximate values of $\zeta_{a.c0}$, Φ_{z0} could be taken from Fig. 2.4.7 and from table 2.4.4.

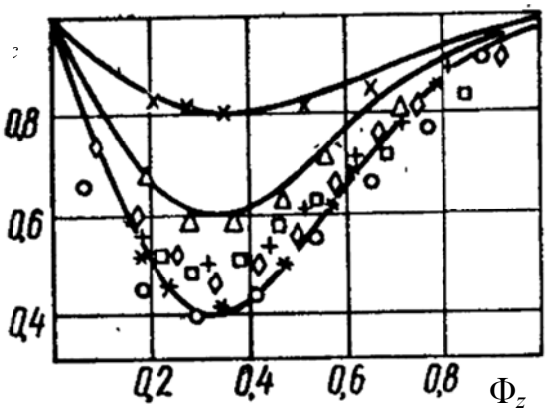

Fig. 2.4.7. Experimental data for air usage function behavior:
x – high-speed engine with indirect injection Д-130, **Δ** – high-speed two-stroke opposed-piston engine with direct injection JUMO-4, □ – medium-speed two-stroke opposed-piston engine with direct injection 2Д100, ◊ – high-speed two-stroke engine with uniflow scavenging and direct injection ЯАЗ-204, + – high-speed four-stroke engine with direct injection СМД-60, ○ – high-speed four-stroke engine with direct injection Renault, * – medium-speed four-stroke engine with direct injection Д-70.

Table 2.4.4

Air usage function approximate setup

Engine type	$\zeta_{a.c0}$	Φ_{z0}
Indirect injection (swirl chamber or pre-chamber)	0.75…0.9	0.35…0.45
High-swirl two-stroke engines with direct injection	0.55…0.65	0.35…0.4
High-speed and medium-speed two-stroke engines	0.4…0.5	0.3…0.35
High-speed four-stroke engines with direct injection	0.35…0.7	0.3…0.4
Medium-speed four-stroke engines with direct injection	0.35…0.55	0.25…0.35
Low-speed two-stroke engines with direct injection	0.35..0.5	0.25…0.4

Fig. 2.4.8 shows the interrelations between fuel injection, evaporation and combustion processes for Razlejtzev combustion model and the influences of setup factors on the heat-release diagram. This figure is also accessible by pressing button “Factors for heat release equations”.

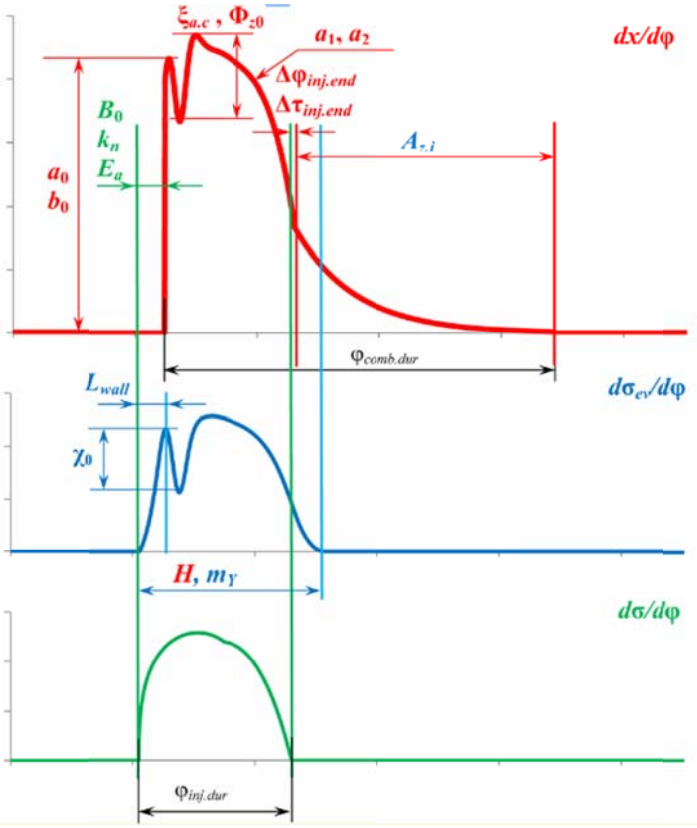

Fig. 2.4.8. Interrelations between fuel injection, evaporation and combustion processes and setup parameters (green color is referred to fuel injection, blue to fuel evaporation and red – to fuel combustion)

2.5. Toxic emissions models setup

The mathematical models of NO, CO and Soot formation are built-in into the Blitz-PRO core as a separate module, which runs after the operation cycle simulation is successfully completed.

2.5.1. NO and CO formation calculation

Calculations of the NO_x concentration at the exhaust gas are based on the Zeldovich mechanism for "thermal" nitric oxide (NO). This chained mechanism includes three equations:

$$N_2 + O \underset{K_{1r}}{\overset{K_{1p}}{\Leftrightarrow}} NO + N;$$

$$N + O_2 \underset{K_{2p}}{\overset{K_{2n}}{\Leftrightarrow}} NO + O;$$

$$N + OH \underset{K_{3r}}{\overset{K_{3p}}{\Leftrightarrow}} NO + H,$$

where K_{1p}, K_{1r}, K_{2p}, K_{2r}, K_{3p}, K_{3r} – constants for direct and reverse chemical reactions.

First equation is the most important in terms of total NO formation kinetics. The equation for NO kinetics could be expressed as:

$$\frac{d[NO]}{d\tau} = K_{1p}[N_2][O] - K_{1r}[NO][N] + K_{2p}[O_2][N] - K_{2r}[NO][O] + K_{3p}[N][OH] - K_{3r}[NO][H],$$

where square brackets "[]" express the volumetric concentration of the corresponding matter.

Blitz-PRO currently utilizes the NO formation kinetic equation, which considers only first and second equations according to Zvonov's approach [13]:

$$\frac{d[NO]}{d\tau} = \frac{2K_{1p}[N_2][O]}{1 + \frac{K_{1r}[NO]}{K_{2p}[O_2]}}\left(1 - \frac{[NO]^2}{K_4[O_2][N_2]}\right);\ K_4 = \frac{K_{1p}K_{2p}}{K_{1r}K_{2r}};$$

Notice, that $K_4[O_2][N_2] = [NO]_{eq}$ – is the equilibrium concentration of NO.

Conversion of the equation into volumetric fraction units gives:

$$\frac{d[NO]}{d\tau} = \frac{p}{RT_{burned}} \frac{2K_{1p}[N_2][O]}{1 + \frac{K_{1r}[NO]}{K_{2p}[O_2]}}\left(1 - \left(\frac{[NO]}{[NO]_{eq}}\right)^2\right), \qquad (2.5.1)$$

where p – incylinder pressure, bar, R = 8.3144 J/(mole·K) – gas constant, T_{burned} – temperature of the burned gases.

The Arrhenius law equations are used for reaction rate constants calculation:

$$K = AT^B \exp\left(-\frac{E_a}{RT}\right),$$

where A, B – empirical coefficients, E_a – activation energy.

The values of A, B could be chosen by the User from table 2.5.1.

Table 2.5.1.

Coefficients for reaction rate constants calculations

Constant,	A, $cm^3/(mole \cdot s)$	B	E_a, J/mole	Source
K_{1p}, $cm^3/(mole \cdot s)$	$7 \cdot 10^{13}$	0	316103	[7]
	$1{,}36 \cdot 10^{14}$	0	315600	[8]
	$4{,}93 \cdot 10^{13}$	0,0472	316480	[9]
	$1{,}3 \cdot 10^{14}$	0	317849	[10]
K_{1r}, $cm^3/(mole \cdot s)$	$3{,}2 \cdot 10^{13}$	0	1670	[8]
	$1{,}32 \cdot 10^{13}$	0	0	[11, 12]
	$1{,}6 \cdot 10^{13}$	0	0	[9]
	$1{,}55 \cdot 10^{13}$	0	0	[7]
	$2{,}8 \cdot 10^{13}$	0	0	[10]
K_{2p}, $cm^3/(mole \cdot s)$	$1{,}33 \cdot 10^{10}$	1	29600	[8]
	$1{,}81 \cdot 10^{9}$	1,5	12560	[11]
	$1.21 \cdot 10^{13}$		29700	[13]
	$1{,}48 \cdot 10^{8}$	1,5	23781	[9]
	$6{,}4 \cdot 10^{9}$	1	26147	[10]
K_{2r}, $cm^3/(mole \cdot s)$	$3{,}2 \cdot 10^{9}$	1	163700	[7]
	$3{,}6 \cdot 10^{12}$	0	162300	[12]
	$1{,}25 \cdot 10^{7}$	1,612	157800	[9]
	$1{,}5 \cdot 10^{9}$	0	161848	[10]

It is important to know the temperature and composition of burned gases to make the usage of the equation 2.5.1 for instantaneous NO concentration rate calculations possible.

The temperature of the burned gases T_{burned} is calculated according to the two-zone model for the combustion period. The working medium in the cylinder is assumed as two-component system – "fresh charge" and "burned gases", separated by the imaginable movable boundary. The pressure for both zones is assumed the same, while temperatures are calculated according to equations, described in section 1.2.

The gas composition for the burned gases zone is calculated according to the professor Zvonov's method [13]. According to this approach the burned gases are assumed as 18-components mixture of O, O2, O3, H, H2, OH, H2O, C, CO, CO2, CH4, N, N2, NO, NO2, NH3, HNO3, HCN.

To find the concentration of each component the set of 14 balance equations together with 4 bound equations is used. This equations set is nonlinear and is solved numerically.

The calculated concentration of CO at the end of combustion process is used as an output data for the "Report" page. So [CO] is calculated as equilibrium concentration of CO at this point.

For diesel engines case the important parameter, which allows precise tuning of NO formation mathematical model, is α_{loc} – the value of the local air excess ratio at the combustion zone. It is assumed, that α_{loc} has linear dependence on the crank angle, reaching $\alpha_{loc} = 1$ at the end of combustion:

$$\alpha_{loc} = \alpha_{loc.start} + (1 - \alpha_{loc.start}) \frac{\varphi - \varphi_{comb.start}}{\varphi_{comb}},$$

where $\alpha_{loc.start}$ indicates the value of α_{loc} at the beginning of combustion process.

Generally $\alpha_{loc.start} = 0.8 \ldots 0.95$, increasing of $\alpha_{loc.start}$ results in rise of calculated NO concentration.

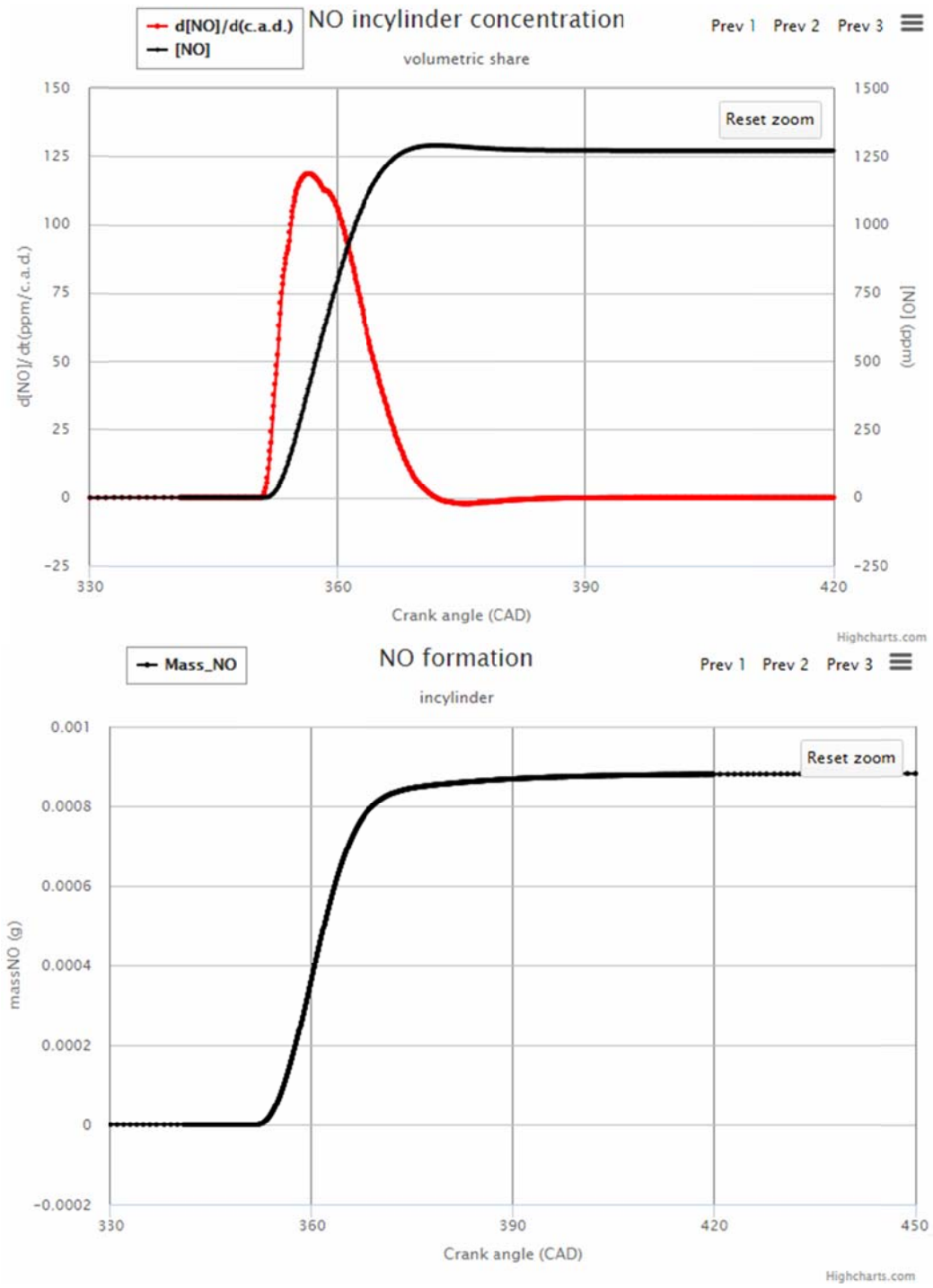

Fig. 2.5.1. Calculated diagrams of incylinder NO formation.

Fig. 2.5.1 shows an example of diagrams of NO formation for automotive diesel engine. The volumetric concentration as well as the mass of NO in the engine cylinder is presented. The resulting amount of nitric oxides is considered for the moment

of exhaust valves (or ports) opening. It is expressed as incylinder and exhaust manifold volumetric concentration and as specific NO emission g_{NO} (see Fig. 2.5.2).

Toxic emissions prediction			
$[CO]_{cyl}$	9.09472	ppm	Incylinder CO concentration at the exhaust openning
$[CO]_{exh}$	9.06256	ppm	Exhaust manifold CO concentration
$[NO]_{cyl}$	1271.51671	ppm	Incylinder NO concentration at the exhaust openning
$[NO]_{exh}$	1267.01994	ppm	Exhaust gases NO concentration
g_{NO}	5.23185	g/(kW h)	Specific emissions of NO_x
$[C]_{cyl}$	0.06639	g/m^3	Incylinder soot concentration at the exhaust oppening
$[C]_{n.cyl}$	0.0216	g/m^3	
$[C]_{n.cyl.Bosch}$	0.77523	Bosch units	Incylinder soot concentration at the exhaust oppening reffered to normal conditions
$[C]_{n.cyl.Hartrige}$	8.67844	HSU (%)	

Fig. 2.5.2. Calculation results of diesel engine toxic emissions (from "Report" page).

The difference between exhaust manifold and incylinder NO concentration is explained because of mixing of the exhaust gases and with some volume of fresh charge during scavenging period.

2.5.2. Calculation of soot formation

Calculation of soot formation is executed for diesel engines only using prof. Razlejtsev approach [4].

The instantaneous volumetric soot concentration rate is given by equation:

$$\frac{\mathrm{d}[C]}{\mathrm{d}\tau} = \left(\frac{\mathrm{d}[C]}{\mathrm{d}\tau}\right)_{kin} + \left(\frac{\mathrm{d}[C]}{\mathrm{d}\tau}\right)_{pol} - \left(\frac{\mathrm{d}[C]}{\mathrm{d}\tau}\right)_{burn} - \left(\frac{\mathrm{d}[C]}{\mathrm{d}\tau}\right)_{vol},$$

where $\left(\frac{\mathrm{d}[C]}{\mathrm{d}\tau}\right)_{kin}$ – kinetic soot formation rate (in the flame), $\left(\frac{\mathrm{d}[C]}{\mathrm{d}\tau}\right)_{pol}$ – core polymerization of fuel droplets rate, $\left(\frac{\mathrm{d}[C]}{\mathrm{d}\tau}\right)_{burn}$ – burning of the soot particles rate, $\left(\frac{\mathrm{d}[C]}{\mathrm{d}\tau}\right)_{vol}$ – change in soot concentration rate due to cylinder volume change.

$$\left(\frac{\mathrm{d}[C]}{\mathrm{d}\tau}\right)_{kin} = B_{1soot}\frac{q_{fuel}}{V}\frac{dx}{dt};$$

$$\left(\frac{\mathrm{d}[C]}{\mathrm{d}\tau}\right)_{pol} = B'_{2soot}\delta_d\frac{q_{fuel}}{V}\frac{1-\exp\left(-\left(\frac{\sqrt{K_{ev}\left(\tau-\tau_{inj.start}\right)}}{d_{32}^{inst}}\right)^{n_{disp}}\right)}{\tau_{inj}}$$ (fuel injection period);

$$\left(\frac{\mathrm{d}[C]}{\mathrm{d}\tau}\right)_{pol} = B''_{2soot}\delta_d\left(1-x_{inj.end}\right)\frac{n_{disp}q_{fuel}}{2V\left(\tau-\tau_{inj.end}\right)}\left(\frac{\sqrt{K_{ev}\left(\tau-\tau_{inj.start}\right)}}{d_{32}^{inst}}\right)^{n_{disp}}\frac{1-\exp\left(-\left(\frac{\sqrt{K_{ev}\left(\tau-\tau_{inj.start}\right)}}{d_{32}^{inst}}\right)^{n_{disp}}\right)}{\tau_{inj}}$$

(soot polymerization after injection end);

$$\left(\frac{\mathrm{d}[C]}{\mathrm{d}\tau}\right)_{burn} = B_{3soot} k_{O_2} \sqrt{n} \cdot p \cdot [C];$$

$$\left(\frac{\mathrm{d}[C]}{\mathrm{d}\tau}\right)_{vol} = B_{4soot} \frac{6n}{V} \frac{dV}{d\varphi},$$

where B_{1soot}, B'_{2soot}, B''_{2soot}, B_{3soot}, B_{4soot} – empiric coefficients; δ_d – droplets core size, d_{32}^{inst} – instantanious Sauter diameter of the injected fuel, K_{ev} – evaporation constant, $\tau_{inj.start}$, $\tau_{inj.end}$ – moments of tome for injection start and injection end, $x_{inj.end}$ – burned fuel fraction for the moment of injection end, n_{disp} – distibution constant to consider fuel injection uniformity, [C] – volumetric soot concentration.

Approximate values of empiric coefficients are given at table 2.5.2 and must be defined more precisly for current engine.

Table 2.5.2

Approximate values of empiric coefficients
for soot formation equation

Parameter	Value
B_{1soot}	0.004
$B'_{2soot}\,\delta_d$	0.0017
$B''_{2soot}\,\delta_d$	0.0028
B_{3soot}	0.0000031
B_{4soot}	0.75
n_{disp}	2…3

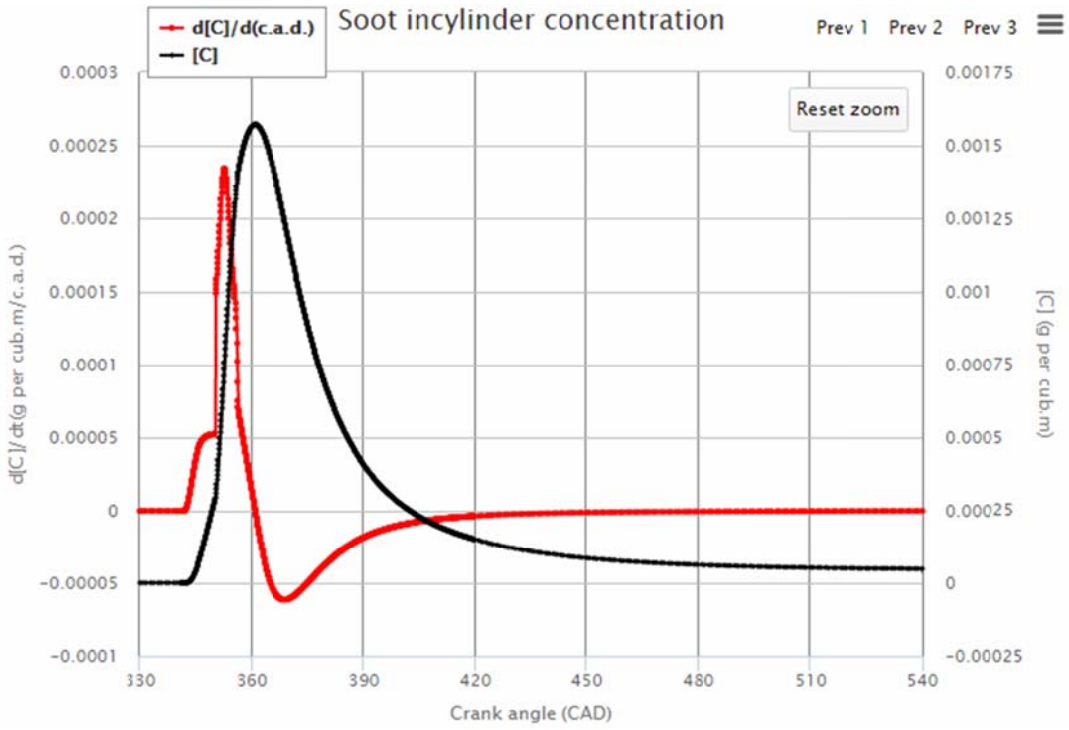

Fig. 2.5.3. Calculated diagrams of diesel engine soot formation.

Fig 2.5.3 illustrates the kinetics of incylinder soot formation and burning for the automotive diesel engine,

The resulting exhaust gases soot concentration referred to normal conditions is calculated by equation:

$$[C]_{n.cyl} = \left(\frac{101.3}{p_{\varphi=\varphi_{e.o}}} \right)^{1/k_{exh}} \frac{1}{6n} \int_{\varphi_{inj.start}}^{\varphi_{e.o}} \left(\frac{d[C]}{d\tau} \right) d\varphi ,$$

where $\varphi_{e.o}$ – exhaust openning, c.a.d.

This value of the volumetric soot concentration is also converted to Bosch and Hartrige scales using the corresponding regressions.

2.6. Supercharging system setup.

The setup of engine's gas-exchange system includes choosing of configuration and geometrical properties of air receiver and exhaust manifold, method of the cylinder aspiration, type and number of superchargers and their arrangement. Blitz-PRO enables calculations for naturally-aspired engine, engines with single-stage supercharging (via mechanically driven turbocharger or with turbocharger), register and two-stage supercharging.

Ambient conditions and flow resistances

The ambient air conditions setup includes the temperature, pressure and humidity of the air at the air filter inlet.

The air filter resistance and resistance of exhaust piping (which is considered as the resistance of pipes, muffler and neutralizers from the turbocharger outlet to the exit to atmosphere) can be set directly or calculated from functions. To set the resistances by calculation, the user should check the checkbox "Use equations to find pressure losses" and set the rated values of resistances and the exponents values for functions on the "Transient" page (see section 2.7).

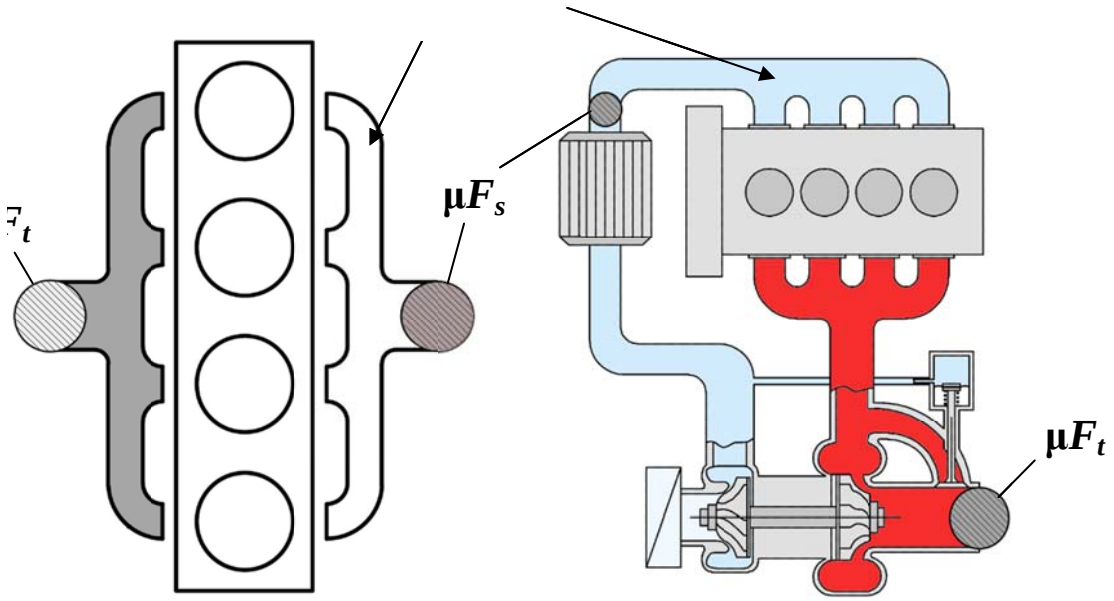

Fig. 2.6.1. Estimation of intake receiver inlet flow area μF_s and exhaust manifold flow area μF_t for naturally aspired (left) and turbocharged engine (right).

Intake and exhaust manifolds geometry

It is important to set correctly the areas of the intake receiver inlet flow area μF_s and exhaust manifold outlet flow area μF_t (see Fig. 2.6.1). For spark-ignition engines with carburetor μF_s could be referred to carburetor diffuser minimal flow area.

The geometrical parameters of intake receiver and exhaust manifold are to be set by their equivalent diameters ($d_{int.eqv}$ and $d_{exh.eqv}$) and relative volumes. The relative volumes are defined as the volume of the part of receiver/manifold to the displacement volume of engine cylinder. Intake receiver as well as exhaust manifold can be made as single part, which combine all engine cylinders, or consist of some parts,

each of the part combine several engine cylinders (see Fig. 2.6.2 for the example). It is important to set correctly the number of the cylinders, combined with one part of the manifold $i_{cyl.1exh}$, $i_{cyl.1int}$. Please note, due to utilizing average cylinder approach the total number of engine cylinders i_{cyl} must be divisible by $i_{cyl.1exh}$ and $i_{cyl.1int}$. That means, for example, if $i_{cyl} = 9$, than $i_{cyl.1exh}$ could be set to 1, 3 or 9.

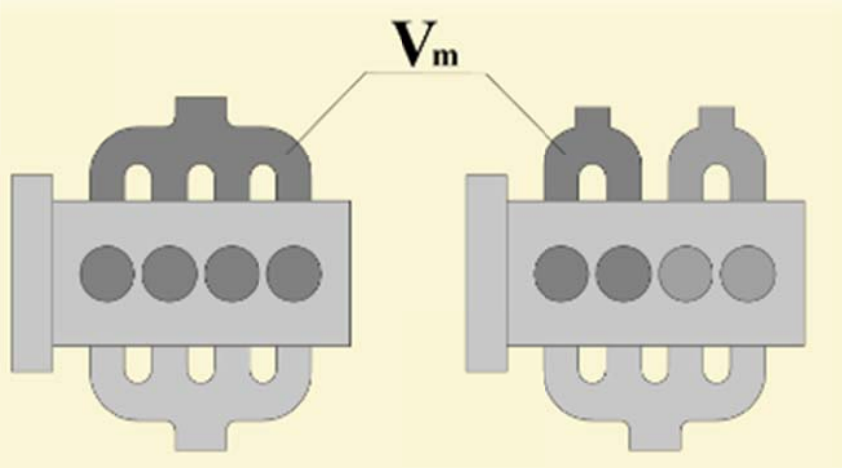

Fig. 2.6.2. Definition of the manifold volume for the single manifold (left) and for the manifold separated in parts, which combine some number of engine cylinders.

Considering unsteady flow behavior

As it is mentioned above, the synthesis of the working processes in the intake receiver and exhaust manifold is executed on the 0-D quasy-steady approach. This approach makes impossible to consider the unsteady flow phenomena due to pressure waves propagation in the pipes of gas-exchange system as well as inertia of the gas flow. For high-speed engines and for engines with specially designed intake and exhaust pipe neglecting of unsteady phenomena leads to high level of inaccuracy of calculations.

Blitz-PRO suggests two methods of considering the unsteady flow effects: 1) simplified 1-D approach, suggested by prof. Orlin; 2) complete 1-D approach for the ideal gas model (currently unavailable).

These both approaches are based on the same computational layout (Fig. 2.6.3). The exhaust manifold and intake receiver are considered assembled with two types of piping: 1) "dynamic" pipes with 1-D unsteady flow calculations, 2) "steady" pipes with 0-D quasysteady calculations.

Please note, that the User sets the relative volumes $V_{int.m}/V_s$, $V_{exh.m}/V_s$ only of "steady" part of the manifold, while the volumes of "dynamic" pipes are calculated automatically and added to the volume of "steady" piping.

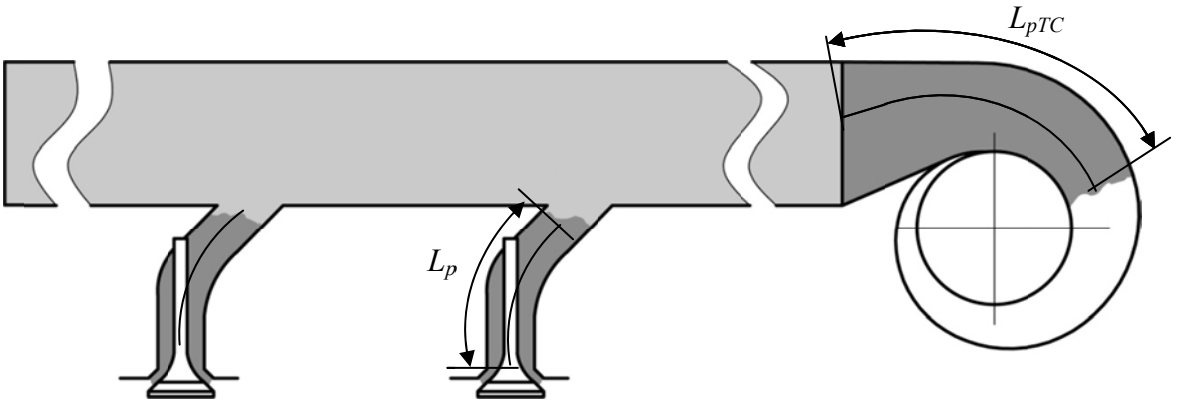

Fig.2.6.3. Intake receiver / exhaust manifold schematic layout.
darkgray – 1-D unsteady approach, lightgray – 0-D quasysteady approach.
L_p – dynamic length of intake/exhaust pipe,
L_{pTC} – dynamic length of compressor/turbine volute (calculated automatically).

The simplified Orlin's approach is based on the pulse conservation equation for 1-D unsteady flow of ideal gas:

$$w\frac{\partial w}{\partial x}+\frac{\partial w}{\partial t}=-\frac{1}{\rho}\frac{\partial p}{\partial x},$$

where x – the coordinate, w – gas velocity, t – time, p – gas pressure, ρ – gas density.

This equation is simplified and adopted to the current task:

$$w^{i+1}=w^{i}+\frac{w_{static}\cdot\left|w_{static}\right|-w^{i}\cdot\left|w^{i}\right|}{2L_p}\Delta\tau,$$

where i – number of computational step, w – gas velocity at the equivalent flow area, w_{static} – gas velocity calculated with the static flow equations, L_p – effective dynamic length of the pipe, $\Delta\tau$ – computational time step.

The Orlin's approach helps to consider the inertia of the gas flow and provide very fast and more accurate calculations for the gas-exchange processes.

The complete 1-D approach is based on the full set of equations for 1-D unsteady ideal gas flow:

$$\begin{cases}\dfrac{\partial\rho}{\partial t}+w\dfrac{\partial\rho}{\partial x}+\rho\dfrac{\partial w}{\partial x}=-\lambda_{fr}\dfrac{w|w|}{2d};\\ \dfrac{\partial u}{\partial t}+w\dfrac{\partial w}{\partial x}+\dfrac{1}{\rho}\dfrac{\partial p}{\partial x}=-w\rho\dfrac{\mathrm{d}\ln f}{\mathrm{d}x};\\ \dfrac{\partial S}{\partial t}+w\dfrac{\partial S}{\partial x}=\dfrac{1}{T}\left(\lambda_{fr}\dfrac{\left|w^3\right|}{2d}-\dfrac{4\alpha}{\rho d}\left(T_{\text{wall}}-T\right)\right);\\ S-S_{no}=\dfrac{R_\mu}{k-1}\ln\dfrac{p/p_{no}}{\left(\rho/\rho_{no}\right)^{k}},\end{cases}$$

where λ_{fr} – coefficient of friction, α – heat transfer coefficient from gas to the pipe wall, T_{wall} – pipe wall temperature, T – gas temperature, S – entropy, "no" – referred to normal conditions, d – pipe diameter, k – adiabatic exponent.

This set of equations completed with boundary conditions is solved with two-stage predictor-corrector numeric method. The "dynamic" pipe length is divided by number of cells (from 10 to 50).

The complete 1-D approach provides more accurate results, but takes much more computational time for execution.

Manifolds friction losses setup

Although the 0-D quasy-steady model is utilized for intake and exhaust piping working processes synthesis, there is an ability to consider the friction losses in the intake receiver and exhaust manifold. The User can set the roughness for intake receiver and exhaust manifold inner walls $R_{a.int}$ and $R_{a.exh}$. The additional frictional backpressure is calculated by:

$$\Delta p_{pipe} = \lambda_{pipe} \frac{L_{pipe}}{d_{pipe}} \rho_G \frac{w_G^2}{2},$$

For the smooth inner surface:

$$\lambda_{pipe} = \frac{64}{\mathrm{Re}}, if\ \mathrm{Re} < 2000;$$

$$\lambda_{pipe} = \frac{0.3164}{\mathrm{Re}^{0.25}}, if 2000 < \mathrm{Re} < 4000;$$

$$\lambda_{pipe} = \frac{1}{(1.81\lg \mathrm{Re} - 1.64)^2}, if\ \mathrm{Re} > 2000.$$

For the rough inner surface:

$$\lambda_{pipe} = 0.11\left(\overline{\Delta} + \frac{68}{\mathrm{Re}}\right)^{0.25}, if\ \mathrm{Re} > 2090 \cdot \left(\frac{1}{\overline{\Delta}}\right)^{0.0635}$$

$$\overline{\Delta} = \frac{R_a}{d_{pipe}}$$

where λ_{pipe} – coefficient of resistance, L_{pipe} – length of the piping, d_{pipe} – inner diameter of the pipe, w_G – gases average velocity, ρ_{EG} – gases density, $\overline{\Delta}$ - relative roughness, R_a – roughness of the pipe inner surface.

Reynolds number for gases flow:

$$\mathrm{Re} = \frac{w_G d_{pipe}}{\nu_G};$$

where ν_G – kinematic viscosity of gases.

The calculated frictional backpressure in the exhaust manifold is added to the exhaust system pressure losses Δp_t and is considered for the exhaust gases flow calculation through the gas turbine or through the outer pipe of exhaust system. At the same way the calculated frictional backpressure in the intake receiver is added to the air filter resistance $\Delta p_{int.f}$ and is considered for the intake air flow calculation through the air compressor or through the inlet pipe of intake system.

Supercharger performance and charge air cooler setup

For supercharged internal combustion engines the User should define the type and parameters of the supercharger. Blitz-PRO allows calculations for the mechani-

cally driven supercharger (with dynamic ore displacement type of the compressor) and for the turbocharger.

The User has two options: to set the parameters of the supercharger (or turbocharger) manually or to use the supercharger's performance maps. This choice triggers the gas-exchange calculation mode. Usage of the performance maps provides much more accurate calculations.

The parameters of supercharged air cooler are given by the temperature of the coolant at the air coolant enter $T_{w1.CAC}$ and the efficiency of air cooler η_{CAC}, which is considered as:

$$\eta_{CAC} = \frac{T_k - T_s'}{T_k - T_{w1CAC}},$$

where T_k – the air temperature at the compressor outlet, T'_s – the air temperature at the air cooler outlet.

Please note, that supercharged air after the air cooler can be heated from the air receiver walls, so the average temperature of the air in the air receiver T_s is different to T'_s.

Fig 2.6.4 shows the setup for mechanically driven supercharger for two cases: manual setup and setup with the performance maps.

For mechanically driven supercharger the User should set the driving gear ratio:

$$i_{cmpr.g} = \frac{n_{SC}}{n},$$

where n_{SC} – the speed of supercharger rotor, n – the crankshaft speed.

In the case of manual setup, the User should set the adiabatic efficiency of the compressor, which is considered as:

$$\eta_{ad.cmpr} = \frac{T_0(\Pi_{cmpr}^{\frac{k-1}{k}} - 1)}{T_k^* - T_0},$$

where T_k^* – the total temperature at the compressor's outlet.

To use the performance maps, the User should check this option from the checkbox and then either choose the corresponding performance maps from the list of maps or upload new performance map from file.

Fig. 2.6.5 shows an example of extrapolated performance maps for the mechanically driven compressor (Lysholm LYS2300AX). Performance maps are presented with two maps: compressor flow map and compressor efficiency map.

Compressor flow map presents the function $\Pi_{cmpr} = f(G_{cmpr.ref}, n_{cmpr.ref})$ as a set of the lines for constant referred speeds of the compressor rotor $n_{cmpr.ref}$ (isotahoes). Compressor efficiency map shows the function $\eta_{cmpr.ad} = f(G_{cmpr.ref}, n_{cmpr.ref})$ as a set of isotahoes. The referred air flow and referred rotor speed are calculated by:

$$G_{\text{cmpr.ref}} = G_{cmpr}\sqrt{\frac{T_{\text{int}}}{T_{ref}}}\frac{p_{ref}}{p_{\text{int}}}, \quad n_{cmpr.ref} = n_{SC}\sqrt{\frac{T_{ref}}{T_{\text{int}}}},$$

where p_{int}, T_{int} – pressure and temperature of air at the compressor inlet, p_{ref}, T_{ref} – referred pressure and temperature (generally p_{ref} = 96 kPa, T_{ref} = 303 K).

The compressor flow map also shows the isolines for constant compressor adiabatic efficiencies, calculated from the efficiency map to provide easier compressor-to-engine matching.

The set of multipliers – μG_k, $\mu \Pi_k$, $\mu \eta_k$, μn_k – helps to scale the maps for better matching the supercharger to the engine. It is strongly recommended do not use the values for multipliers out of range of **0.8…1.2** to provide the proper accuracy of calculations (see section 5).

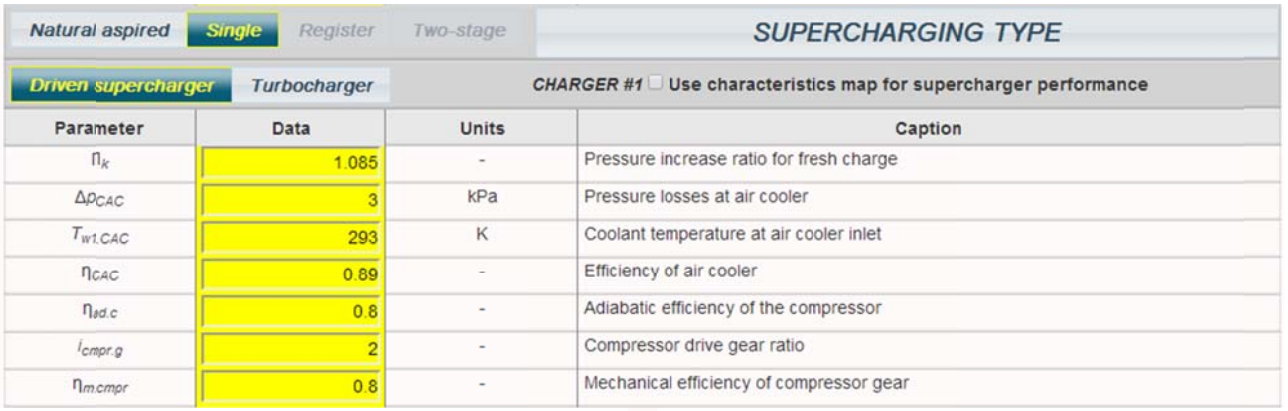

a)

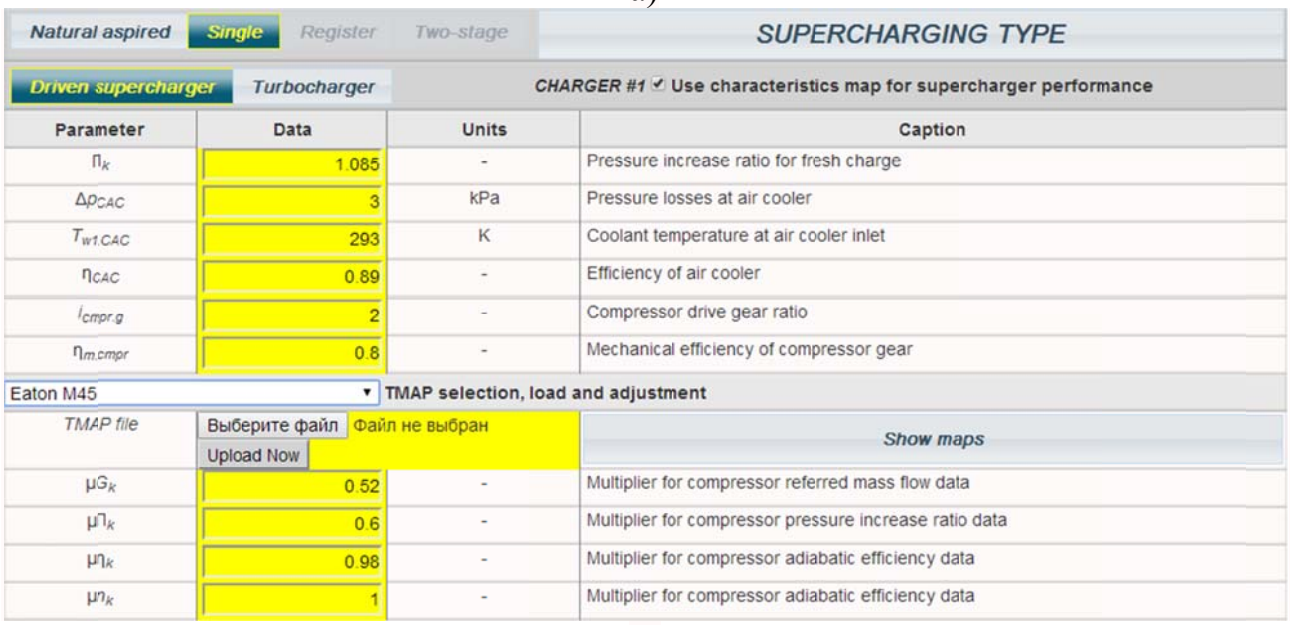

b)

Fig. 2.6.4. Mechanically driven supercharger setup:
a) manual setup, b) setup with performance maps.

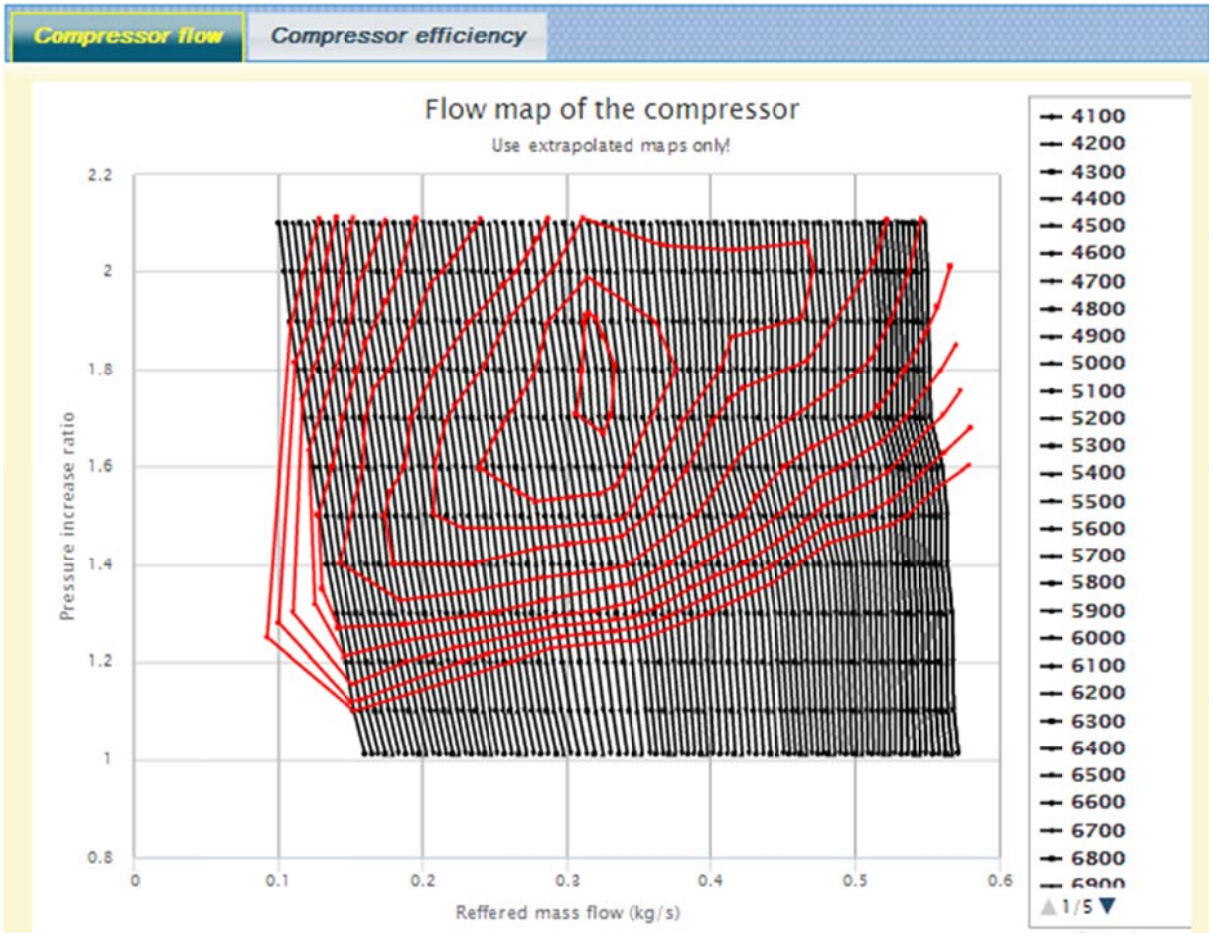

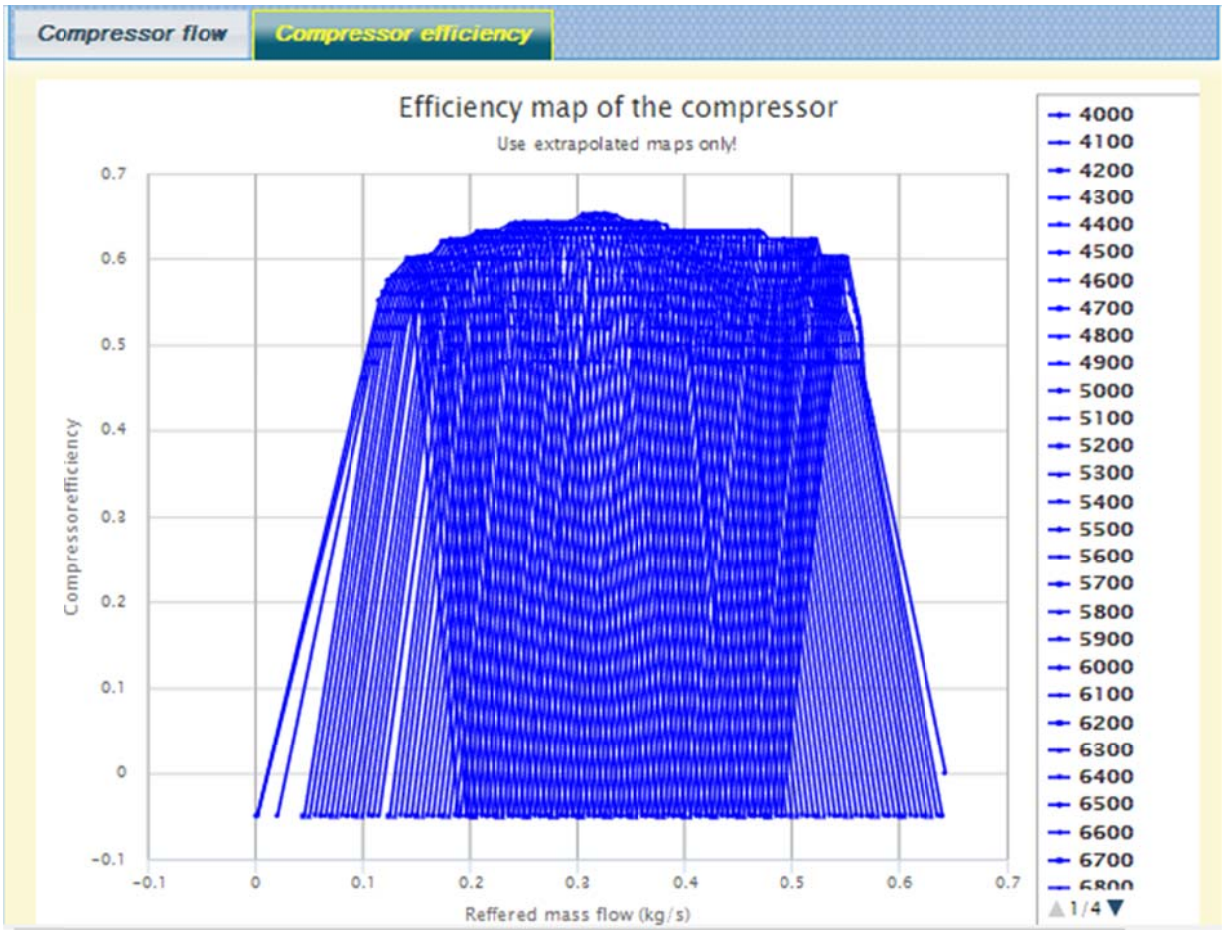

Fig. 2.6.5. Performance maps for the screw-type mechanically driven supercharger.

Fig 2.6.6 shows the setup for **turbocharger** for two cases: manual setup and setup with the performance maps. The manual setup of the turbocharger performance sets directly the turbine efficiency η_{et}, which is considered as:

$$\eta_{e.t} = \frac{T_t^* - T_{z.t}^*}{T_t^*\left(1 - \Pi_{turb}^{\frac{k_t - 1}{k_t}}\right)} \eta_{m.TC},$$

where T_t^*, $T_{z.t}^*$ – the total temperature at the turbine inlet and outlet correspondently, Π_{turb} – turbine pressure expansion ratio (ratio between pressure at the turbine inlet and pressure at the turbine outlet), $\eta_{m.TC}$ – mechanical efficiency of the turbocharger.

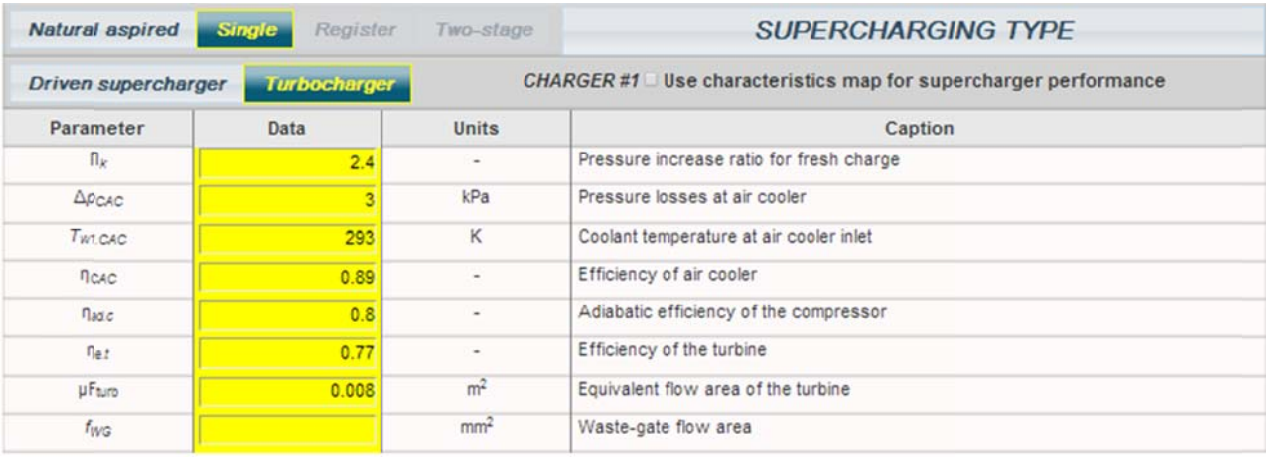

a)

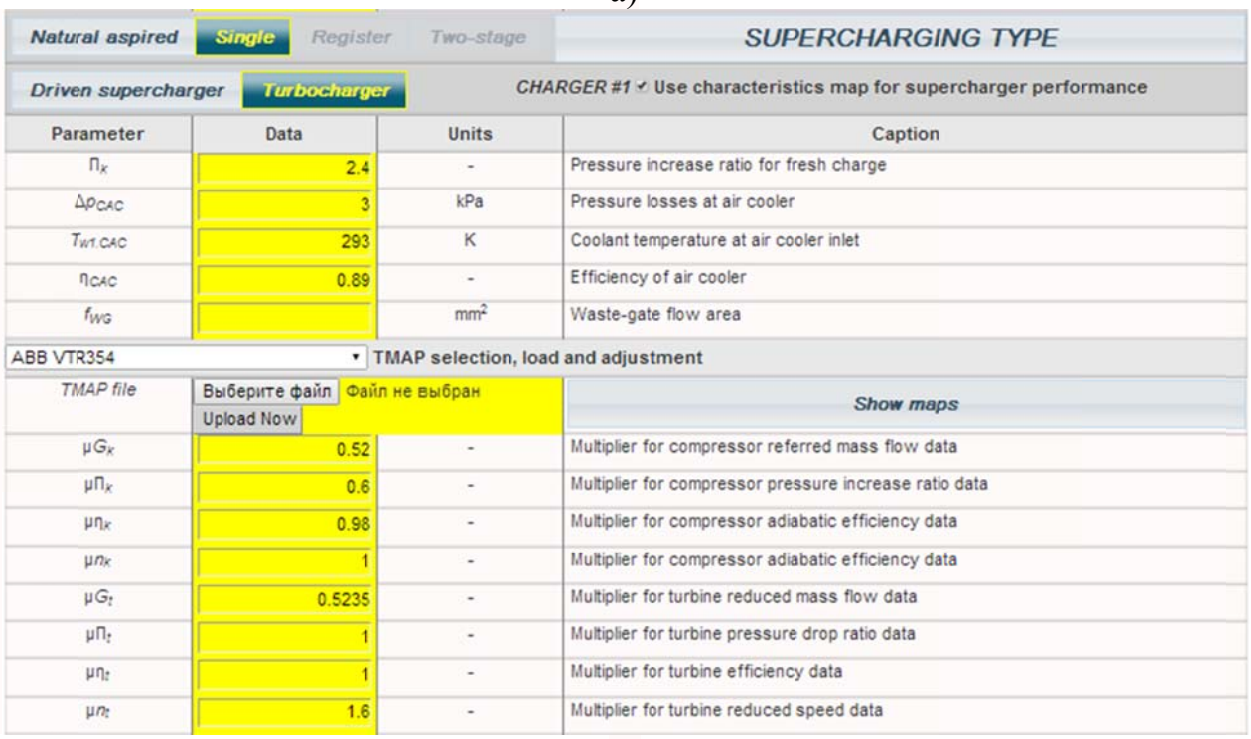

b)

Fig. 2.6.6. Turbocharger setup:
a) manual setup, b) setup with the performance maps.

Another parameter which is necessary for the manual setup: the equivalent turbine flow area μF_{turb}. It is important to set the initial value of μF_{turb} properly – basically it can be assumed from $(0.2\ldots0.4)\cdot\mu F_t$ for initial calculations.

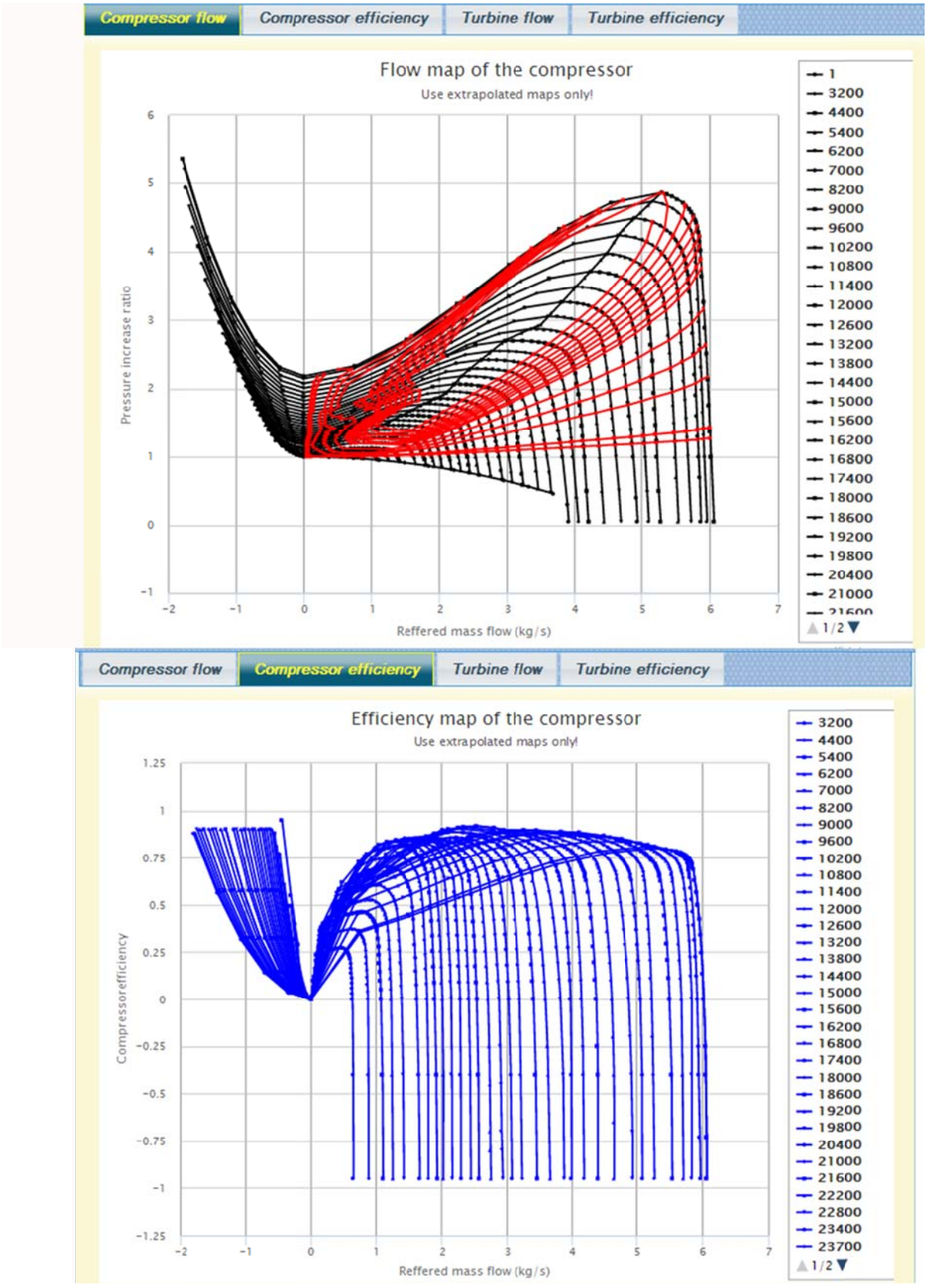

Fig. 2.6.7. Performance maps for the centrifugal-type compressor of turbocharger.

The example of extrapolated performance maps for centrifugal compressor of the turbocharger ABB VTR354 is presented on the Fig. 2.6.7, while Fig. 2.6.8 represents the extrapolated performance maps for the axial-type turbine for the same turbocharger.

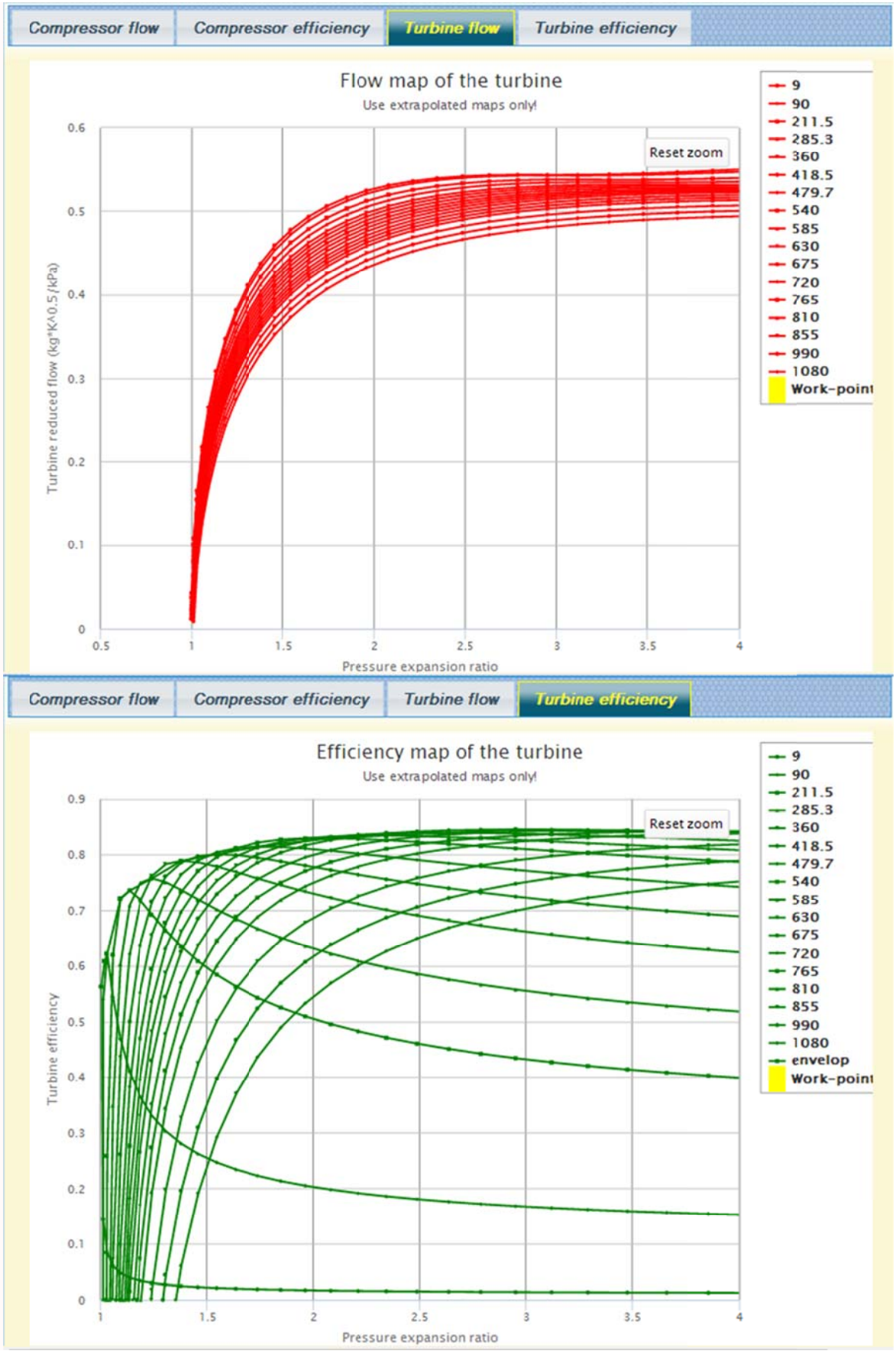

Fig. 2.6.7. Performance maps for the axial-type turbine of turbocharger.

Turbine performance maps are presented with two maps: turbine flow map and turbine efficiency map.

Turbine flow map presents the function $G_{turb.red} = f(\Pi_{turb}, n_{turb.red})$ as a set of the lines for constant reduced speeds of the turbine rotor $n_{turb.red}$ (isotahoes). Turbine efficiency map shows the function $\eta_{e.t} = f(\Pi_{turb}, n_{turb.red})$ as a set of isotahoes. The reduced gas flow and reduced rotor speed are calculated by:

$$G_{turb.red} = \frac{G_{turb}\sqrt{T_t^*}}{p_t^*}, \quad n_{turb.red} = \frac{n_{TC}}{T_t^*},$$

where n_{TC} – turbocharger's rotor speed, p_t^*, T_t^* – total pressure and temperature of gases at the turbine inlet.

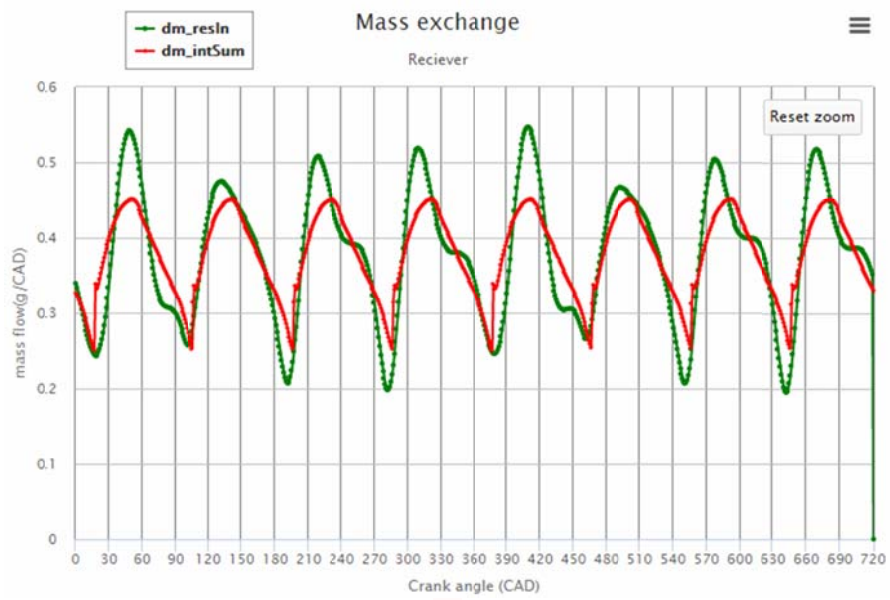

a)

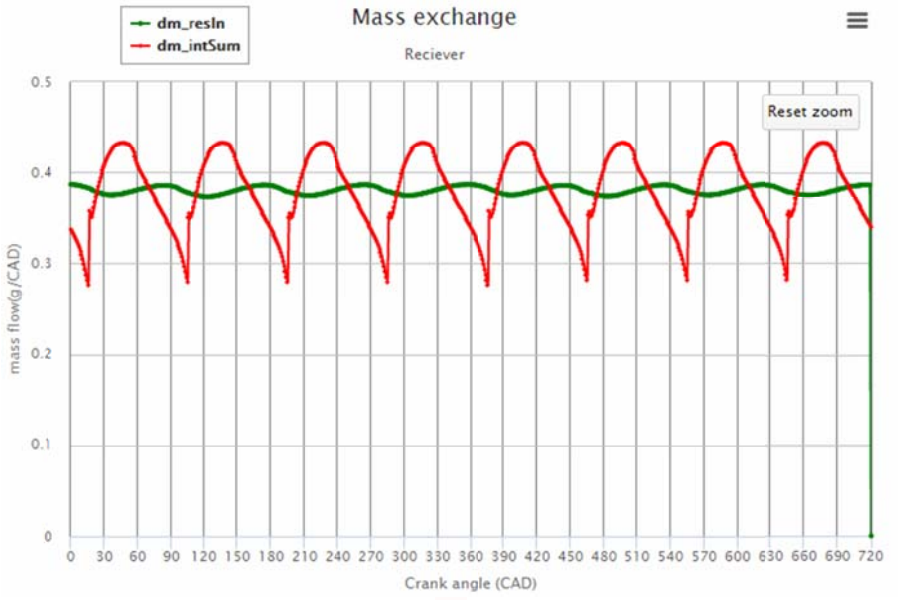

b)

Fig. 2.6.9. Intake receiver mass exchange diagrams ($dm_{res.in}$ – compressor air mass flow, $dm_{int.sum}$ – total mass flow through intake valves):
a) manual turbocharger setup, b) calculations with performance maps

The difference in calculation approach for manual supercharger performance setup and for setup with performance maps significant. The reason is that for the first case (manual setup) the efficiency of compressor and turbine assumed constant through the entire operating cycle, and the effective flow area of the turbine doesn't

depend on the pressure drop ratio and gas temperature at the turbine inlet. The air pressure at the compressor outlet is also considered constant for the current operating cycle. So, please, for correct simulations use the performance maps of the supercharger at the earliest opportunity. Fig. 2.6.9 shows the difference in simulation results for manual and performance maps supercharger setup.

2.7. Transient calculations setup.

"Transient" page serves for transient calculations setup. Transient calculations include various types of engine's non-steady behavior:

1) operation of the engine as part of automotive vehicle power plant for different types of load and speed changing conditions;
2) operation of the main ship engine with direct or geared power transmission with fixed pitch or controllable pitch propeller;
3) operation of engine, coupled with various types of alternators;
4) engine start/stop, warming, etc.

All these cases mean the change in engine operating process for each consecutive cycle because of speed/load/environment/fuel injection conditions change. Thus, before calculation of the transient performance, the User must presetup the conditions, which cause the transient process. The most common of these conditions are: 1) fuel injection and timing maps for diesel engines and fuel ignition and combustion maps for spark-ignition engines; 2) the law of engine load change in respect of engine speed or time of the process.

The change in engine speed and load causes the change in hydraulic losses at the intake and exhaust systems. To consider this, the User setups the set of parameters, as it is shown on Fig. 2.7.1.

Calculations of instantaneous intake air filter, exhaust piping and air cooler resistances are provided with following functions:

$$\Delta p_{\text{int}.f} = \Delta p_{\text{int}.f.rated}\left(\frac{G_{\text{int}}}{G_{\text{int}.rated}}\right)^{m_{\text{int}.f}};$$

$$\Delta p_{exh} = \Delta p_{exh..rated}\left(\frac{G_{\text{int}}}{G_{\text{int}.rated}}\right)^{m_{exh}};$$

$$\Delta p_{CAC} = \Delta p_{CAC.rated}\left(\frac{G_{\text{int}}}{G_{\text{int}.rated}}\right)^{m_{CAC}}$$

Typical value for exponents $m_{int.f}$, m_{exh}, m_{CAC} is 1.8…2.2.

Parameter	Data	Units	Caption
$G_{k.rate}$	0.3	kg/s	Air flow at rated speed and load
$\Delta p_{int.f.rate}$	0.5	kPa	Air pressure drop in the intake air filter at rated speed and load *Generally is to be less then 0.5...1 kPa*
$\Delta p_{CAC.rate}$	4	kPa	Air pressure drop in the charge air cooler at rated speed and load *Generally is to be less then 4...5 kPa*
$\Delta p_{CAC.rate}$		kPa	Air pressure drop in the second stage charge air cooler at rated speed and load *Generally is to be less then 4...5 kPa*
$\Delta p_{exh.rate}$	10	kPa	Exhaust gases pressure drop in the outlet manifold at rated speed and load *Generally is to be less then 7...10 kPa*
$m_{int.f}$	2	-	Exponent for intake air filter pressure drop equation *1.7...2.5*
m_{CAC}	2	-	Exponent for CAC pressure drop equation *1.7...2.5*
m_{exh}	2	-	Exponent for exhaust manifold pressure drop equation *1.7...2.5*
$p_{max.rate}$	10000	kPa	Incylinder maximum pressure at rated power
$dp/d\varphi_{max.rate}$	700	kPa/c.a.d.	Incylinder maximum pressure rate at rated power

Fig. 2.7.1. Rated parameters of hydraulic pressure losses at intake and exhaust and incylinder maximum pressure and maximum pressure rate.

During transient operation the maximum permissible value of incylinder pressure $p_{max.rated}$ or incylinder pressure rate $dp/d\varphi_{max.rated}$ could be limited, so the User setups these parameters, and the routine corrects the ignition/injection timing.

Fig. 2.7.2. Applying the limit for minimal value of air excess ratio for compression-ignition engines

Another limit could be applied for the minimal permissible value of the air excess ratio during transient (for CI engines only). If the User checks the checkbox "Adjust the fuel injection to limit the air excess ratio α", the routine will decrease the fuel flow at some stage of transient to keep α in desired range.

The setup of fuel-injection maps for diesel engines and fuel-ignitions maps for spark-ignition engines is made by importing the corresponding .csv files (described in section 1.5). The maps are to be displayed by pressing the "Show graphs" button (see Fig. 1.5.2 for example).

Fig. 2.7.3. Import and displaying of engine control maps.

Heat inertia

The transient behavior is also characterized by effect of non-steady temperatures of engine parts – piston, cylinder liner and head, exhaust manifold and intake receiver. Due to phenomena of heat inertia it takes time to warm and cool the parts of an engine, so their temperatures differ from the temperatures of steady operation at the same combination of speed and load. To consider these phenomena the User should set the masses and specific heats for engine parts, as it is shown on Fig. 2.7.4.

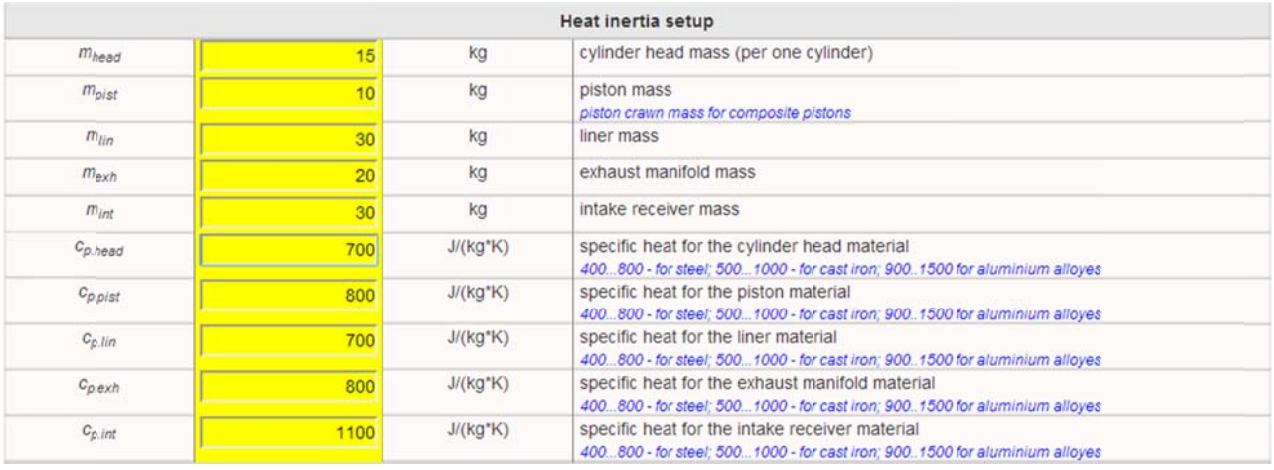

Fig. 2.7.4. Setup of heat inertia for engine parts.

To consider heat inertia, assume the heat balance equation for engine part:

$$Q_h = Q_c + \Delta I,$$

where Q_h – the heat, taken from the hot source, Q_c – the heat, rejected to the cold source, ΔI – the enthalpy, accumulated for part heating.

The change in engine part enthalpy is considered in respect of the part temperature change ΔT_m as:

$$\Delta I = c_p m \Delta T_m .$$

The part temperature is assumed as average value between temperatures of hot surface $T_{wall,h}$ and cold surface $T_{wall,c.}$:

$$T_m = (T_{wall.h} + T_{wall.c})/2.$$

So the heat balance equation could be expressed as:

$$\alpha_h F_h (T_h - (T^{i+1}_{wall.h} + T^{i}_{wall.h})/2)\tau = \alpha_c F_c ((T^{i+1}_{wall.c} + T^{i}_{wall.c})/2 - T_c)\tau + c_p m (T^{i+1}_{m} - T^{i}_{m}),$$

where α_h and α_c – heat transfer coefficients from hot source to the hot wall and from the cold wall to cold source, F_h and F_c – areas of the hot and cold surfaces of engine part, T_h and T_c – temperatures of the hot and cold source respectively, τ – the time of current operating cycle, i – number of calculated consecutive cycles.

This equation is added with equations of heat transfer trough the part wall:

$$Q_c = (\lambda/\delta_{wall} + 1/R_{wall}) F_c ((T^{i+1}_{wall.h} + T^{i}_{wall.h})/2 - (T^{i+1}_{wall.c} + T^{i}_{wall.c})/2)\tau,$$

where λ – heat conductivity coefficient for the wall material, δ_{wall} – wall thickness, R_{wall} – thermal resistance of fouling on the wall surfaces.

Solving this set of equations gives values of $T^{i+1}_{wall.h}$, $T^{i+1}_{wall.c}$ for the next operation cycle calculation.

Types of engine installation

Blitz-PRO offers three types of engine installation for transient calculations: wheeled vehicle, ship and stationary installation. The User can switch between these three options with radio-button set as it is shown on Fig. 2.7.5.

For wheeled vehicle the Newton's law of motion is expressed as:

$$T - F_{fr} - R_{air} - m_{veh} g \sin\alpha_{incl} = m_{veh} j_{veh} + \sum_{j=1}^{N} \frac{I_j \varepsilon_j}{r_j},$$

where T – is the thrust force, applied by driving wheels, F_{fr} – total friction force, including friction in tires, shafts and bearings of slave wheels, R_{air} – air drag force, j_{veh} – vehicle acceleration, I_j, ε_j and r_j – moment of inertia, angular acceleration and referred radius for j rotating part.

The rotational parts (wheels, shafts, etc) inertia consideration is made with multiplier β_{inert}:

$$\beta_{inert} = 1 + \frac{\sum_{j=1}^{N} \frac{I_j \varepsilon_j}{r_j}}{m_{veh} a_{veh}}.$$

Thus, the main equation changes as:

$$T - F_{fr} - R_{air} - m_{veh} g \sin \alpha_{incl} = \beta_{inert} m_{veh} a_{veh} .$$

The common value of β_{inert} is 1.01…1.2.

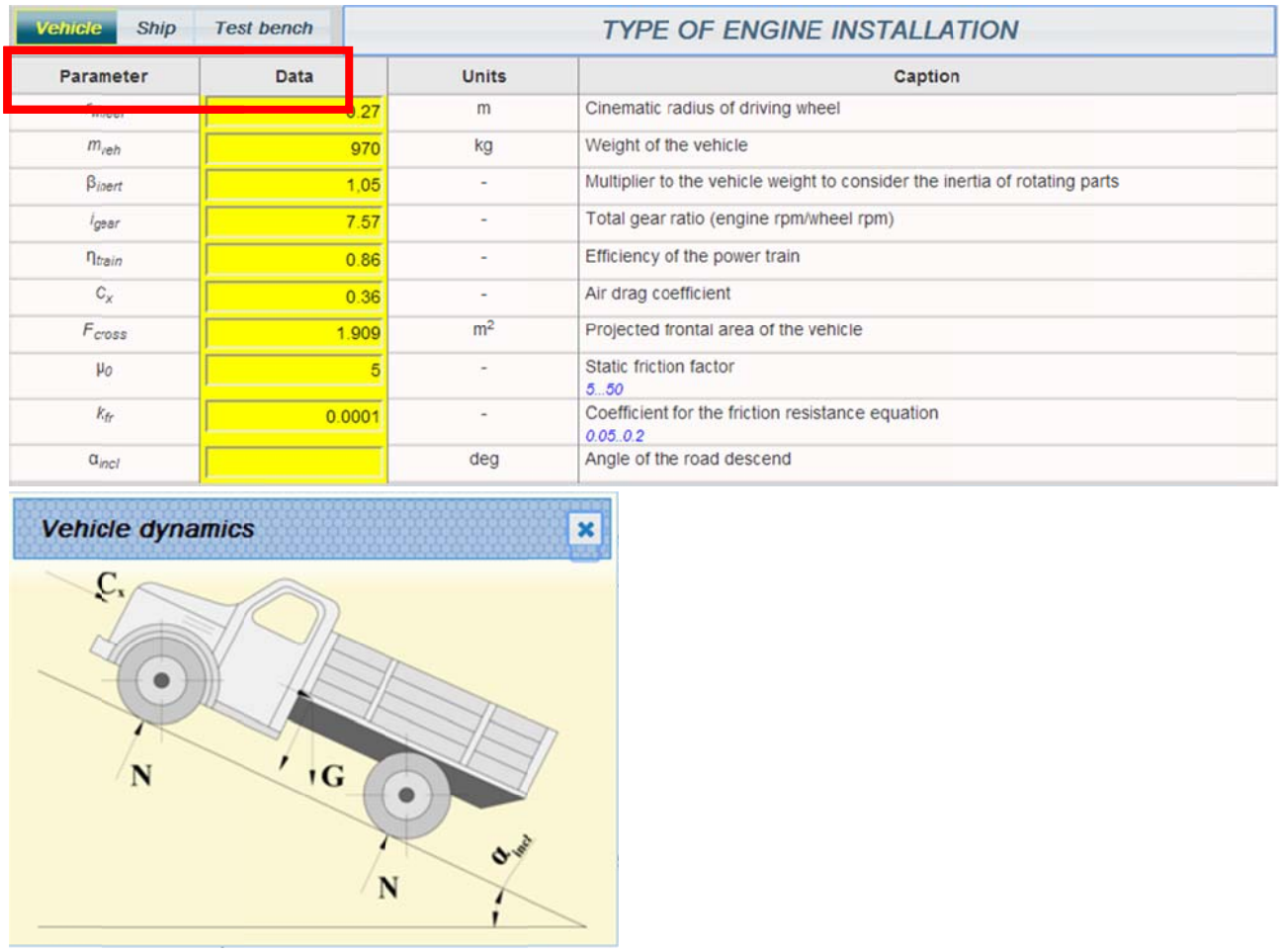

Fig. 2.7.5. Radio button set for installation type selection (marked with red frame) and the set of parameters for the wheeled vehicle case.

The trust force is calculated from the engine brake torque T_b:

$$T = \frac{T_b i_{gear}}{\eta_{\text{train}}} r_{wheel} .$$

The friction force is considered as:

$$F_{fr} = \mu_{fr} m_{veh} g = \left(\mu_0 10^{-3} + 10^{-5} k_{fr} v_{veh}^2\right) m_{veh} g ,$$

де μ_{fr} – coefficient of friction, v_{veh} – vehicle velocity.

The values of μ_0 and k_{fr} depend on tires dimensions and pressure as well as on road surface characteristics. In general μ_0 = 5…50, while k_{fr} = 0.05…0.2.

The air drag force equation is:

$$R_{air} = C_x F_{cross} \rho_{air} \frac{v_{veh}^2}{2} .$$

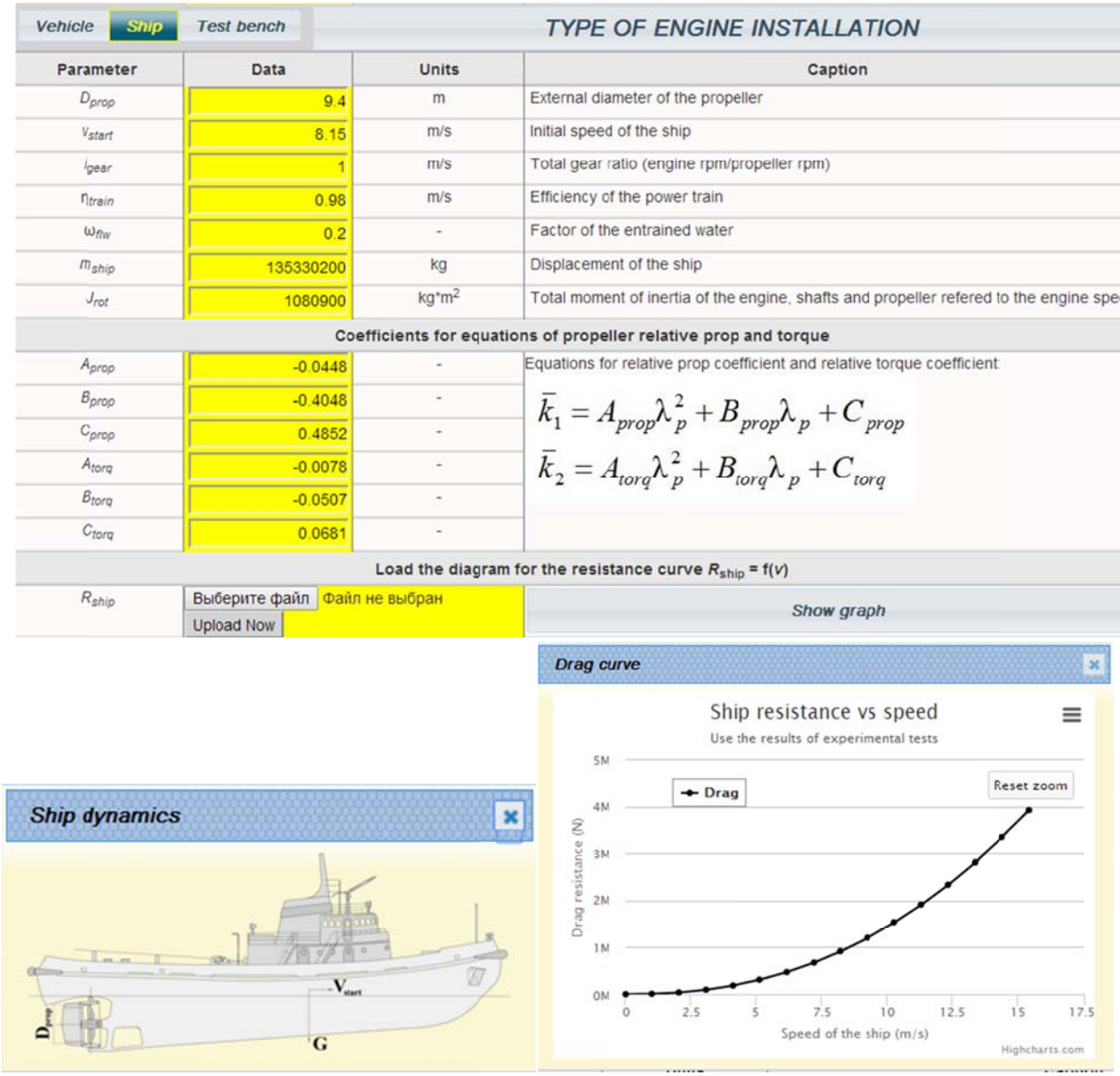

Fig. 2.7.6. Set of parameters for the ship installation.

The transient calculations of the ship dynamics are based on the Newton's law of motion:

$$p_{prop}(1-t) - R_{ship} = m_{ship}a_{ship};$$

$$T_b\eta_{train} - T_{prop} = J_{rot}\frac{\pi}{30}\frac{\mathrm{d}n}{\mathrm{d}t},$$

where p_{prop}, T_{prop} – propeller thrust and torque, R_{ship} – ship towing resistance, t – thrust deduction coefficient.

The rotational moment of inertia J_{rot} includes the moments of inertia of engine moving parts, shafts, gears and propeller with added water referred to the engine speed.

Propeller thrust and torque are given with the propeller characteristics (see Fig. 2.7.7 for example) in respect with the relative propeller advance coefficient λ_{prop}:

$$\lambda_{prop} = \frac{v_{ship}(1-\omega_{flw})}{n_{prop}D_{prop}};$$

$$p_{prop} = k_1 \rho_w n_{prop}^2 D_{prop}^4 ;$$

$$T_{prop} = k_2 \rho_w n_{prop}^2 D_{prop}^5 ,$$

where k_1, k_2 – coefficients of propeller thrust and torque respectively, ρ_w – water dencity.

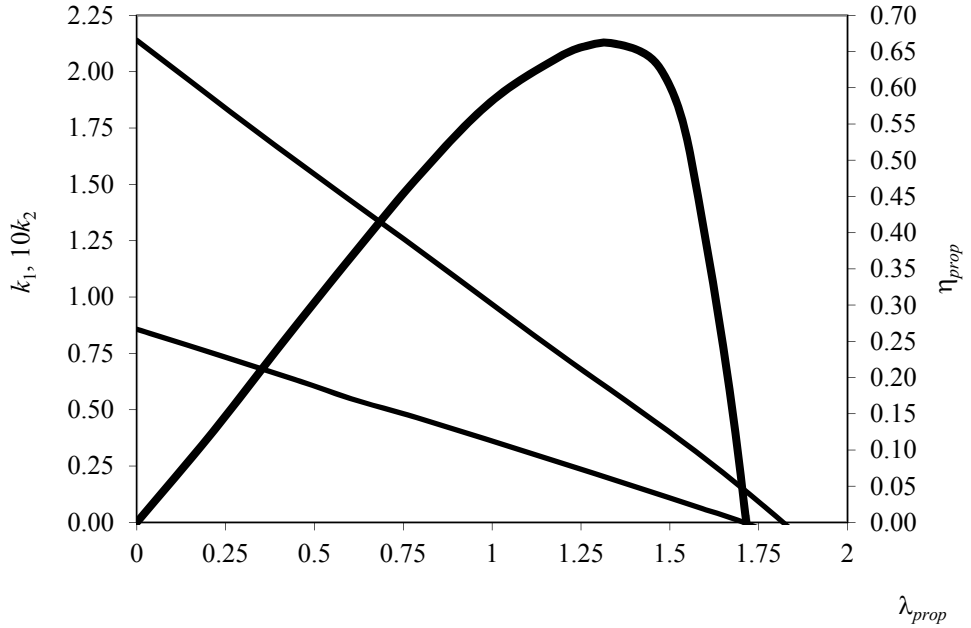

Fig. 2.7.7. Example of propeller performance characteristics (η_{prop} represents propeller efficiency).

The ship towing resistance R_{ship}, which include all components of resistance (friction, wave, wake and air drag) is given as a function with respect to the ship speed by .csv file (see section 1.5 and Fig. 2.7.6).

The test bench case of engine installation needs minimal number of initial parameters (Fig. 2.7.8). The power of engine load P_{load}, which mean the power of consumer is given by function:

$$P_{load} = P_{e.load} \left(\frac{n}{n_{load}} \right)^{m_{load}} ,$$

where n – engine speed.

The Newton's law of motion is expressed as:

$$P_b - P_{load} = J_{rot} \left(\frac{\pi}{30} \right)^2 n \frac{\mathrm{d}n}{\mathrm{d}t} .$$

Vehicle | Ship | Test bench — TYPE OF ENGINE INSTALLATION

Parameter	Data	Units	Caption
$N_{e.load}$	100	kW	Power of the load at the end of the transient period
n_{load}	1960	rpm	Speed of the engine at the end of the transient period
m_{load}	1.79817	-	Exponent for the load curve
J_{rot}	3.9	kg*m^2	Total moment of inertia of the engine, shafts and load refered to the engine speed

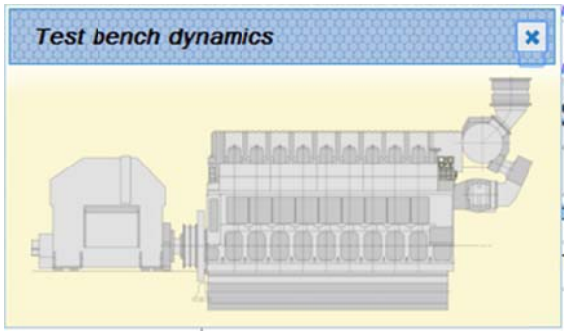

Fig. 2.7.8. Test bench installation

Turbocharger transient

Calculations of turbocharger transient are based on the Newton's law of motion:

$$P_{turb.pulse} - P_{compr} = J_{TC}\left(\frac{\pi}{30}\right)^2 n_{TC}\frac{\mathrm{d}n_{TC}}{\mathrm{d}t},$$

where $P_{turb.pulse}$ – the power of turbine in a pulse flow, P_{compr} – the power of compressor, J_{TC} – the moment of inertia of turbocharger rotor, n_{TC} – turbocharger speed.

The User can switch between three options of turbocharger control: bypassing turbine with waste-gate (WG), changing the turbine nozzle (VNT) or without control (Free).

For the waste-gate arrangement, which consists of the waste-gate valve and pneumatic actuator, the Newton's law of motion is applied (see Fig. 2.7.9):

$$P_{res} + P_{exh} - F_{spring} = m_{act} j_{WG},$$

$$P_{res} = \frac{\pi d_{diafr}^2}{4} p_s,\ P_{exh} = \frac{\pi d_{seatWG}^2}{4} p_t - \frac{\pi d_{WG}^2}{4} p_{zt},\ F_{spring} = F_{spr.static} + C_{spr} h_{WG},$$

where P_{res}, P_{exh} and F_{spring} – forces from air pressure, applied to diaphragm, exhaust gases pressure, applied to waste-gate and from the spring, j_{WG} – the acceleration of the waste-gate, p_s, p_t, p_{zt} – receiver pressure, pressure before and after turbine respectively.

The User can use the predicted value of waste-gate opening pressure, which is calculates with assumption, that $p_s = p_t$ and p_{zt} = 100 kPa, for setup the parameters for waste-gate control system. The actual value of opening pressure will differ from predicted.

WG | VNT | FREE

TURBOCHARGER#1 TRANSIENT & CONTROL

Parameter	Data	Units	Caption
J_{TC}	0.0025	kg*m^2	Moment of inertia of the turbocharger
d_{diafr}	43	mm	Diameter of the diafragm
C_{spr}	3500	N/m	Actuator spring rate
$F_{spr.st}$	15	N	Static spring tight *Predicted reciever pressure p_s for WG opening ($p_s = p_t$ and p_0 = 100 kPa), kPa:* **69.5**
m_{act}	10	g	Mass of actuator mooving parts
d_{WG}	35	mm	Diameter of the waste-gate valve
$d_{seat.WG}$	26	mm	Diameter of the waste-gate valve seat
h_{WG}	6	mm	Waste-gate valve lift
μ_{WG}	0.6	-	Average discharge coefficient of the waste-gate valve

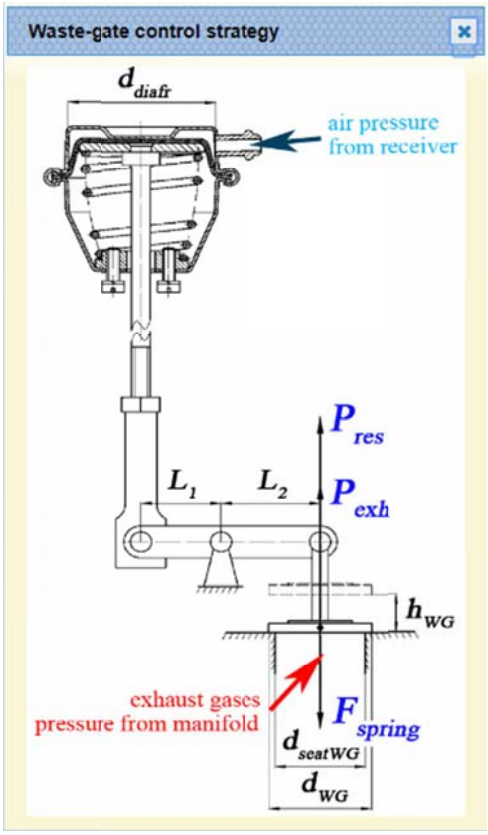

Fig. 2.7.9. The turbine control with waste-gate.

For the variable nozzle turbine control strategy the actuator is also assumed for the nozzle position change (see Fig. 2.7.10). For this case the Newton's law of motion is:

$$P_{res} - F_{spring} = m_{act} j_{VNT} .$$

The User can also use the prediction for the activating pressure for actuator.

The change in nozzle blades position causes the change in the turbine performance maps. This change is considered with the multipliers for turbine flow map μG_t and turbine efficiency map $\mu\eta_t$, which are calculated from equations:

$$\mu G_t = \left[\mu G_t^{\min} + \frac{h_{VNT}}{h_{VNT}^{\max}} \left(\mu G_t^{\max} - \mu G_t^{\min} \right) \right] / \mu G_t^{nom} ;$$

$$\mu\eta_t = a_1 (\mu G_t)^2 + b_1 \mu G_t + c_1 \text{ if } \mu G_t < 1;$$

$$\mu\eta_t = a_2 (\mu G_t)^2 + b_2 \mu G_t + c_2 \text{ if } \mu G_t \geq 1.$$

WG | VNT | FREE

TURBOCHARGER#1 TRANSIENT & CONTROL

Parameter	Data	Units	Caption
J_{TC}	0.00002	kg*m^2	Moment of inertia of the turbocharger
d_{diafr}	50	mm	Diameter of the diafragm
C_{spr}	5000	N/m	Actuator spring rate
$F_{spr.st}$	375	N	Static spring tight *Predicted reciever pressure p_s for VNT opening (p_0 = 100 kPa), kPa:* **291.0**
m_{act}	250	g	Mass of actuator mooving parts
h_{VNT}	7	mm	VNT actuator lift
μG_t^{nom}	1	-	Nominal (basic) value for μG_t
μG_t^{max}	1.4	-	Maximum for μG_t
μG_t^{min}	0.45	-	Minimum for μG_t
a_1	-0.1169	-	Coefficients for the equation of $\eta_{et} = f(\mu G_t)$ for the range of μG_t = min...1
b_1	0.3834	-	
c_1	0.1962	-	
a_2	-0.3055	-	Coefficients for the equation of $\eta_{et} = f(\mu G_t)$ for the range of μG_t = 1...max
b_2	0.5688	-	
c_2	0.1332	-	

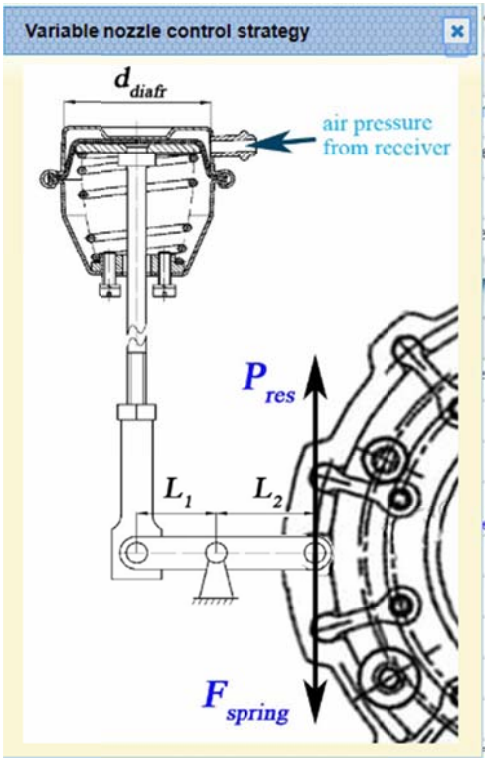

Fig. 2.7.10. The turbine control by variable nozzle.

3. Computation options and core setup

BlitzPRO offers flexible setup of the computation options depending on the particular goal of the current calculation. These options are grouped in the “Calculations setup” dialog, which opens by click on the “Calculate” button on the main page or by click on the “Calculate” icon at the page header.

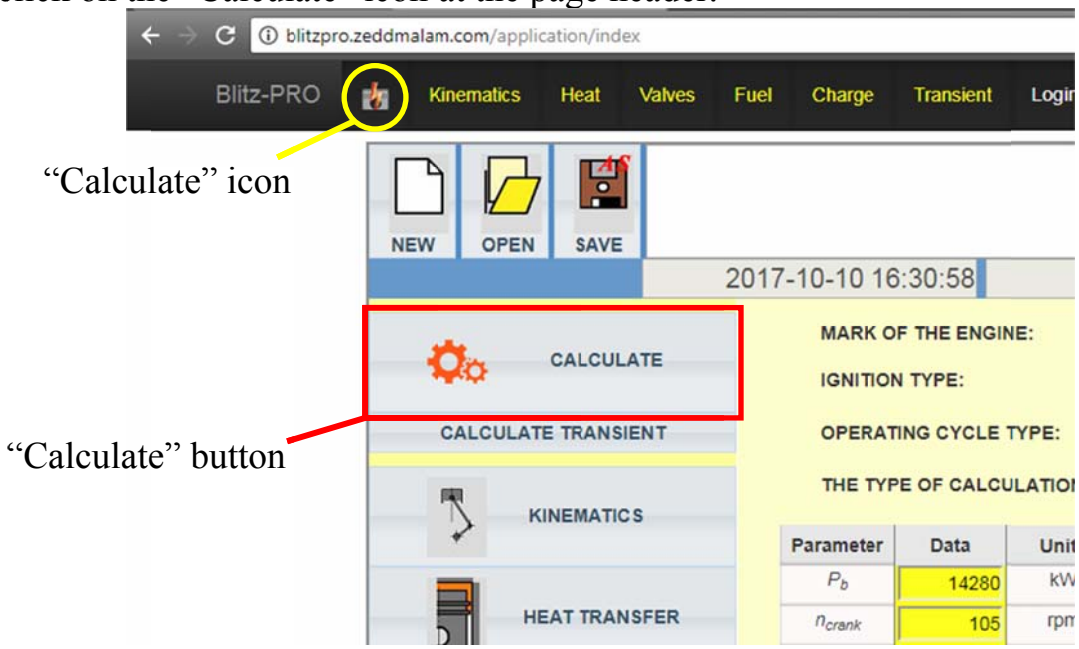

Fig 3.1. “Calculate” button (available on the main page only) and “Calculate” icon (available on any page except “Report”) both trigger the “Calculations setup” window.

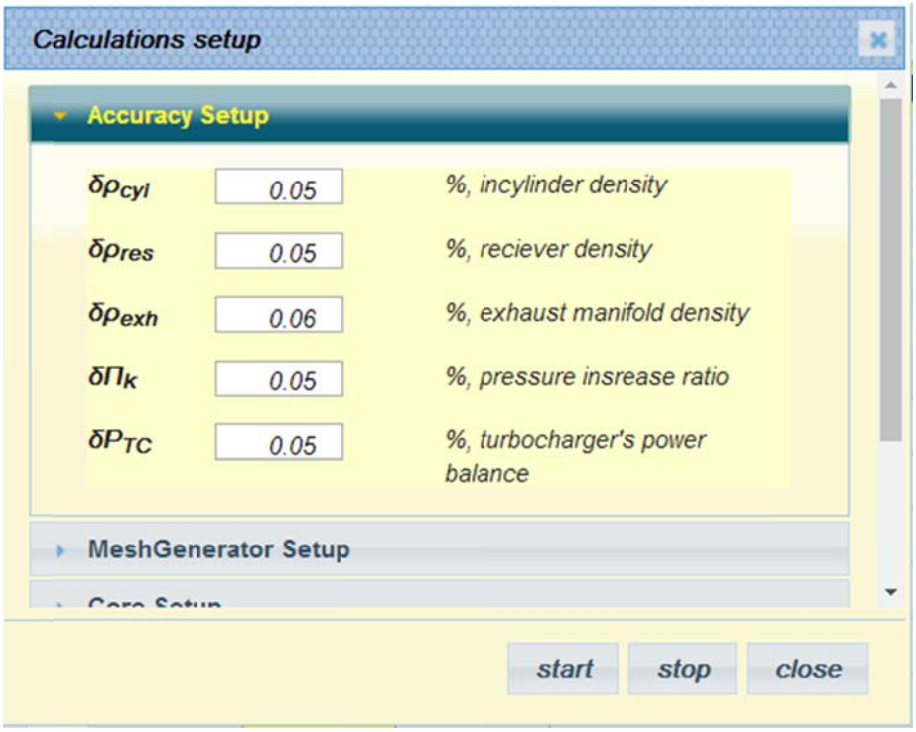

Fig. 3.2. Accuracy setup.

Calculation setup dialog offers the number of options, grouped in the sections: accuracy setup, mesh generator setup, core setup and configure solutions options. It also has the compute log option to display the progress of calculations.

"Accuracy setup" options include the set of calculations accuracies or precisions of numeric calculations. These accuracies for same parameter y are calculated by equation:

$$\delta y = \frac{|y(\varphi = 360/\chi) - y(\varphi = 0)|}{y(\varphi = 360/\chi) + y(\varphi = 0)} \cdot 200,\% .$$

For incylinder, receiver and exhaust manifold densities $y(\varphi = 0)$ means the value of corresponding parameter at the beginning of the operating cycle, and $y(\varphi = 360/\chi)$ indicates the value of this parameter at the end of the cycle (χ – stroke factor, $\chi = 0.5$ for four-stroke engines and $\chi = 1.0$ for two-stroke engines).

For pressure increase ratio accuracy ($\delta\Pi_k$) $y(\varphi = 0)$ means the value of Π_k for previously calculated cycle, while $y(\varphi = 360/\chi)$ is the value of Π_k for the last cycle.

Turbocharger's power balance accuracy is given as:

$$\delta P_{TC} = \frac{|P_{turb} - P_{compr}|}{P_{turb} + P_{compr}} \cdot 200,\% ,$$

where P_{turb} – power, delivered by the turbine, P_{compr} – power, consumed by compressor.

Generally, the recommended value for all accuracies is 0.04…0.06 %, and in most cases there is no reason to change them. But sometimes at some computational iteration for numerical calculations reasons the solver can't find the solution for current set of accuracies. From "Compute log" the User can find out which accuracy can't be reached and then change its value in the "Accuracy setup" window.

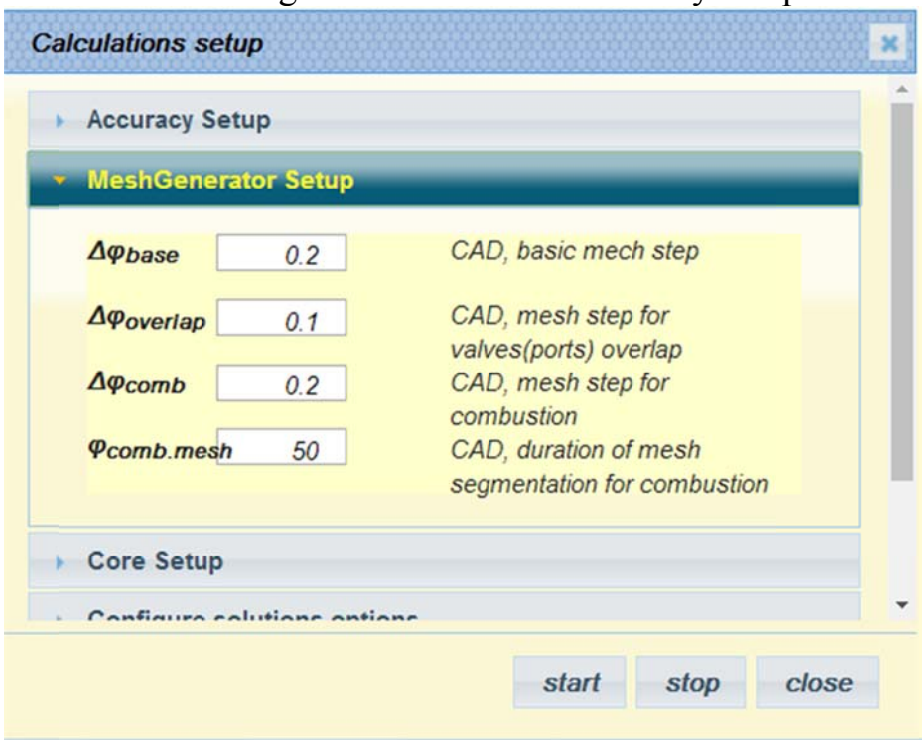

Fig. 3.3. MeshGenerator setup.

"MeshGenerator setup" options help to generate the computational mesh as the sequence of time steps, expressed in crank angle degrees.

The User currently can set any value of the time steps, which obey the condition $\Delta\varphi \geq 0.1$ and multiple to 0.1 ($\Delta\varphi = 0.1, 0.2, 0.3\ldots$ etc).

To increase the speed of calculations and for memory saving reasons BlitzPRO offers the ability to set the computational mesh with variable step by crank angle.

The calculation time step influences greatly on the overall accuracy of calculations. Fig. 3.4 illustrates this relation for the test task: comparison of analytic and numerical computation results for incylinder pressure p at the end of adiabatic compression of the air. The simple Euler method is extremely sensitive to the calculation time step (the calculation error rises up to ≈ 2 % at the step $\Delta\varphi$ = 1 c.a.d), while Runge-Kutta methods demonstrate much more accurate results. But even for the second order implicit Runge-Kutta method change of time step from 0.1 to 1 c.a.d. leads to computation error rise from 0.0001 to about 0.02 % (200 times!).

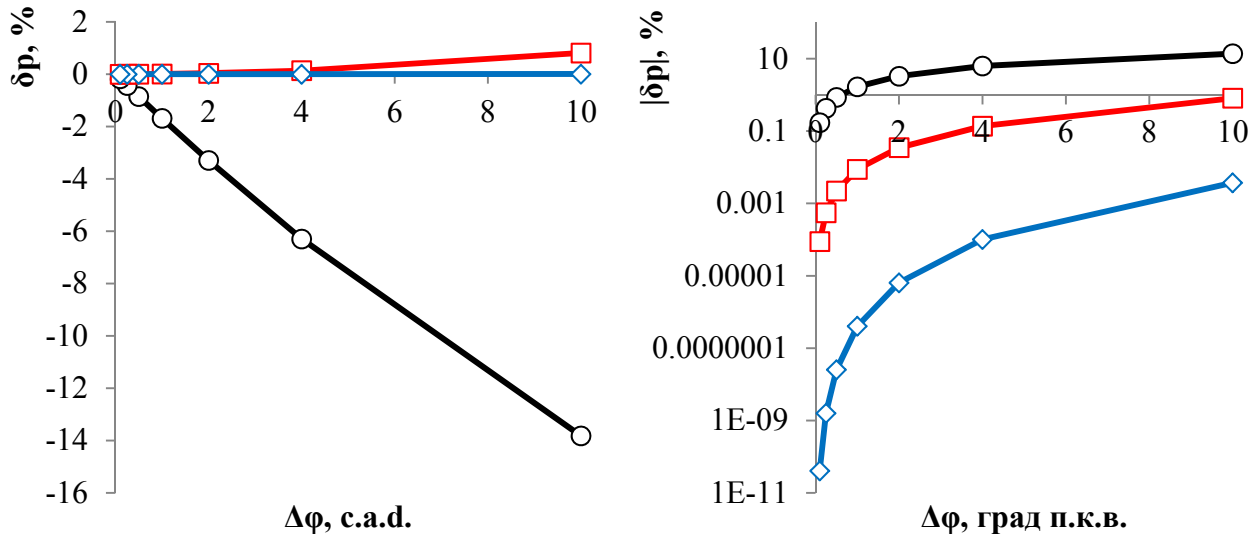

a *b*

Fig. 3.4. Computational accuracy of numeric methods for the adiabatic compression of air test task (*a* – absolute scale; *b* – logarithmic scale for norms of accuracies):

–○– simple Euler method,

–□– fourth order Runge-Kutta method,

–◊– second order implicit Runge-Kutta method.

Fig. 3.4 demonstrates, that in terms of numerical errors the largest reasonable time step is about $\Delta\varphi$ = 2 c.a.d. for Runge-Kutta second order implicit method and about $\Delta\varphi$ = 0.2 c.a.d. for simple Euler method.

But for some processes of the cycle the computation step has to be decreased. These processes are: fuel injection (which can take time about 1 c.a.d. for pilot injection), fuel combustion (especially the kinetic combustion phase for diesel engines), scavenging period of gas exchange processes and the period of free exhaust (exhaust blowdown). Using for these sections of operating cycle the steps $\Delta\varphi > 0.5$ c.a.d. for Runge-Kutta is not recommended.

The base time step for entire cycle is given by $\Delta\varphi_{base}$ and with $\Delta\varphi_{overlap}$ the User can set the time step for valves and ports overlap period (which means the period when both exhaust and intake valves/ports are opened), and for fuel injection-evaporation-combustion period the User can change the values of $\Delta\varphi_{comb}$ (time step) and φ_{comb} (period of time for combustion time step).

Generally it is recommended to use $\Delta\varphi_{base}$ = 1 c.a.d., $\Delta\varphi_{overlap}$ = 0.2 c.a.d., $\Delta\varphi_{comb}$ = 0.1 c.a.d. and φ_{comb} = 40…70 c.a.d.

Table 3.1 illustrates the example of influence of mesh steps generation on the computational results. To define the total calculations error the equation being used:

$$\delta_{\Sigma} = \sqrt{\frac{\sum_{i=1}^{N}\left(x_i - x_i^{E}\right)^2}{N}},$$

where N – total number of engine cycle controllable parameters (air excess rato, indicated efficiency, bsfc, etc), x_i , x_i^{E} – values of the i-parameter for current mesh and etalon mesh correspondently.

Table 3.1

Mesh time steps and calculation results.
For-stroke eight-cylinder truck diesel engine (bore 12 cm, stroke 12 cm), injected fuel mass per cycle q_{fuel} = 42 mg/cycle at 1600 rpm.

Param.	***Units***	***Value***													
$\Delta\varphi_{base}$	° c.a.d.	**0.1**	**0.2**	**0.5**	**0.5**	**0.5**	**1**	**1**	**1**	**1**	**2**	**2**	**2**	**2**	**2**
$\Delta\varphi_{overlap}$	° c.a.d.	0.1	0.2	0.1	0.2	0.5	0.1	0.2	0.5	1	0.1	0.2	0.5	1	2
$\Delta\varphi_{comb}$	° c.a.d.	0.1	0.2	0.1	0.2	0.5	0.1	0.2	0.5	1	0.1	0.2	0.5	1	2
N_{nodes}	-	7200	3600	2220	1732	1440	1612	1117	820	720	1311	811	511	411	360
$\delta\rho_{cyl}$	%	0.007	0.015	0.004	0.016	0.014	0.027	0.006	0.005	0.040	0.019	0.009	0.009	0.013	0.006
$\delta\rho_{res}$	%	0.012	0.014	0.005	0.008	0.013	0.033	0.005	0.005	0.038	0.043	0.009	0.028	0.038	0.005
$\delta\rho_{exh}$	%	0.005	0.014	0.004	0.015	0.012	0.009	0.005	0.002	0.034	0.027	0.008	0.010	0.013	0.016
δP_{TC}	%	0.015	0.033	0.027	-0.010	0.044	0.035	-0.044	-0.005	-0.030	0.008	-0.015	-0.022	-0.035	-0.036
$\delta\Pi_k$	%	0.034	0.039	0.040	0.044	0.045	0.026	0.044	0.011	0.034	0.046	0.047	0.044	0.022	0.040
N_{it}	-	293	311	360	307	323	281	308	320	391	212	267	297	365	349
τ_{Σ}	s	292.04	146.81	125.072	79.887	67.794	78.373	57.261	48.646	55.38	51.713	42.749	34.873	37.231	32.71
τ_{it}	s	0.997	0.472	0.347	0.260	0.210	0.279	0.186	0.152	0.142	0.244	0.160	0.117	0.102	0.094
Π_{cmpr}	-	1.5700	1.5721	1.5703	1.5726	1.5748	1.5676	1.5724	1.5747	1.5864	1.5625	1.5695	1.5758	1.5849	1.6007
α	-	3.306	3.310	3.305	3.306	3.310	3.298	3.300	3.302	3.325	3.286	3.281	3.287	3.314	3.336
η_i	%	45.49	45.45	45.46	45.43	45.62	45.44	45.40	45.60	45.36	45.30	45.29	45.48	45.32	45.50
η_m	%	64.82	64.77	64.82	64.77	64.87	64.82	64.80	64.91	64.61	64.72	64.80	64.92	64.61	64.45
b_b	g/(kW·h)	284.0	284.4	284.1	284.5	282.9	284.3	284.6	282.9	285.7	285.6	285.2	283.6	285.9	285.5
P_b	kW	56.80	56.72	56.77	56.69	57.02	56.74	56.68	57.02	56.46	56.48	56.55	56.88	56.42	56.50
p_{max}	kPa	6676.2	6663.7	6678.4	6662.6	6612.3	6670.5	6656.9	6603.0	6492.6	6659.4	6614.4	6562.8	6493.8	6485.1
t_{max}	°C	1056.2	1052.0	1056.3	1052.5	1051.3	1057.3	1053.4	1052.7	1030.6	1059.1	1056.9	1055.1	1032.5	1009.5
t_t	°C	430.1	429.2	430.4	429.7	425.3	431.0	430.3	426.2	422.5	432.4	432.2	427.8	422.9	411.6
$\eta_{cmpr.ad}$	%	67.63	67.60	67.64	67.60	67.57	67.44	67.63	67.59	67.42	66.81	67.39	67.62	67.45	67.39
$\eta_{e.t}$	%	53.30	53.30	53.31	53.30	53.25	53.28	53.31	53.27	53.20	53.22	53.24	53.24	53.17	52.92
η_{tc}	%	36.05	36.03	36.06	36.03	35.98	35.93	36.05	36.01	35.87	35.56	35.88	36.00	35.86	35.67
δ_{Σ}	%	0.00	0.34	0.12	0.33	1.55	0.39	0.44	1.50	3.39	1.24	1.45	1.88	3.32	5.30

In Table 3.1: N_{nodes} – number of computation steps, N_{it} – total number of iterations for successive calculation, τ_{Σ} – total computational time, τ_{it} – average time per one iteration, δ_{Σ} – overall calculation error.

Fig. 3.5 illustrates the example of the total number of computation nodes influence on the computational iteration average time and overall calculation accuracy.

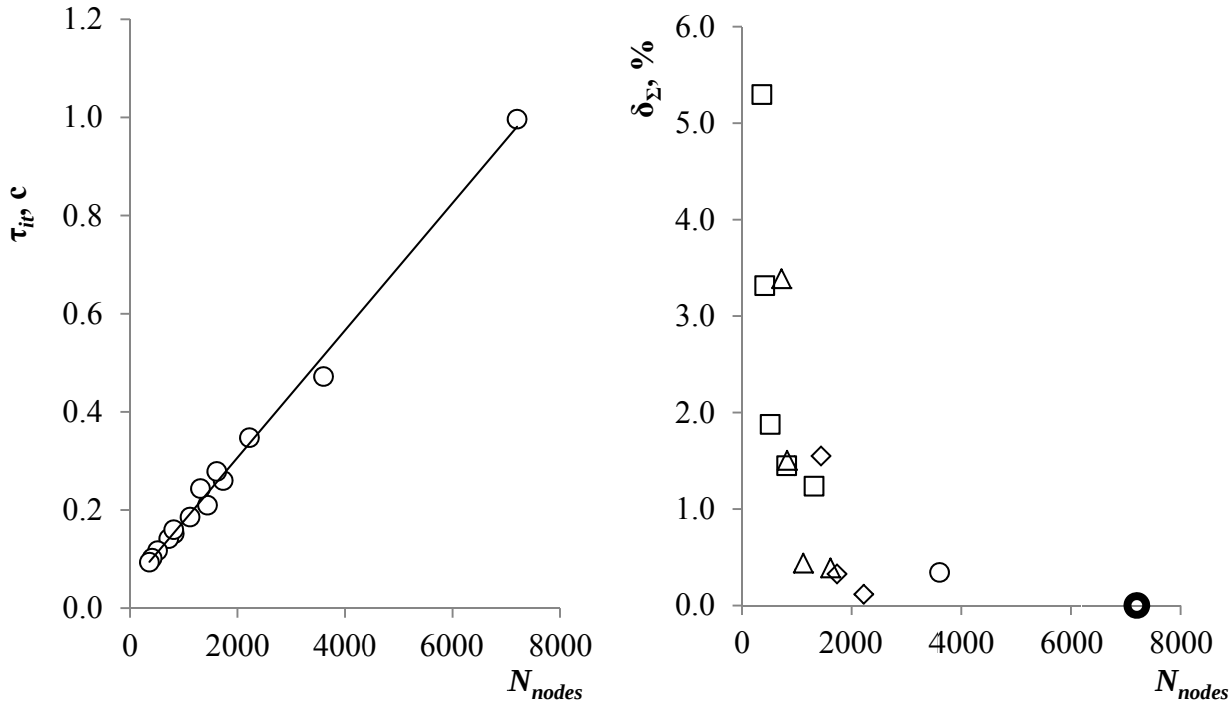

Fig. 3.5. Influence of the total mesh size on the average one iteration time and overall error of calculations.

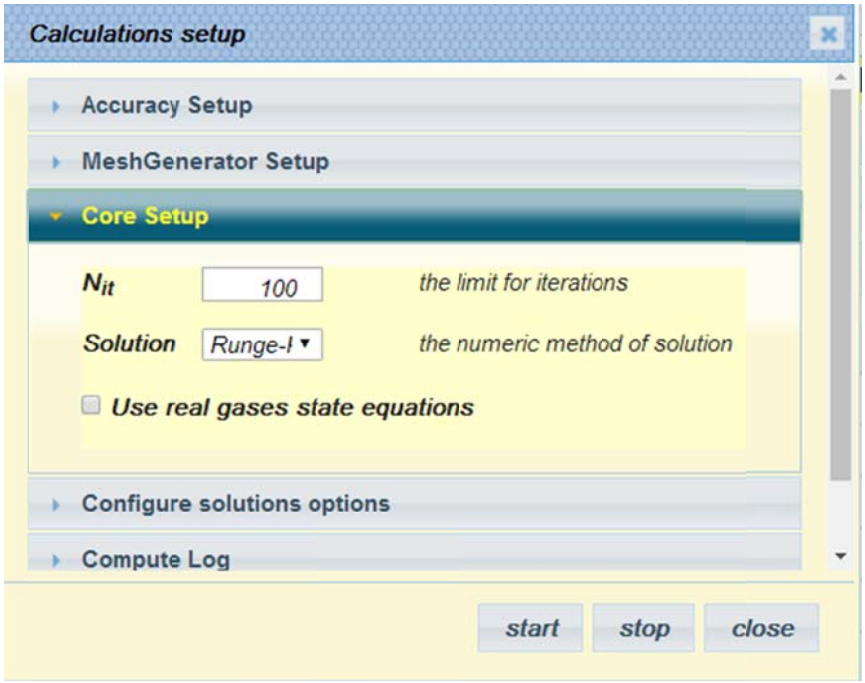

Fig. 3.6. Core setup.

"Core setup options" window is used to set the limit of iterations for current calculation, to choose the numeric method of solution and to trigger the type of gases state equations. The limit for iterations sets the maximum number of iteration, if this number exceeds – the calculation stops even if the desired accuracy of calculation is not reached. It prevents the endless calculation loop if the solver cannot find the solution for current set of accuracies and the User forgets to stop it with the "Stop" button.

The User can choose between simple Euler and second order implicit Runge-Kutta method. The simple Euler method provides the maximum speed of calculation (generally more than twice faster at the same mesh), but has significant numeric errors (see Fig. 3.4) and is recommended for rough calculations only.

The second order implicit Runge-Kutta method provides much more stable and accurate calculations and is preferred. Let's consider this method using an example for the adiabatic air compression task. It has two steps:

1) at the first step (predictor), which is actually a simple Euler method, the predicted values of the next time layer parameters are calculated:

$$T^{i+1} = T^i + \frac{p^i \Delta V^i}{m \cdot c_v},$$

$$p^{i+1} = \frac{m R_\mu T^{i+1}}{V^{i+1}};$$

2) at the second step (corrector) the more accurate calculation executes using predicted parameters:

$$T^{i+1} = T^i + \frac{p^i + p^{i+1}}{2} \frac{\Delta V^i}{m \cdot c_v},$$

$$p^{i+1} = \frac{m R_\mu T^{i+1}}{V^{i+1}}.$$

The checkbox "Use real gases state equations" is to trigger between the ideal gas state equations for open thermodynamic systems and Berthelot equations for real gases (see section 1.2). The Berthelot equations are to be applied to all gases, which form the incylinder gases mixture (including fuel vapor). It provides more accurate calculations in the high pressure range (about 1% calculations accuracy increment at 10 MPa, 1.5% at 15 MPa, 5 % at 20 MPa and up to 15% at 30 MPa).

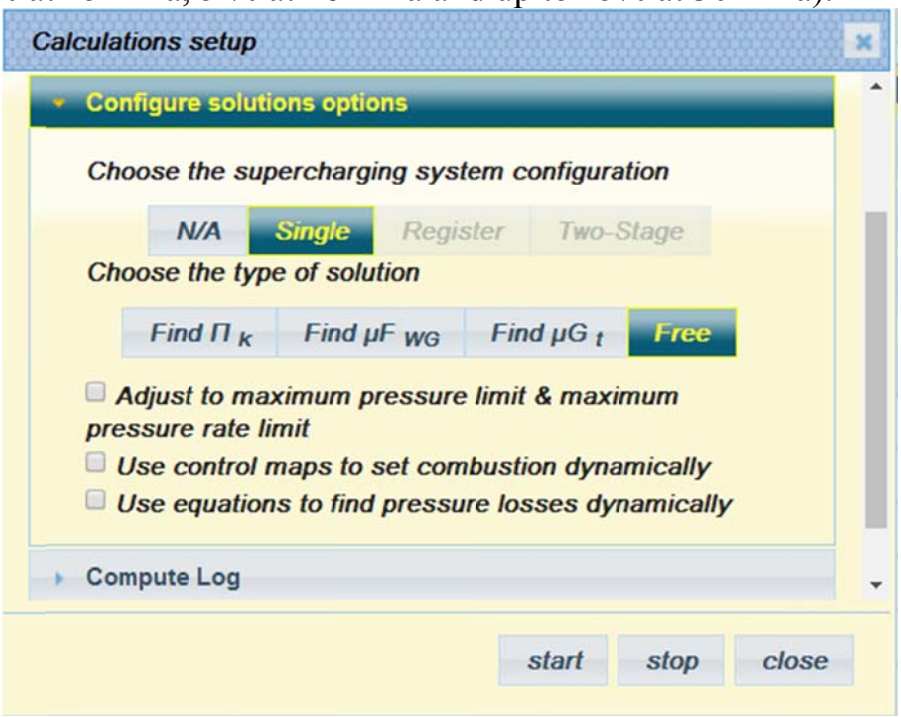

Fig. 3.7. Solution options setup.

"Configure solution options" window is used to switch between different modes of calculation routine. The simulation core can be assumed as combination of

internal loop, which executes until the values of densities errors reach the limit ($\delta\rho_{cyl}$, $\delta\rho_{res}$, $\delta\rho_{exh}$), and external loops (see Fig. 3.8). Number and purpose of these external loops varies depending on the current configuration of the engine and could be set by the User. External loops can be switch into sequence or parallel arrangement on each step (iteration), depending on the current conditions.

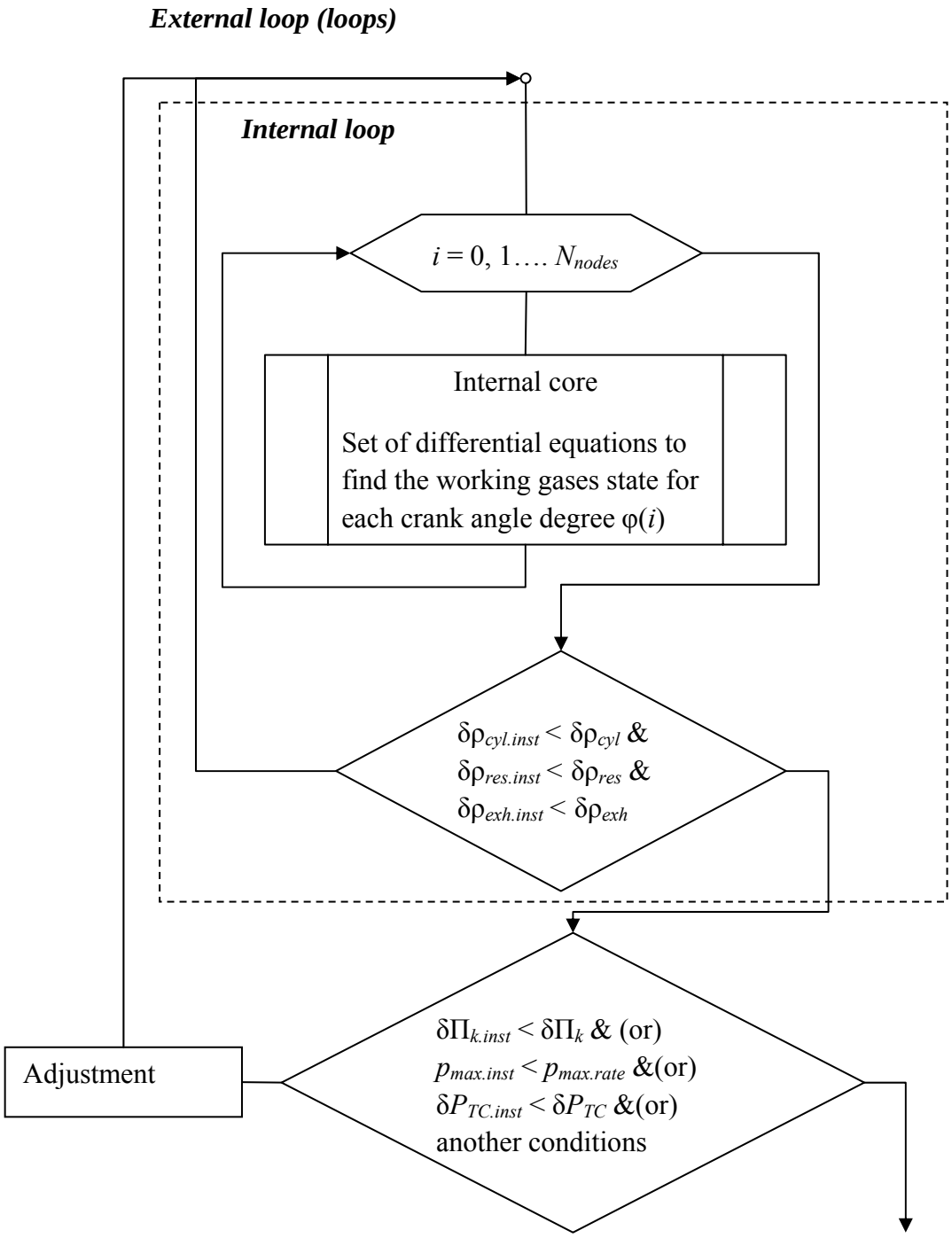

Fig. 3.8. Internal and external loops of simulation algorithm.

The User can set external loops for:

1. Adjustment injected fuel mass per cycle to reach desired brake power. It is activated for diesel engines only by selecting this option from “Type of calculation” list on the main page.

2. Adjustment fuel injection advance (spark timing advance) to limit desired maximum pressure in the cylinder and (or) maximum pressure rate. It is activated by "Adjust to maximum pressure limit & maximum pressure rate limit" checkbox on the "Configure solution options" window.

3. Find conditions for turbocharger's turbine and compressor power balance:

3.1. The User can opt "Find Π_k" to set the loop for search of the value of Π_k, which provides the equality of compressor and turbine power, while turbine geometry remains the same.

3.2. Another option is to obtain the desired value of Π_k by changing the flow area of turbine's waste-gate valve μF_{WG} (by selecting "Find μF_{WG}" option).

3.3. Option "Find μG_t" triggers the loop of adjusting turbine geometry (value of turbine equivalent flow area μF_t for calculations without using turbocharger's performance maps or turbine reduced flow multiplier μG_t if performance maps of turbocharger are activated) for desired level of Π_k.

3.4. Calculations under "Free" mode provide the fastest result, but the manual adjustment of turbocharger performance to reach the compressor and turbine power balance is needed!

For diesel engines the User can also activate automatic adjustment of fuel injection parameters using the interpolation of Control maps (whip can be uploaded on "Transient page"). For spark-ignition engines Control maps are used to set the combustion parameters of Wiebe combustion model. Usage of Control maps is activated by opting "Use control maps to set combustion dynamically" checkbox.

Option "Use equation to find pressure losses dynamically" checkbox activates the equations for air inlet filter resistance, charge air cooler resistance and turbine backpressure adjustment in respect to engine air flow.

"Compute Log" window activates when the User runs calculation by pressing "Start" button. This window displays the log of calculation on-line. It shows information about calculation steps (iterations) in reverse order. For each step the current values of computation errors (which are set at "Accuracy setup" window) are displayed.

The User can break off the calculations by pressing "Stop" button. The routine will continue iterations until it reach the closest iteration number divisible by 10 (i.e. 10, 20, 30 … etc).

The calculation also stops if:

1. The routine finds the solution with desired values of errors. In this case the first raw of compute log is filled with -1.000 values.

2. Some error occurs during calculation. In this case the error is displayed above compute log table. The error message contains information about current exception, which helps to understand its origin. To fix the error the User should inspect initial data and make necessary changes.

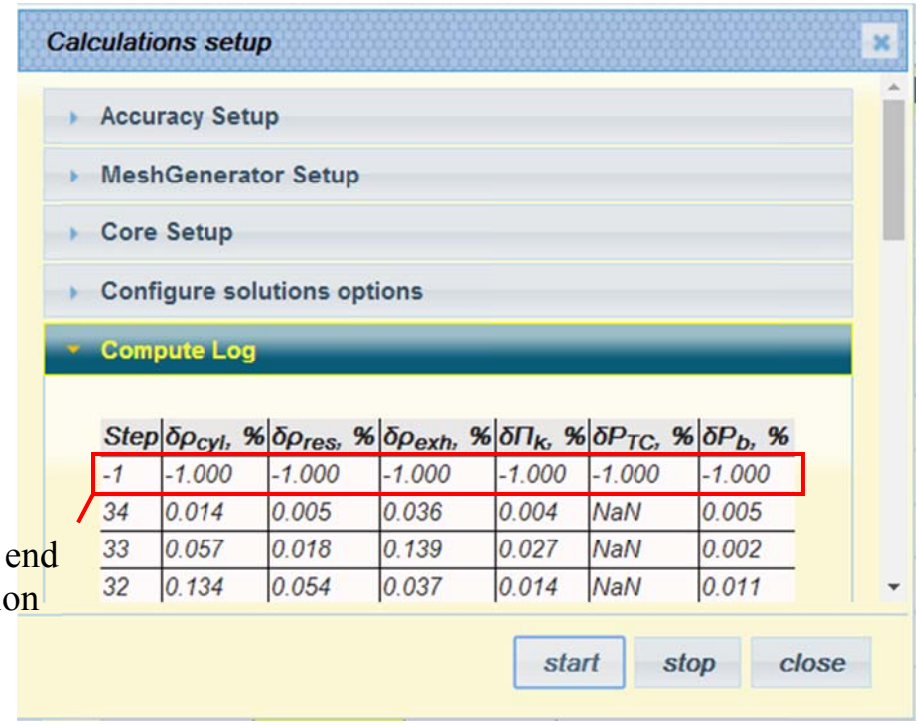

Successful end of calculation

Fig. 3.9. Compute Log widow.

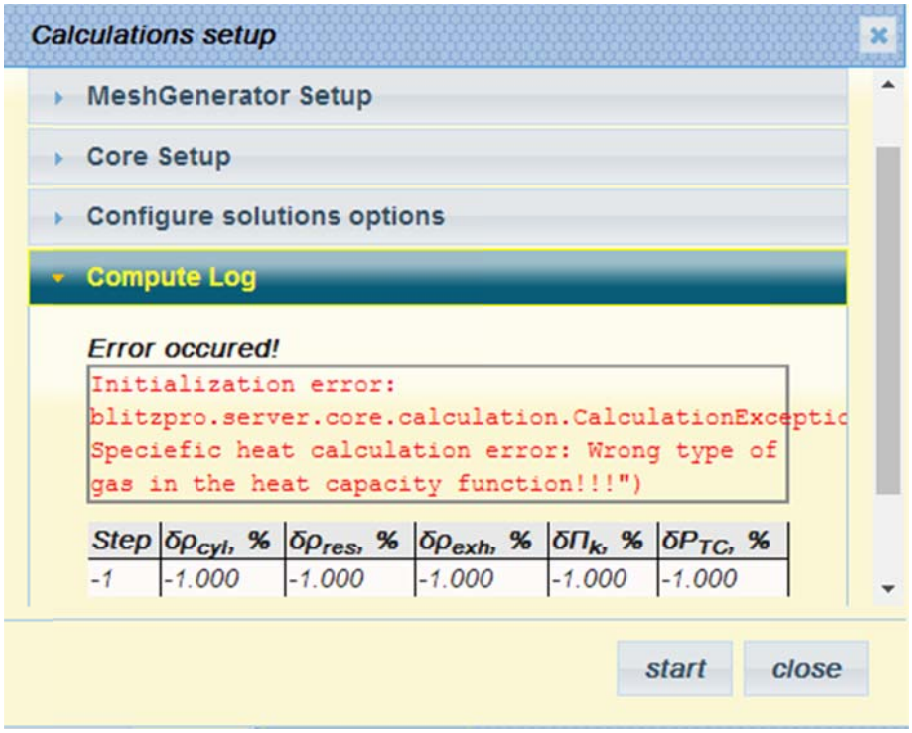

Fig. 3.10. Error message for emergency calculation shutdown.

4. Report and analysis

4.1. Report table

The results of calculations are gathered in “Report” and “Charts” pages.

“Report” page is a table, which is filled with data after successful calculation and presents the main information about engine’s operating cycle and some calculation statistics.

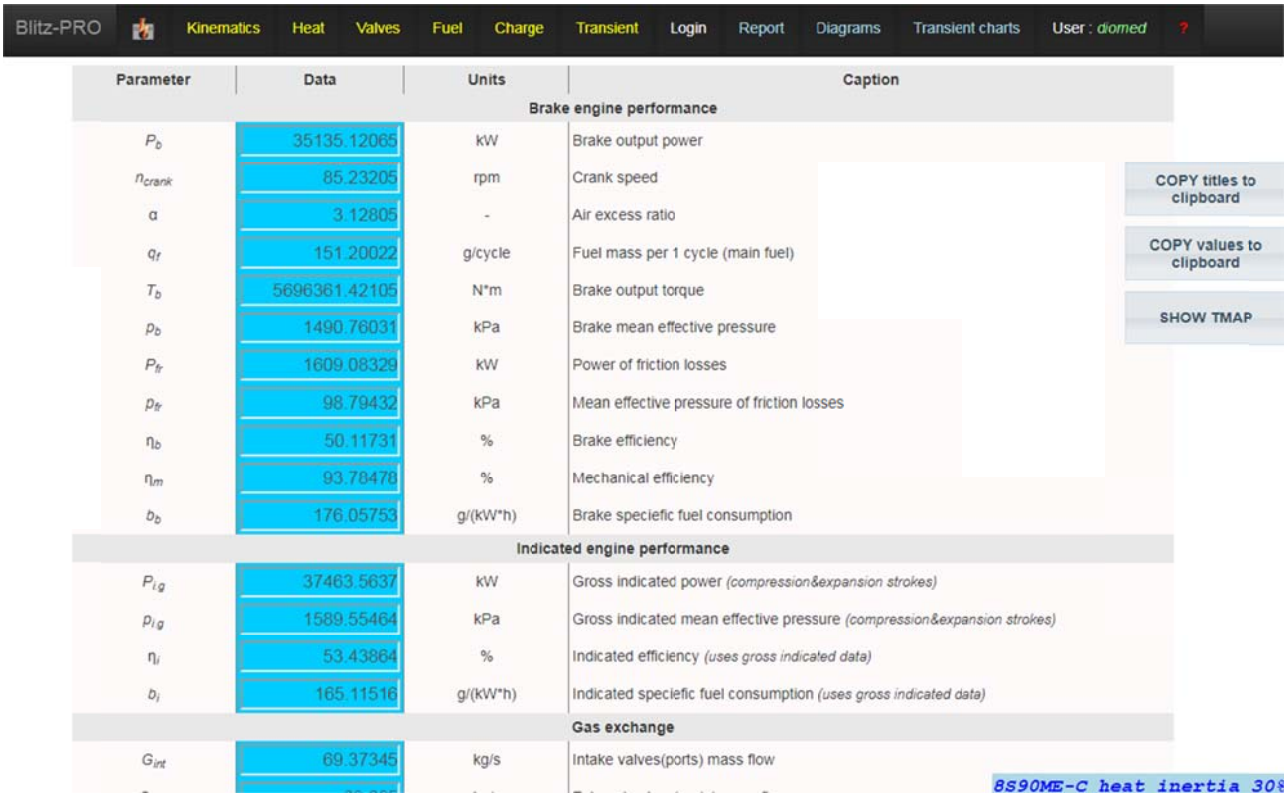

Parameter	Data	Units	Caption
Brake engine performance			
P_b	35135.12065	kW	Brake output power
n_{crank}	85.23205	rpm	Crank speed
α	3.12805	-	Air excess ratio
q_f	151.20022	g/cycle	Fuel mass per 1 cycle (main fuel)
T_b	5696361.42105	N*m	Brake output torque
p_b	1490.76031	kPa	Brake mean effective pressure
P_{fr}	1609.08329	kW	Power of friction losses
p_{fr}	98.79432	kPa	Mean effective pressure of friction losses
η_b	50.11731	%	Brake efficiency
η_m	93.78478	%	Mechanical efficiency
b_b	176.05753	g/(kW*h)	Brake speciefic fuel consumption
Indicated engine performance			
$P_{i\,g}$	37463.5637	kW	Gross indicated power *(compression&expansion strokes)*
$p_{i\,g}$	1589.55464	kPa	Gross indicated mean effective pressure *(compression&expansion strokes)*
η_i	53.43864	%	Indicated efficiency *(uses gross indicated data)*
b_i	165.11516	g/(kW*h)	Indicated speciefic fuel consumption *(uses gross indicated data)*
Gas exchange			
G_{int}	69.37345	kg/s	Intake valves(ports) mass flow

Fig. 4.1.1. “Report” page.

The information is grouped into blocks: “brake engine performance”, “indicated engine performance”, “gass exchange”, “pressures & temperatures”, “combustion”, “toxic emissions prediction”, “walls temperatures and heat transfer parameters”, “supercharger(s) parameters”, “energy balance” and “accuracy of calculations”.

The button “walls temperatures and heat transfer parameters” is interactive and triggers the dialog window with cylinder liner hot surface temperature distribution (see Fig. 2.2.1).

The button “Show TMAP” activates the dialog window with supercharger performance maps superimposed with the average for cycle operating point (yellow). The interpolated lines for current compressor speed are also presented on the compressor’s flow and efficiency maps (Fig. 4.1.2).

The button “COPY titles to clipboard” fills the clipboard with the list of parameters titles, which can be pasted to any table editor.

The button “COPY values to clipboard” serves the same purpose for parameters values.

With the last two buttons the User can form the table with calculations results (see Fig. 4.1.3 for the example).

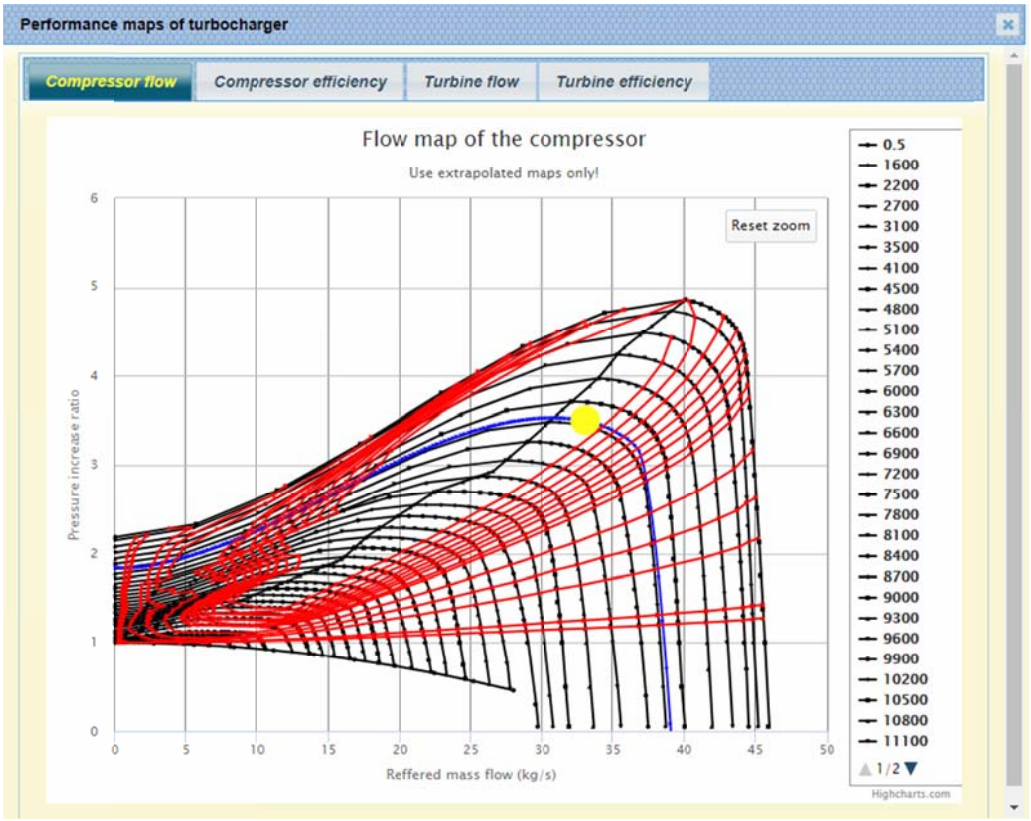

Fig. 4.1.2. Performance map of turbocharger's centrifugal compressor with average operating point (yellow). Blue line shows the current speed of turbocharger.

	B	C	D	E	F	G	H	I	J	K	L
1											
2											
3	*Number of strokes*		Four-stroke	Four-stroke	Four-stroke	Four-stroke	Four-stroke	Four-stro	Four-stro	Four-stroke	
4	*Ignition type*		Compressio	Compressio	Compressic	Compressi	Compressi	Compres	Compres	Compression-igniti	
5	*Combustion model*		combust_op	combust_op	combust_op	combust_op	combust_o	combust_	combust_	combust_opt1	
6	*Supercharging system*		sc_opt2	sc_opt2	sc_opt2	sc_opt2	sc_opt2	sc_opt2	sc_opt2	sc_opt2	
7	*Type of the supercharger*		scl_opt2	scl_opt2	scl_opt2	scl_opt2	scl_opt2	scl_opt2	scl_opt2	scl_opt2	
8	*TMAP1 check*		checked	checked	checked	checked	checked	checked	checked	checked	
9	*TMAP1 name*		ABB TPL76	ABB TPL76	ABB TPL7	ABB TPL7	ABB TPL'	ABB TPI	ABB TPI	ABB TPL76	
10	*del ro_cyl, %*		0.0467625	0.0311859	0.0111322	0.005091	0.005164	0.00184	0.00514	0.00183	
11	*del ro_res, %*		0.0420594	0.0017986	0.0186156	0.0048382	0.014882	0.00213	0.00072	0.00012	
12	*del ro_exh, %*		0.0236189	0.0188957	0.0162797	0.0067738	0.000215	0.00278	0.00018	0.00186	
13	*del Power_TC, %*		0.0655115	-0.1329678	0.169605	-0.040061	-5.84164	-609887	-47268	-54627	
14	*del Pik, %*		0.0164441	0.0076221	0.0244039	0.0127933	0.005216	0.00547	0.01146	0.00028	
15	*Number of iterations*		16	18	15	175	36	35	74	30	
16	*Brake power, kW*		2940.2728	2657.060	2122.447	1511.006	1088.993	747.005	482.999	268.001	
17	*crank speed*		1000	966	896	797	720	654	600	550	
18	*Air excess ratio*		2.471	2.4150566	2.2935262	2.1387305	1.96106	1.84947	2.36165	3.35648	
19	*Fuel mass per cycle, g*		1.2147151	1.1411	0.9989	0.8298643	0.70068	0.57875	0.45931	0.3305	
20	*Friction power, kW*		432.60895	406.51534	355.49582	290.4425	243.1246	205.313	178.412	155.914	
21	*Brake torque, N*m*		28077.537	26266.1	22620.401	18104.202	14443.22	10907.3	7687.17	4653.13	
22	*Brake mep, kPa*		1538.3266	1439.0807	1239.3382	991.90236	791.3228	597.595	421.169	254.938	
23	*Friction mep, kPa*		226.33745	220.17131	207.58091	190.6614	176.6678	164.248	155.573	148.314	
24	*Brake efficiency, %*		42.720377	42.433111	41.62297	40.108081	38.1732	35.4584	31.6191	26.7341	
25	*Mechanical efficiency, %*		87.173907	86.730689	85.653593	83.877284	81.74902	78.4407	73.0256	63.2205	
26	*Brake sfc, g/(kW*h)*		196.89	198.22292	202.08109	209.71372	220.3435	237.214	266.017	314.625	
27	*Gross indicated power, kW*		3396.7031	3077.623	2481.9899	1804.8271	1344.346	976.396	680.946	438.652	
28	*Net indicated power, kW*		3372.8817	3063.5752	2477.9432	1801.449	1332.118	952.319	661.411	423.915	
29	*Pumpins strokes power, kW*		-23.821407	-14.047719	-4.046676	-3.378167	-12.2275	-24.077	-19.534	-14.737	
30	*Gross mean indicated pressure, kPa*		1777.1272	1666.8603	1449.2821	1184.7814	976.8758	781.104	593.775	417.271	
31	*Net mean indicated pressure, kPa*		1764.664	1659.252	1446.9191	1182.5638	967.9906	761.843	576.742	403.252	
32	*Indicated efficiency, %*		49.005922	48.92514	48.594541	47.817572	46.6956	45.2041	43.2986	42.2871	
33	*Indicated sfc, g/(kW*h)*		171.63671	171.9201	173.08971	175.90217	180.1286	186.072	194.261	198.908	
34	*Volumetric efficiency, %*		95.828416	96.011566	96.248273	96.245514	94.95815	90.4751	91.0549	91.7238	
35	*Residual gases fraction, %*		1.1234716	1.1226201	1.1495262	1.2704558	1.819116	3.50991	2.9739	2.3167	
36	*Scavenging factor*		1.0221393	1.0221243	1.0217914	1.0203725	1.013057	1.00275	1.00314	1.00487	

Fig. 4.1.3. Example of the report table, exported to table editor (for series of calculations)

4.2. Charts and diagrams of the operating cycle

The “Diagrams” page displays the number of diagrams with results of performed calculations. The diagrams are thematically grouped into seven blocks and are displayed by clicking on one of the buttons:

1. “Indicated diagrams”:
   - *p*-*V* diagram,
   - *p*-φ diagram for incylinder pressure (**p_cyl**), intake receiver pressure (**p_res**) and exhaust manifold pressure (**p_exh**),
   - *T*-φ diagram for incylinder temperature (**T_cyl**), intake receiver temperature (**T_res**), exhaust manifold temperature (**T_exh**), temperature of gases, refluxed in the receiver (**T_ZG**), fresh zone (**T_II (fresh)**) and burned gases zone (**T_I (burned)**) temperatures;
2. “Combustion diagrams”:
   - heat-release diagram for burned fuel fraction (**X**), fuel burn rate (**dX_comb**), used heat fraction (**Ksi**),
   - detailed heat-release diagrams (CI-engines only) for burned fuel fraction (**X**), fuel burn rate (**dX_comb**), evaporated fuel fraction (**SigmaEv**), fuel evaporation rate (**SigmaEv**), injected fuel fraction (**Sig**) and fuel injection rate (**dSig**),
   - heat-release diagrams for main and ignition fuels (Dual-fuel engines only);
3. “Gas exchange diagrams”:
   - *m*-φ diagram for incylinder mass (**m_cyl**), intake receiver mass (**m_res**), exhaust manifold mass (**m_exh**), burned and fresh gases zones masses (**m_I(burned)** and **m_II(fresh)** correspondently), mass of air in the cylinder (**m_air**), mass of fuel vapor for SI-engines (**m_benz**) and mass of gases refluxed into intake manifold (**m_ZG**),
   - *A*-φ diagram for intake (**A_int**) and exhaust (**A_exh**) valves/ports areas;
   - d*m*-φ diagram for intake valves/ports mass flow rate (**dm_int**), exhaust valves/ports mass flow rate (**m_exh**) an refluxed gases flow rate (**dm_ZG**),
   - d*m*-φ diagram for intake receiver incoming flow rate (**dm_resIn**) and the outcoming mass flow from the intake receiver (**dm_intSum**),
   - d*m*-φ diagram for exhaust manifold incoming flow rate (**dm_exhSum**) and the outcoming mass flow from the exhaust manifold (**dm_exhOut**),
   - turbocharger efficiency diagram for compressor’s (**eff_compr**) and turbine’s (**eff_turb**) efficiency;
4. “Heat transfer diagrams”:
   - heat transfer diagrams for heat rate, rejected to cylinder walls (**dQw**), heat rate, rejected to piston crown (**dQw_pist**), heat transfer rate between fresh and burned gases zone (**dQ_2zone**), heat transfer rate to intake receiver walls (**dQres**), heat transfer rate to exhaust madifold

walls (**dQexh**), heat transfer rate, rejected to walls from fresh zone (**dQw_II(fresh)**) and burned gases zone (**dQw_I(burned)**);

5. "Kinematics & dynamics diagrams":
   - *V*-φ – volume diagram for the cylinder (**Volume**), volume of burned gases (**V_I**) and volume of fresh charge (**V_II**),
   - diagram for piston velocity (**Piston speed**) and piston acceleration (**Piston acceleration**),
   - *F*-φ diagram for piston force (**Piston force**), inertia forces (**Inertia force**) and connecting rod force (**Connecting rod force**),
   - *F*-φ diagram for normal force (**Normal force**), tangential force (**Tangential force**) and radial force (**Main bearing radial force**);
6. " Heat balance diagrams":
   - *Q*-φ cylinder internal heat balance diagram for the cylinder intake enthalpy (**I_int**), cylinder exhaust enthalpy (**I_exh**), heat released from fuel burning (**Q_fuel**), heat rejected to cylinder walls (**Q_walls**), work performed by piston (**Work**), incylinder internal energy (**U**) and energy conservation accuracy (**balance**),
   - *Q*-φ receiver internal heat balance diagram for the intake enthalpy (**I_resIN**), outcoming enthalpy (**I_resOUT**), heat rejected to receiver walls (**Q_res**), internal energy of the receiver gases (**U_res**) and energy conservation accuracy (**balance**),
   - *Q*-φ exhaust manifold heat balance diagram for the incoming enthalpy (**I_exhIN**), outcoming enthalpy (**I_exhOUT**), heat rejected to manifold walls (**Q_exh**), internal energy of the manifold gases (**U_exh**) and energy conservation accuracy (**balance**),
   - *S*-φ diagram for incylinder enthropy (**S_cyl**);
7. "Emissions formation diagrams":
   - NO formation diagram for NO volumetric concentration in the cylinder (**[NO]**) and NO volumetric concentration rate (**d[NO]/d(c.a.d)**),
   - NO formation diagram for NO mass in the cylinder (**Mass_NO**),
   - Soot formation diagram for soot concentration (**[C]**) and soot concentration rate (**d[C]/d(c.a.d)**).

There are some options for displaying and export of diagrams.

The User can switch between low-resolution and full-resolution of diagrams in respect to number of points for the chart. The low-resolution diagrams are displayed after first click on the button for diagrams block and have uniform step by crank angle revolution $\Delta\varphi = 1$ c.a.d. (this provides 720 points charts for four-stroke and 360 points charts for two-stroke engines). The button after been clicked is added with the inscription "press for full-resolution" (see number 1 on Fig. 4.2.1). The second click on the same button will display the charts with full resolution (total mesh size) with support of variable step by c.a.d. (see Fig. 4.2.2).

The diagrams allow zooming charts framing the desired range by mouse. The button "Reset zoom" returns the full scope of the chart.

For diagrams with multiple rows the User can hide some of them by clicking on their names on the legend.

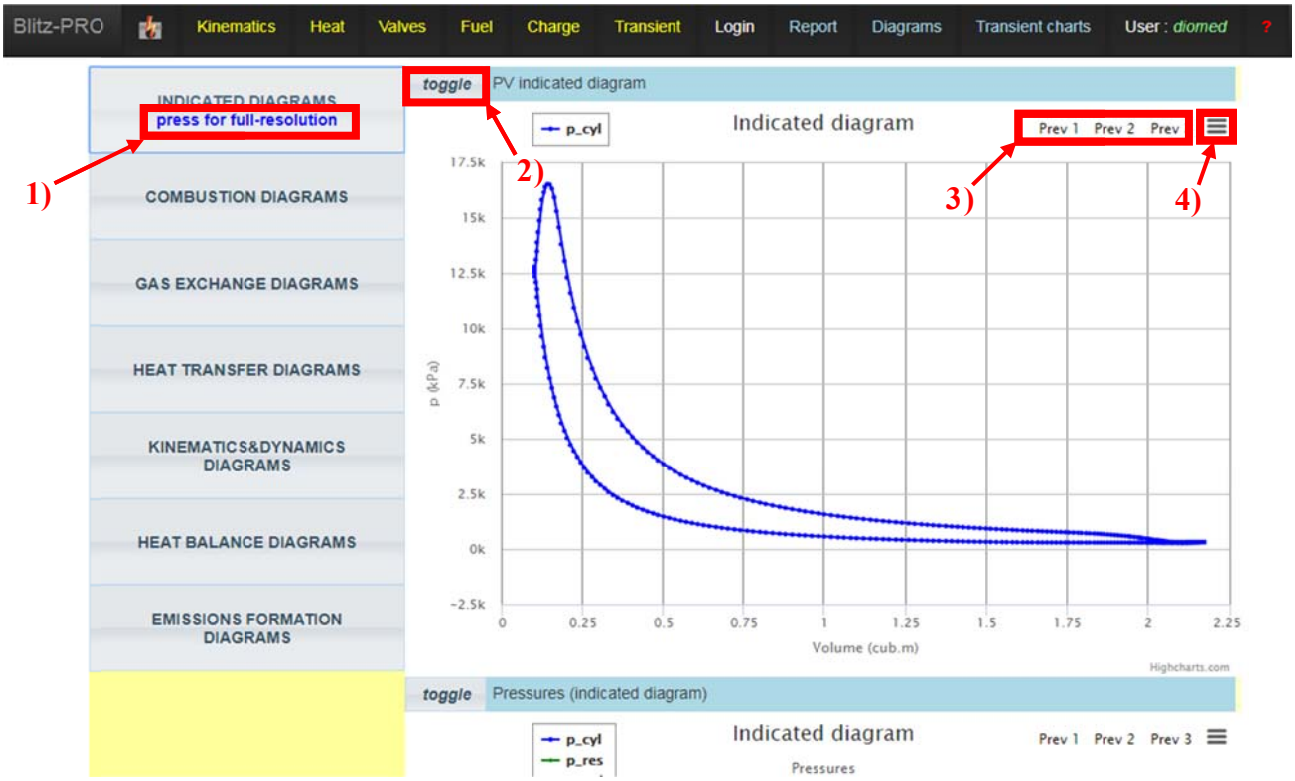

Fig. 4.2.1. “Charts” page with activated “Indicated diagrams” button: 1 – mesh resolution information, 2 – “Toggle” button to show and hide the current diagram, 3 – buttons which add the previously calculated diagrams, 4 – block of options for diagram export.

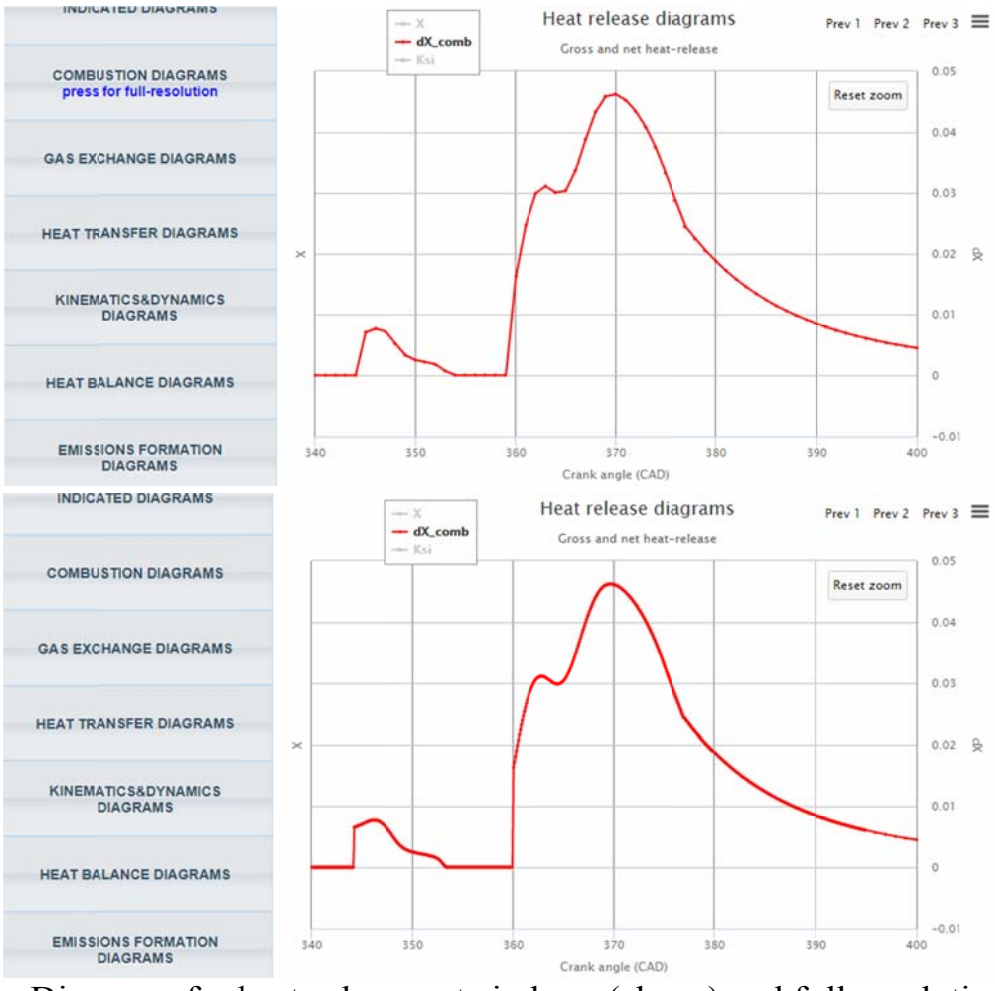

Fig. 4.2.2. Diagrams for heat-release rate in low- (above) and full-resolution (below).

The User can also superimpose the chart for several consecutive calculations he made before using buttons “Prev 1”, “Prev 2” and “Prev 3” (number 3 on fig 4.2.1). “Prev 1” displayes previous calculation, “Prev 2” – the calculation before previous and “Prev 3” – the calculation executed before “Prev 2” (see Fig. 4.2.3).

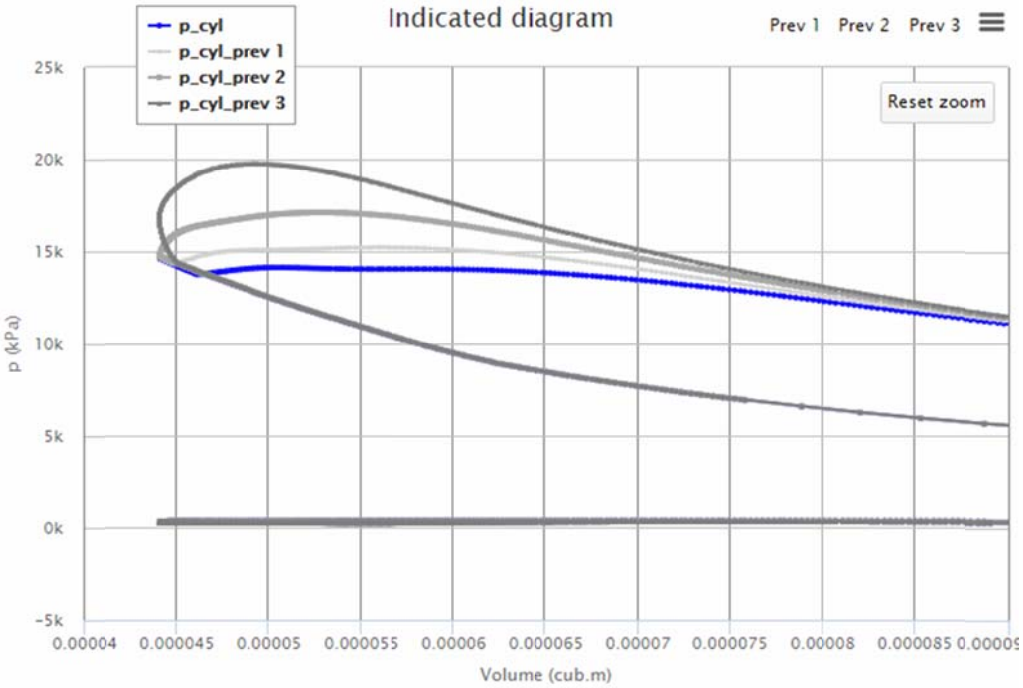

Fig. 4.2.3. The indicated pressure build-up for different fuel-injection advance angles.

The “Prev” buttons offer the ability to compare calculation results for different projects – the previous calculations are stored in database by User unique id.

Clicking on chart context menu button (position 4 on Fig. 4.2.1) displays the number of options for diagram export, shown on Fig. 4.2.4. The diagram can be exported as .png or .jpeg image, .pdf document, .svg vector image, .csv and .xls files.

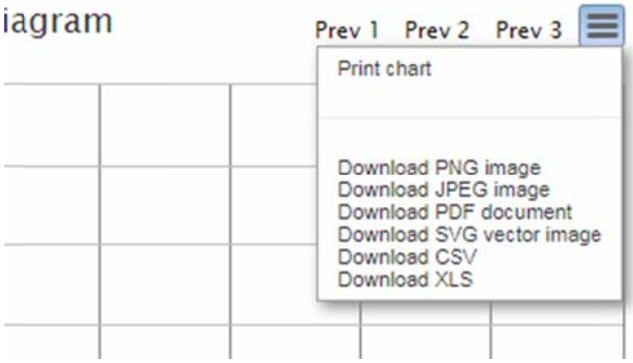

Fig. 4.2.4. Diagram export options.

4.3. Charts and diagrams of engine and installation transient

Transient calculations results are displayed on pages “Report” and “Transient charts”. The “Report” page contains the results of the last calculated operating cycle, while the “Transient charts” page offers the diagrams of the transient processes. The diagrams are grouped in fallowing blockes (see Fig. 4.3.1): engine transient, installation transient, supercharger transient, heat transfer transient, injection&combustion transient, incylinder transient, emissions transient. These blocks are activated with corresponding buttons. All diagrams have the time of transient process as abscissa.

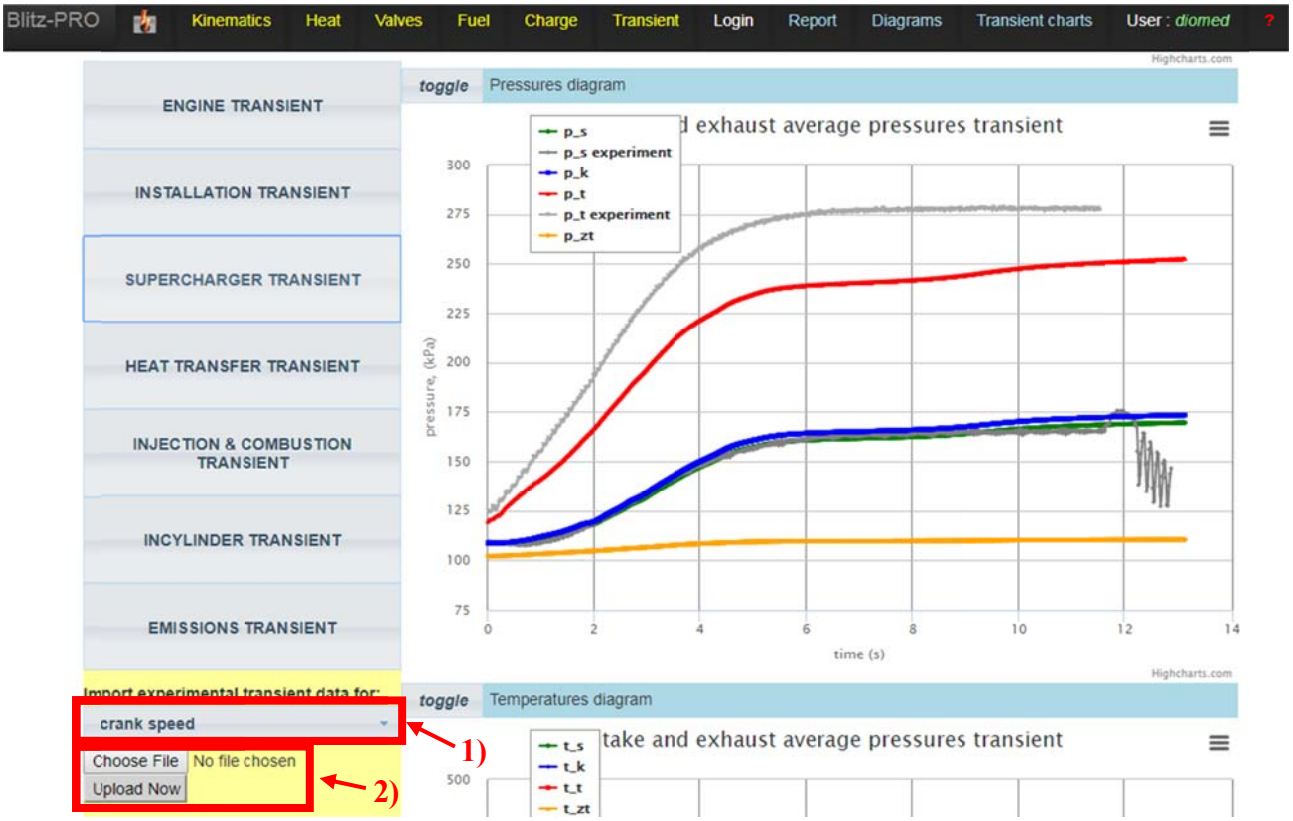

Fig. 4.3.1. “Transient charts” page.

Click on the button “Engine transient” displays diagrams:

- n_{crank}-τ diagram for engine speed (**rpm**),
- *P*-τ diagram for engine brake power (**Pb**), indicated power (**P ind**), power of engine load (**P load**), power of friction losses (**Pfr**), power of pumping stroke (**P pump**),
- gas exchange transient diagrams for air excess ratio (***alpha***), trapped air ratio (***Fi scav***), residual gases fraction (**gamma r**),
- η-τ diagrams for brake efficiency (**eff brake**), indicated efficiency (**eff ind**), mechanical efficiency (**eff mech**) and volumetric efficiency (**eff v**),
- *p*-τ diagrams for intake receiver pressure (**p_s**), the pressure after conpressor (**p_k**), exhaust manifold pressure (**p_t**) and the pressure after turbine (**p_zt**),

- t-τ diagrams for intake receiver temperature (**t_s**), the temperature after conpressor (**t_k**), exhaust manifold temperature (**t_t**) and the temperature after turbine (**t_zt**).

The "Installation transient" button shows the diagrams:

- v-τ diagram for installation speed (**speed**),
- s-τ and j-τ diagrams for vehicle travel (**travel**) and acceleration (**acceleration**),
- λ_p-τ and η_p -τ diagrams for propeller relative pitch (**relative pitch**) and propeller efficiency (**efficiency**),
- diagrams for propeller thrust (**thrust**) and torque (**torque**).

The "Supercharger transient" button shows the diagrams:

- P-τ diagram for supercharger's compressor power (**Power_compr**), turbine power in static (**Power_turb**) and pulsating flow, or actual turbine power (**Power_turb_imp**) and supercharger's speed (**rpm_TC**),
- η-τ diagrams for compressor adiabatic efficiency (**eff_compr**), turbine efficiency in static (**eff_turb**) and pulsating flow (**eff_turb_imp**),
- Π-τ diagrams for compressor pressure increase ratio (**Π_cmpr**) and turbine pressure drop ratio (**Π_turb**),
- G-τ diagrams for intake valve/ports total flow (**G_int**), exhaust valve/ports total flow (**G_exh**), exhaust gases flow through the waste-gate (**G_WG**) and waste-gate effective area (**f_WG**).

The "Heat transfer transient" button shows the diagrams:

- Q-τ diagrams for the burned fuel heat (**Q_fuel**), the heat, rejected to the cooling water/air (**Q_w**), the heat rejected to the oil (**Q_m**), the heat taken from scavenge air in charge air cooler (**Q_cac**), the heat of exhaust gases (**Q_exh**) and the heat rejected to the walls of the intake receiver (**Q_int.receiver**) and exhaust manifold (**Q_exh.manifold**).

Click on the "Injection and combustion transient" button displays the diagrams:

- φ-τ diagrams for the injection advance (**Inj_start**), injection duration (**Inj_duration**), the combustion start (**comb_start**) and duration (**comb_duration**),
- q_f-τ diagram for the fuel mass, injected per cycle (**q_z**),
- diagrams for injection average pressure (**press_inj**) and fuel droplets Sauter diameter (**d_32**).

The "Incylinder transient" button shows the diagrams:

- p-τ diagrams for incylinder maximum pressure (**press_max**), fuel ignition pressure (**press_ignition**), and the incylinder maximum pressure rate (**dp_dfi_max**),
- t-τ diagrams for incylinder maximum average temperature (**tempr_max**), burned gases zone maximum temperature (**tempr_I_max (burned)**), fresh charge zone maximum temperature

(**tempr_II_max (fresh)**) and the temperature of fuel ignition (**tempr_ignition**),

- *t*-τ diagrams for walls temperatures of the cylinder head (**tempr_head**), piston crown (**tempr_piston**), cylinder liner (**tempr_liner**), intake receiver (**tempr_receiver**) and exhaust manifold (**tempr_exhaust**),
- α-τ diagrams for average heat transfer coefficients from gases to walls for the cylinder (**alpha_m_cylinder**) and the exhaust manifold (**alpha_m_exhaust**).

The "Emissions transient" button shows the diagrams:

- diagrams for incylinder concentrations of nitric oxides ([**NO] cyl**) and carbon monoxide ([**CO] cyl**) at the exhaust valves/ports opening and diagrams for exhaust manifold concentrations of nitric oxides ([**NO] exh**) and carbon monoxide ([**CO] exh**),
- diagrams for specific emission of nitric oxides (**g_NO**) and soot concentration (**Soot**).

The User can also add the experimental diagrams or diagrams from another source on the corresponding charts to use these diagrams as the reference. The experimental diagrams are to be imported from .csv file (see section 1.5) via the interface, marked 2) on Fig. 4.3.1. Before import the User should select the parameter for impost with the selection list, marked 1) on Fig. 4.3.2.

The options of diagrams zooming and exporting are the same as described in section 4.2.

5. Supercharger matching

As it was mentioned, for the most cases usage of performance maps of the supercharger helps to increase the accuracy of calculations.

The User should match the maps correctly before running calculations. Let's consider some examples of proper matching of the supercharger's performance maps.

Matching the turbocharger to marine main engine.

For marine diesel engines generally the matching point for the turbocharger is the operation of the engine at rated conditions (speed and load).

For example, assume that the engine has 2460 kW rated power at 750 rpm crankshaft speed. The supercharged air pressure is 372 kPa absolute, which means compressor's pressure increase ratio $\Pi_k = 3.72$.

It is recommended to execute calculations with manual set-up of turbocharger parameters first (uncheck the checkbox "Use characteristics map for supercharger performance", see section 2.5). Don't forget to adjust turbine flow area μF_{turb} properly to reach the balance of turbine and compressor power.

From the report table find the values of: intake air flow $G_{int} = 4.749$ kg/s, exhaust gases flow $G_{exh} = 4.7627$ kg/s, pressure drop ratio at the turbine $\Pi_t = 3.0$, exhaust gases pressure $p_t = 335.8$ kPa and temperature $t_t = 538.4$ °C.

Next step is to switch to the turbocharger performance maps mode (check the checkbox "Use characteristics map for supercharger performance") and to set all multipliers for performance map adjustment equal to 1.0 (see Fig. 2.5.6 and 5.1).

ABB VTR354 ▾	TMAP selection, load and adjustment		
TMAP file	Choose File No file chosen Upload Now		Show maps
μG_k	1	-	Multiplier for compressor referred mass flow data
$\mu \Pi_k$	1	-	Multiplier for compressor pressure increase ratio data
$\mu \eta_k$	1	-	Multiplier for compressor adiabatic efficiency data
μn_k	1	-	Multiplier for compressor adiabatic efficiency data
μG_t	1	-	Multiplier for turbine reduced mass flow data
$\mu \Pi_t$	1	-	Multiplier for turbine pressure drop ratio data
$\mu \eta_t$	1	-	Multiplier for turbine efficiency data
μn_t	1	-	Multiplier for turbine reduced speed data

Fig. 5.1. Setting the multipliers equal to 1.0

Next step is to choose the closest turbocharger performance map from the list of maps, or uploading the User own performance map. For this example the ABB VTR354 performance map suites the best. The intersection of blue lines on Fig. 5.2 for standard map shows the predicted operating point of the turbocharger. As it is seen from this figure, the predicted point lies in the range of lower values of compressor's adiabatic efficiency. To adjust the map better to the engine the μG_k is to be altered, but it is better to keep some distance from surge line for stable calculations.

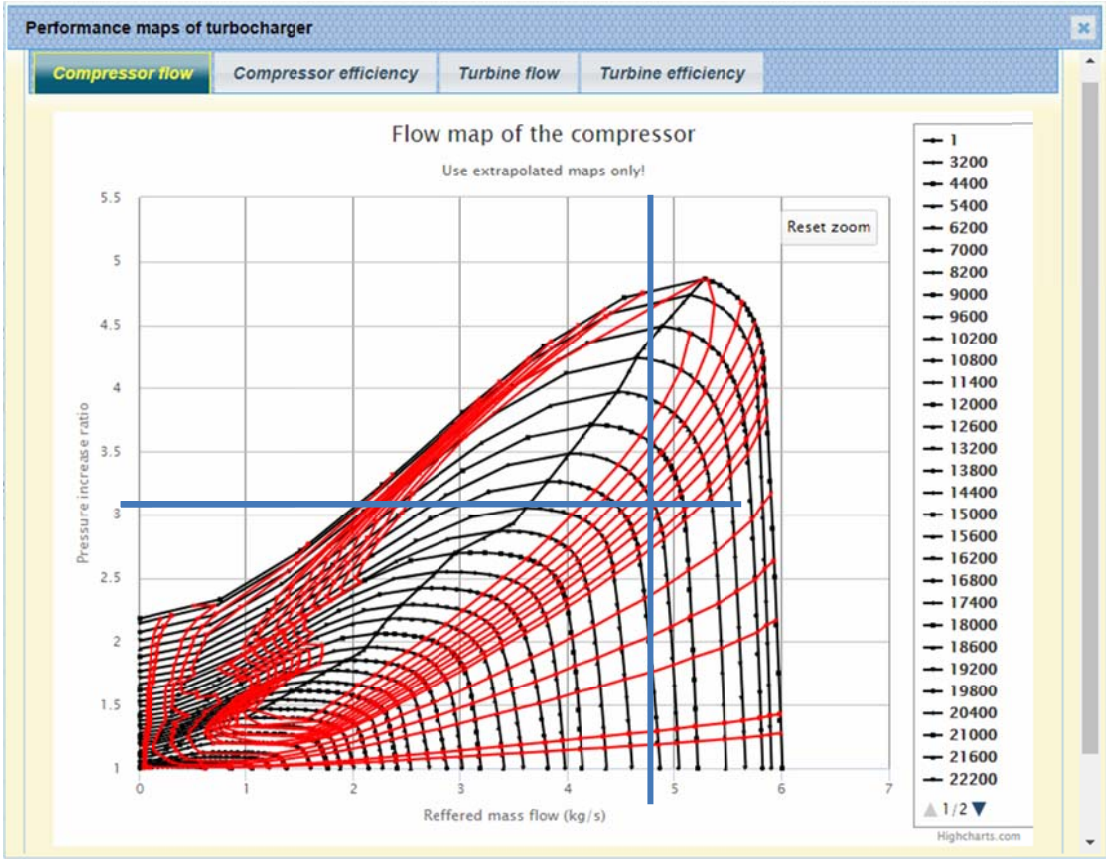

Fig. 5.2. ABB VTR354 compressor standard map (all multipliers set to 1.0).

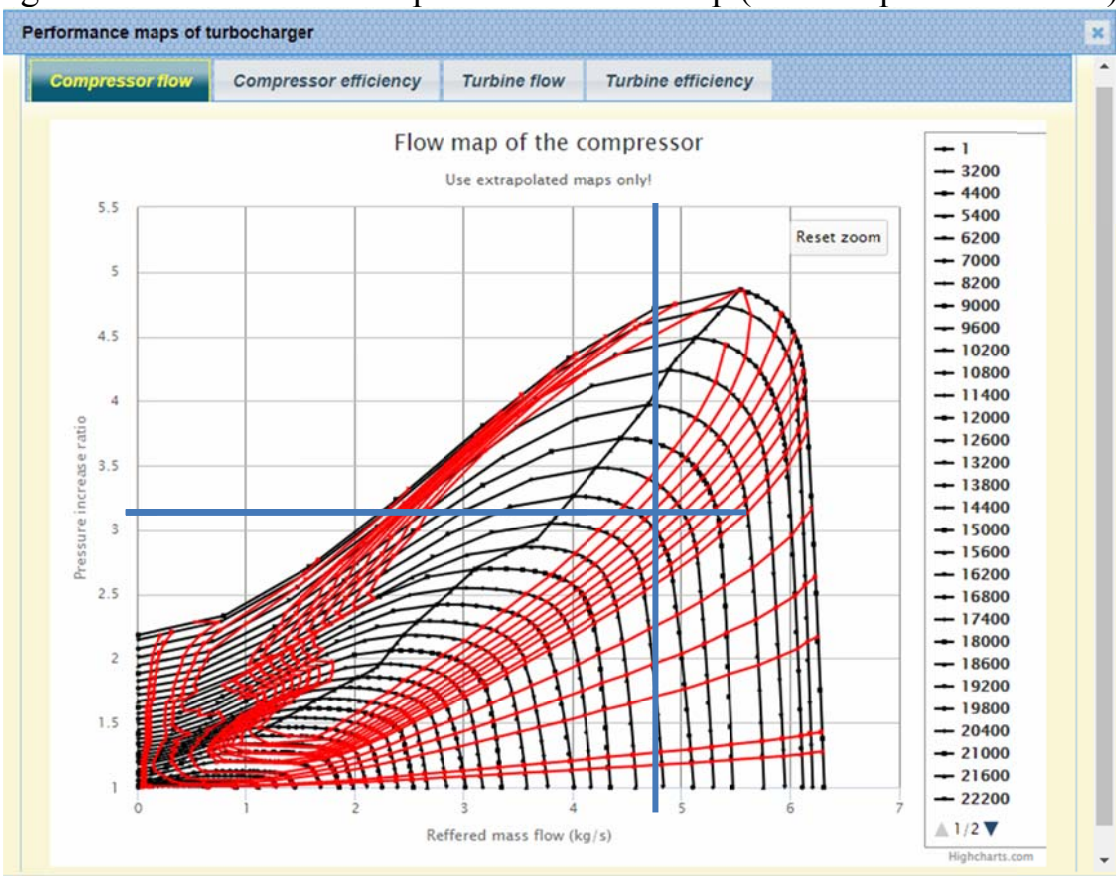

Fig. 5.2. ABB VTR354 compressor scaled map ($\mu G_k = 1.05$).

To match the turbine map the turbine reduced flow must be calculated first:

$$G_{turb.red} = \frac{G_{exh}\sqrt{t_t + 273.15}}{p_t} = \frac{4.763\sqrt{538.4 + 273.15}}{335.8} = 0.4041 \frac{\text{kg/s}\sqrt{\text{K}}}{\text{kPa}} \ .$$

As it is seen from Fig. 5.3 and 5.4 scaling of the turbine flow map could be done with the multiplier μG_t.

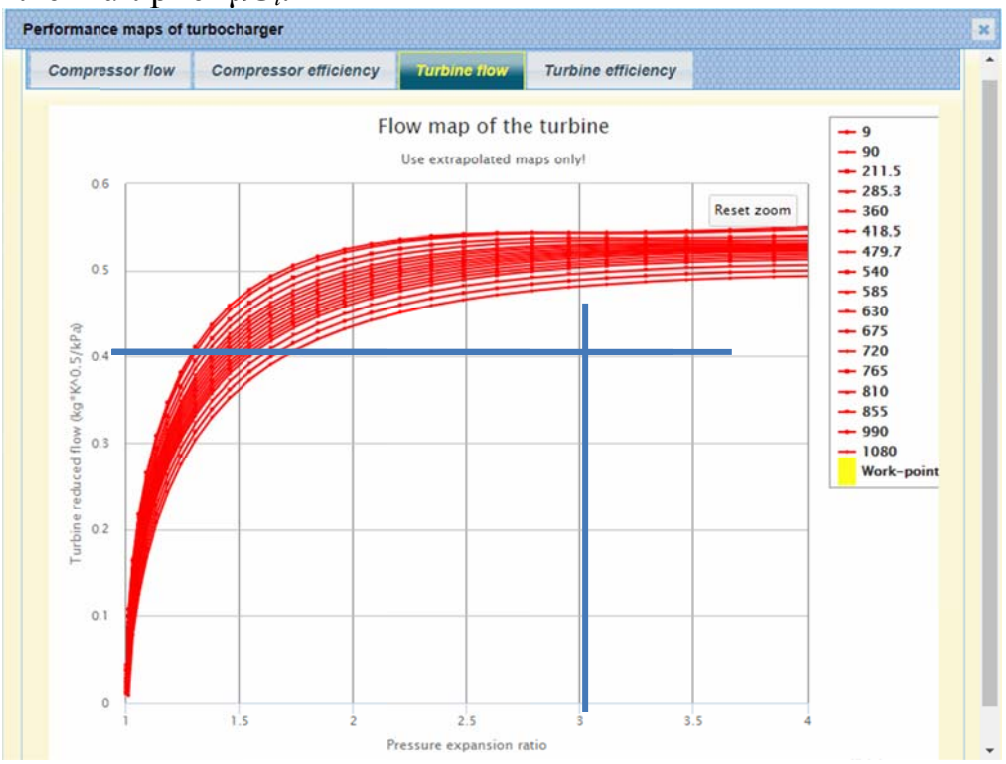

Fig. 5.3. ABB VTR354 turbine standard map (all multipliers set to 1.0).

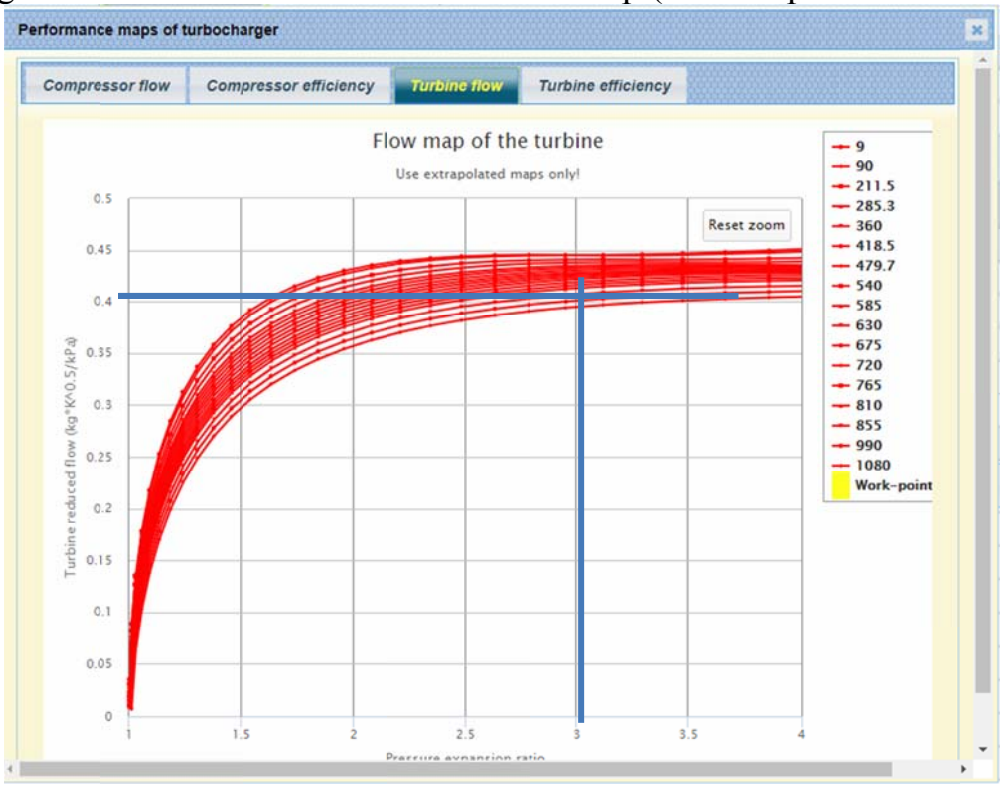

Fig. 5.4. ABB VTR354 turbine adjusted map ($\mu G_t = 0.82$).

The maximum efficiencies of compressor and turbine could be adjusted with the multipliers $\mu\eta_k$ and $\mu\eta_t$.

The next step is to execute calculations with activated turbocharger's maps. To reach the balance of powers of turbocharger compressor and turbine adjust value of μG_t. For this example the balance is reached with $\mu G_t = 0.965$.

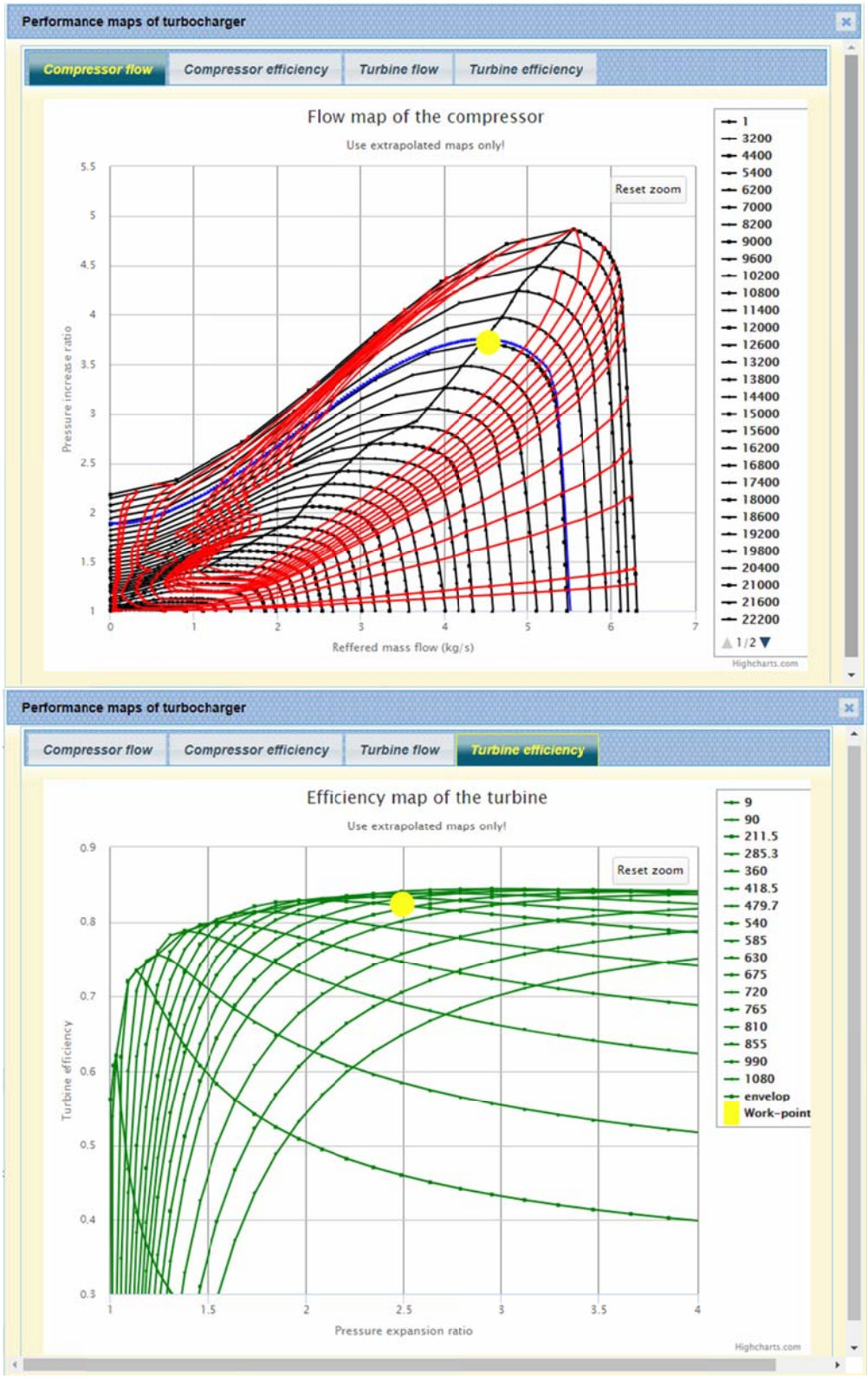

Fig. 5.5. Compressor map and turbine efficiency with the operating points.

From the "Report" page click "Show TMAP" button to see the average operating point on the compressor flow map and turbine efficiency map (Fig. 5.5). Adjust these maps precisely: compressor map altering μG_k and turbine flow map with μn_t multiplier. The last helps to match better the turbine speed to the current compressor. In this example the final values of $\mu G_k = 1.02$ and $\mu \eta_t = 1.15$ provide the best turbocharger map matching.

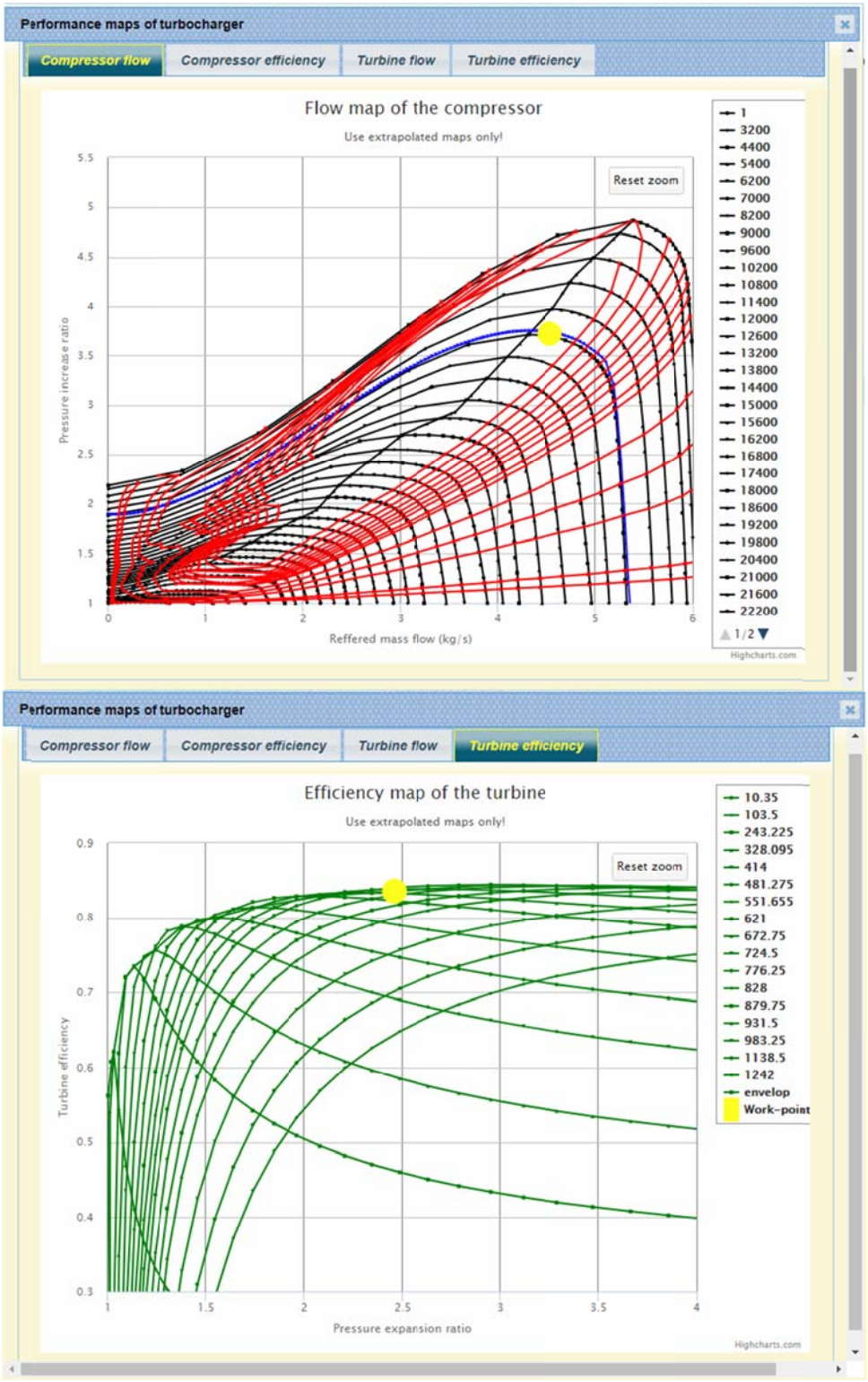

Fig. 5.6. Compressor map and turbine efficiency map after final tuning.

Matching the turbocharger to automotive engine

For automotive engines matching the turbocharger is much more difficult task, because these engines operate in wider range of speed and load at transient conditions. Matching of the turbocharger depends on the type of turbine control: fixed geometry turbine (not controllable), turbine with waste-gate control, variable geometry turbine (VGT or VNT variable nozzle turbine).

Consider the task of waste-gate turbocharger matching to 2.7 liters automotive diesel engine if the rated speed of the engine is 4000 rpm, maximum torque speed is 1800 rpm and the pressure increase ratio at the maximum torque is $\Pi_k = 2.0$.

First, execute three calculations in manual mode (without using the turbocharger map): rated power at 4000 rpm and Π_k = 2.0, maximum torque at 1800 rpm and Π_k = 2.0 and minimum engine speed at 900 rpm and Π_k = 1.0. For these three cases the calculated compressor's air mass flow is 0.19, 0.087 and 0.022 kg/s correspondently.

Fig. 5.7 shows the Garrett GT2252 turbocharger performance maps, superimposed with calculated three points. It is obvious, that the compressor suits perfectly for the engine. The turbine map is presented by manufacturer as single line, which is an envelope of the number of constant-speed lines. Matching of the turbine is to be made for the maximum torque operation. The turbine reduced flow at these conditions, according to the manufacturer's manual is:

$$G_{t.red} = \frac{G_t \sqrt{\frac{T_t}{T_{0t}}}}{\frac{p_t}{p_{0t}}} = 0.09 \frac{\sqrt{\frac{850}{288}}}{1.8} = 0.0859 \text{ kg/s}.$$

From Fig. 5.7 is seen, that the turbine has too big equivalent nozzle area, so the supercharged air pressure at 1800 rpm will be less, then 200 kPa.

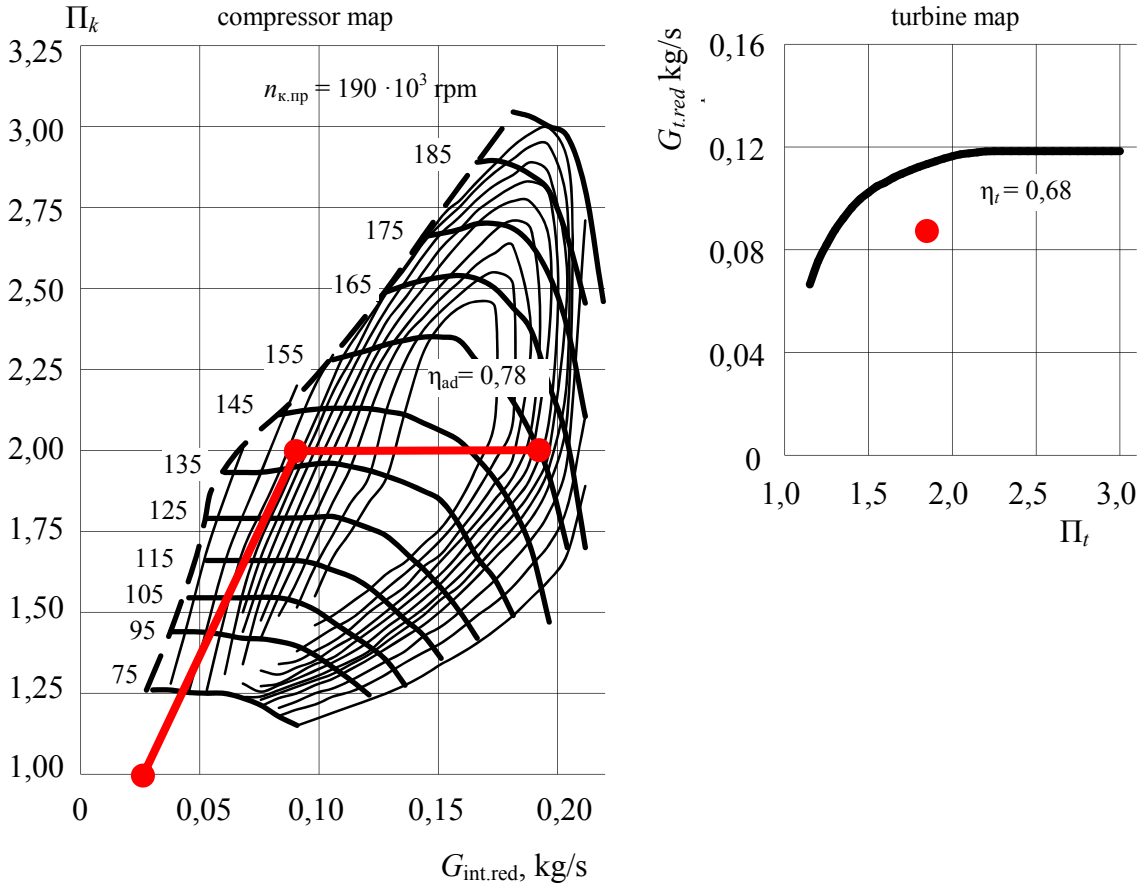

Fig. 5.7. Garrett GT2252 turbocharger performance maps (Garret product catalogue).

Presented turbocharger performance maps must be converted to .tmap file and uploaded to the Project. Calculation of three basic modes of engine operation (rated power, maximum torque and minimum speed) with activated turbocharger's performance maps will help to adjust the maps precisely, using the multipliers.

References

1. Двигатели внутреннего сгорания: Теория поршневых и комбинированных двигателей. Учебник для втузов по специальности «Двигатели внутреннего сгорания» [**text**] /Д. Н. Вырубов, Н.А. Иващенко, В.И. Ивин и др.; под. редакцией А.С. Орлина, М.Г. Круглова. - 4-е издание - М: Машиностроение, 1983. – 372 с.
2. **Woschni, G.** A universally applicable equation for the instantaneous heat transfer coefficient in the internal combustion engine. SAE Trans., 76, 1967, Paper 670931.
3. **Дьяченко, В. Г.** Теория двигателей внутреннего сгорания. Учебник для вузов **[текст]** – Х.: ХНАДУ, 2009 – 500 с.
4. **Разлейцев Н. Ф.** Моделирование и оптимизация процесса сгорания в дизелях. – Харьков. Вища школа, 1980 – 169 с.
5. **Лышевский А. С.** Распыливание топлива в судовых дизелях / А. С. Лышевский – Л. : Судостроение, 1971. – 248 с.
6. **Кулешов, А. С.** Развитие методов расчета и оптимизации рабочих процессов ДВС: дисс. … д.т.н. **[текст]** / А. С. Кулешов. – М, МГТУ, 2011. – 235 с.
7. **Wray K.L., Teare J.D.** Shock-Tube Study of the Coupling of the O2–Ar Rates of Dissociation and Vibrational Relaxation // The Journal of Chemical Physics 37, 1254 (1962)
8. **I.M. Khan, G. Greeves, C.H.T. Wang.** Factors affecting smoke and gaseous emissions from direct injection engines and a method of calculation // SAE Paper No. 730169 (1973)
9. **Pattas K., Häfner G**. Stickoxidbildung bei der ottomotorischen Verbrennung, MTZ 34 (1973)
10. **Urlaub A.** Verbrennungsmotoren. Brand 2. Verfahrenstherie, 1989, 226 S.
11. **Blumberg, P., Kummer, J.,** “Prediction of NOFormation in Spark Ignited Engines—An Analysis of Methods of Control ... 1, 313–326 (1970)
12. **Newhall, H. and Starkman, E.,** "Direct Spectroscopic Determination of Nitric Oxide in Reciprocating Engine Cylinders," SAE Technical Paper 670122, 1967
13. **Звонов. В. А.** Токсичность отработавших газов двигателей внутреннего сгорания. – М.: Машиностроение, 1981 г.